X-RAY STUDIES OF

MONOCHLOROACETAMIDE

AND

BENZANILIDE

by

Paul Graham Collis, G.R.I.C.

A thesis submitted to the University of Keele
in partial fulfilment of the
requirements for the degree of
Doctor of Philosophy

Department of Chemistry
University of Keele

Computer Centre
University of Keele

October 1975

PAGE NUMBERING CLOSE TO THE EDGE OF PAGE, AT SOME POINTS CUT OFF.

ABSTRACT

The crystal structures of monochloroacetamide and benzanilide have been determined by X-ray diffraction methods.

Monochloroacetamide was found to crystallise in the space group $P2_1/c$, with four molecules in the monoclinic unit cell of dimensions

$a = 10.276$ Å $b = 5.152$ Å $c = 7.499$ Å $\beta = 98.8^\circ$

The space group of benzanilide was found to be Ia with four molecules in the monoclinic unit cell of dimensions

$a = 23.383$ Å $b = 5.335$ Å $c = 8.027$ Å $\beta = 92.0^\circ$

Three dimensional intensity data for the monochloroacetamide structure were collected using the multiple film technique, the intensities were measured on a double beam recording microdensitometer. The structure was solved by the interpretation of a three dimensional Patterson Synthesis and was refined using Fourier, difference and least-squares methods. The hydrogen atoms were located in a three dimensional difference synthesis. The carbo-amide plane was found to be planar with the chlorine-carbon bond inclined at 12° to this plane.

Three dimensional intensity data for benzanilide were collected using a three circle diffractometer. The structure was solved by the interpretation of Patterson syntheses. Refinement of the structure by the Parameter Shift method showed the structure to be disordered. This fact was substantiated by Weissenberg photographs. The amount of disorder from least-squares refinement was found to be 39%. The structure has been refined in the space groups Ia and I2/a. In both refinements the N-phenyl bond was found to be rotated by 38° from the amide plane. The C-phenyl bond was found to be rotated by 27° from the amide plane.

PREFACE

This thesis is an account of research performed in the Department of Chemistry at the University of Keele between October 1967 and December 1970. The main theme of the research is an accurate determination of the crystal structures of monochloroacetamide and benzanilide. The work is original except where due acknowledgment is made.

I am indebted to my supervisors Drs. D. O. Hughes, D. T. Dixon, R. W. H. Small and Professor H. D. Springall for their patience and advice. In addition I wish to thank Professor H. D. Springall for the provision of research facilities at Keele and R. W. H. Small for the use of the three circle diffractometer; Mrs. A. F. Grundy for the source listing of the stereo drawing program; many colleagues in the University of Keele for their encouragement; Mrs. C. Goulding who typed the thesis; the Department of Chemistry for a three month grant in October 1969 and the Science Research Council for their financial support during the main course of this research. Finally I would like to thank Marion for her understanding and patience.

Computer Centre
University of Keele

October 1975

CONTENTS

1. INTRODUCTION

1.1. Hydrogen Bonding in Amides

It has long been noticed[1], that a feature of amide crystal structures is the formation of the maximum number of hydrogen bonds. Leiserowitz and Schmidt[2] have summarised the types of hydrogen bond found in primary amides and have tried to relate the packing types to molecular dimensions.

The majority of primary amides achieved one hydrogen bond per amide group in the formation of a centrosymmetric dimer. The orthorhombic form of acetamide[3], in which the dimers form tubes, is the only known example of a dimer which is not centrosymmetric. Primary amides which do not form dimers include the rhombohedral form of acetamide[4], adipamide[5], azodicarbonamide[6], nicotinamide[7] and the metastable form of chloroacetamide[8]. The last is possibly incorrect[9].

In those structures where a dimer is formed the remaining hydrogen bond per amide group is formed between an axis translation-, glide plane- or screw axis related amide group. Leiserowitz and Schmidt demonstrated that unit cell directions containing a non-dimer hydrogen bond are a function of the planarity of the hydrogen bond.

Axis translation hydrogen bonds produce structures in which the dimers are hydrogen bonded in chains. Structures of this type include benzamide[10], monochloroacetamide[11,12], monofluoroacetamide[13] and ethyl carbamate[14]. Glide plane and screw axis related hydrogen bonded structures form puckered sheets of which formamide[15], succinamide[16], crotonamide[17], decanamide[18] and tetradecanamide[19] are examples. The hydrogen bonded sheets or chains are further associated by weaker Van der Waals' forces.

Very few secondary amides (excluding those present in the α- and γ-

helix) have been studied and although the general hydrogen bonding features noted by Leiserowitz and Schmidt should prevail, the formation of hydrogen bonded dimers will be unlikely.

1.2. Non-Bonded Interactions

In a review of amide structures, Hughes[20] stated that "... non-bonded repulsions are of prime importance in determining molecular geometry and the influence of hybridisation, conjugation or hyperconjugation would appear to be small. Conversely the degree of conjugation or hyperconjugation cannot be deduced from bond lengths".

Hughes' work was an extension of Bartell's arguments[21,22,23], and was primarily concerned with the trigonal arrangement of carbon, nitrogen and oxygen atoms about the amide carbon atom. From a number of crystallographic and microwave studies, it was assumed that the non-bonded distances (between the carbon, nitrogen and oxygen atoms) were constant and were determined by the sum of the hard sphere radii of the atoms concerned. Using these constant non-bonded distances, with the observed bond lengths, a value for the calculated bond angle was determined, and compared with the observed bond angle. Good agreement was found, and it was concluded that the geometry of atoms round the amide carbon atom had been a consequence of the non-bonded repulsions.

The agreement found was a consequence of the use of the correct non-bonded distance in the angle calculation. The constancy of the non-bonded distances in these structures does give weight to the hard sphere radii hypothesis, but gives no information about the position of the amide carbon atom; and hence, the carbon-carbon, carbon-oxygen and carbon-nitrogen bond lengths.

Qualitatively, the theory of hybridisation explains the constancy of non-bonded distances, and arguments similar to those used by Mulliken[24]

are not invalidated by Hughes' observations. Within the constant non-bonded triangle, movement of the central carbon atom can be associated with relative changes in the "s" and "p" character of the hybrid orbitals.

1.3. Previous Structure Determinations of Monochloroacetamide

Three independent studies of the structure of monochloroacetamide were undertaken in the mid 1950's. Each study was completed with two-dimensional intensity data and the final results provide a three-fold ambiguity. The unit cell and space group information for each publication is given in Table 1.1.

a (Å)	b (Å)	c (Å)	β	Space Group	Ref.
10.281	5.145	7.429	$98^{\circ}\ 49^{1}$	$P2_1/c$	J.D (11)
10.25	5.18	7.49	$102^{\circ}\ 0^{1}$	$P2_1/c$	P&S (12)
10.27	5.15	7.45	$102^{\circ}\ 30^{1}$	$P2_1/c$*	K (8)

* The a and c axes have been interchanged for this comparison.

TABLE 1.1

Unit Cell Data for Monochloroacetamide

The unit cells selected by Penfold and Simpson, and Katayama are, within experimental error, the same. The final atomic parameters however give rise to significantly different structures. The structure published by Penfold and Simpson showed a typical hydrogen bonded dimer across a centre of symmetry. Katayama found that the "unstable modification", which he had prepared, did not contain hydrogen bonded pairs related by a centre of symmetry and had an unusual screw axis related hydrogen bond.

Dejace[25] brought attention to the fact that the unit cell chosen by himself was related to that chosen by Penfold and Simpson, as were the atomic coordinates. The relationship between the two cells however, showed that centres of symmetry and two-fold screw axes were interchanged in the h0l projection. The h0l projection was not affected and one further projection was not enough to resolve the issue as the related atomic positions both gave reasonable models.*

In comparing amide structures, authors have used each of these determinations as authoritative, and in an attempt to clarify the situation the structure, or structure of each form, of chloroacetamide was undertaken.

1.4. Energies of Hydrogen Bonds

In a thermodynamic study, to estimate the hydrogen bond energies of amides, Aihara[26] has determined the sublimation pressures for a series of amides, using a method which assumes the additivity rule for lattice energies[27,28].

Of the crystals for which data was collected only benzamide[10] and acetanilide[29] had known crystal structures. Benzamide had an estimated hydrogen bond energy of 8.7 Kcal mol^{-1}, that of acetanilide was 4.3 Kcal mol^{-1}. The energy quoted for benzamide is the sum of two hydrogen bond energies, one dimer and one axis translation, per molecule; acetanilide has only one hydrogen bond per molecule, formed between screw axis related amide groups. Benzanilide (N-phenyl benzamide), however had an estimated energy of 0.2 Kcal mol^{-1} per hydrogen bond, which Aihara associated with little or no tendency to hydrogen bond caused by steric hindrance of the two phenyl groups. In the same paper N-methylbenzamide

* Dejace did remark on the short Van der Waals distance between Chlorine atoms in the Penfold and Simpson structure.

was found to have a hydrogen bond energy of 4.0 Kcal mol^{-1}.

1.5. Aims of the Work

The object of the project was the determination of the crystal structures of 1) monochloroacetamide, to remove the ambiguities reviewed earlier and 2) benzanilide, to study a sterically hindered hydrogen bonded system.

PART 1

EXPERIMENTAL TECHNIQUES

2. INTRODUCTION TO CRYSTALLOGRAPHIC WORK

2.1. Unit Cell

A crystal is three dimensionally periodic, and as a result any vector line from a point in the crystal will pass through similar points at regular intervals. Three non-coplanar vectors $\underline{a}$, $\underline{b}$ and $\underline{c}$ bound a parallelepiped known as the unit cell. Simple translations of the unit cell constructs a space lattice of points in the same environment and orientation. There are an infinite number of unit cells which will define the lattice, but it is usual to select the smallest which is still related to the symmetry elements of the lattice.

Depending upon the symmetry of packing there are seven possible types of unit cell. In addition to these primitive lattices there are seven centred lattices. The fourteen types of lattices are known as the Bravais lattices.

In the unit cell of a crystal, the atoms or molecules may be related to each other by various symmetry elements. Consideration of the possible combinations of symmetry elements in the Bravais lattices, shows there to be two hundred and thirty ways in which the symmetry elements can be uniquely combined.

In order to study a crystal structure, the unit cell dimensions ($\underline{a}$, $\underline{b}$, $\underline{c}$, α, β, γ), the space group and the number of molecules in the asymmetric unit must be known. It is usual, in the preliminary study of a crystal, to determine these, as they can be determined directly from photographs and density measurements.

2.2. Reciprocal Cell

Certain aspects of diffraction are more conveniently envisaged in terms of the reciprocal lattice. Each lattice point in the reciprocal lattice represents a set of planes in the direct lattice. The vector,

$\underline{d}^*_{hkl}$, from the origin of the reciprocal lattice to any point, has a length which is inversely proportional to the interplanar spacing, and the direction of the normals to the (hkl) planes in the direct lattice.

The vectors $\underline{a}^*$, $\underline{b}^*$ and $\underline{c}^*$ define the unit cell of the reciprocal lattice. The equation,

$$d^*_{(hkl)} = K/d_{(hkl)}$$

relates the interplanar spacing, $d_{(hkl)}$, of a set of planes (hkl) in the direct lattice to the magnitude of the vector $\underline{d}^*_{(hkl)}$ in the reciprocal lattice. K is a constant which is usually chosen to be unity or λ, the wavelength of the X-radiation. The vector $\underline{d}^*_{(hkl)}$ is related to the reciprocal lattice vectors by the equation,

$$\underline{d}^*_{(hkl)} = h\underline{a}^* + k\underline{b}^* + l\underline{c}^*$$

2.3 Diffraction Geometry

Bragg[30] simplified the theory of diffraction by showing that diffraction could be considered as reflection from lattice planes in the direct lattice. Bragg's law gives the condition for the diffraction of an X-ray beam by a set of crystal planes. It is expressed in the form:

$$\lambda = 2d_{(hkl)} \sin \theta_{(hkl)}$$

where $\theta_{(hkl)}$ is the angle which the incident beam makes with the planes (hkl). Thus diffraction can only occur when Bragg's equation is satisfied. The Bragg angle, θ, can be measured for a number of planes and used to determine the unit cell dimensions.

Bragg's law can be interpreted geometrically in terms of the reciprocal lattice and the Ewald sphere of reflection. The Ewald sphere of reflection is the sphere with radius one reciprocal lattice unit (for $K = \lambda$) which passes through the origin of the reciprocal lattice. The direction of the incident X-ray beam coincides with the diameter of the Ewald sphere which passes through the origin of the reciprocal lattice. It can be shown that diffraction can only occur for a set of planes (hkl) when the corresponding reciprocal

lattice point P_{hkl} (Figure 2.1), lies on the surface of the sphere of reflection.

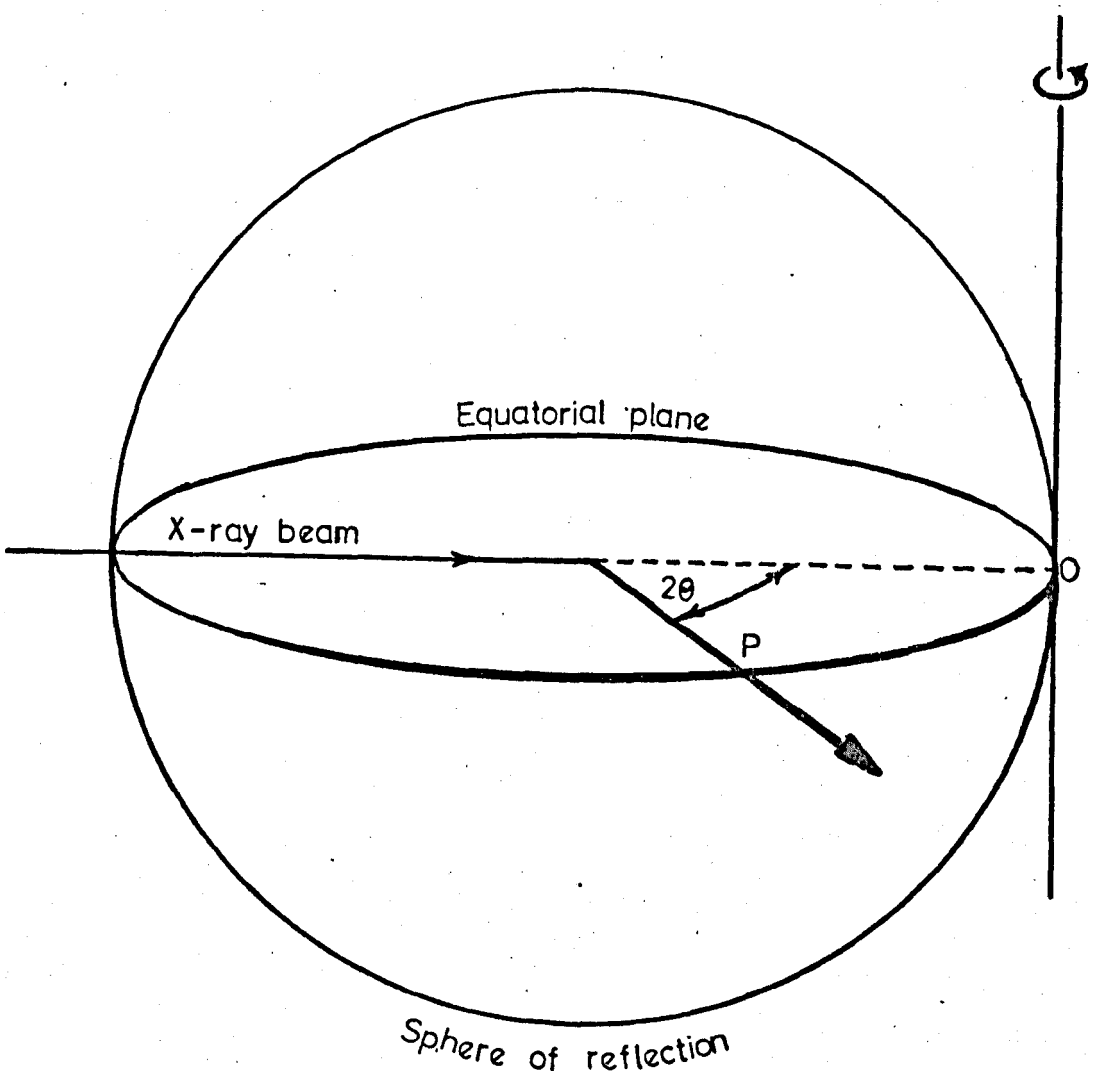

Figure 2.1. The Ewald Sphere of Reflection.

3. THE MEASUREMENT OF INTENSITIES

3.1. Methods of Collection

The measurement of diffracted beam intensities, from which the structure amplitude for every plane can be calculated, is achieved either by photographic or counter techniques. Photographic techniques have been used far more often than those using counters mainly because of the later development of the latter.

The amount of blackening produced by a diffracted beam on a photograph is assumed to be proportional to the intensity of the diffracted beam. The degree of blackening is measured either by visual comparison of a spot with a set of standard exposures, or with the use of a microdensitometer. The limited range of linearity of degree of blackening against exposure for any film produces an experimental difficulty in photographic techniques. The assessment of the relative magnitudes of very strong and very weak intensities is impossible on a single film. The multiple-film technique[31] is usually used to overcome this problem.

Variations on the same photograph in spot size, shape and the amount of background blackening all contribute to the errors likely to accumulate in the collection of intensities by visual estimation. These errors can be considerable, particularly if the X-ray beam shows any divergence and especially at high values of θ, where there is resolution of the $K\alpha_1$ and $K\alpha_2$ doublet. The use of an integrating camera coupled with measurements of optical density on a microdensitometer, can reduce the errors of spot size and resolution of the "doublet".

Counter techniques record individual quanta and thus enable a more accurate estimate to be made of the intensity of the diffracted beam. Geiger-Muller counters have been used for this purpose, but in recent years these have been replaced by proportional and scintillation counters. These

have lower resolving times, lower background counting rates, greater counting efficiencies and can be used in conjunction with pulse height analysers to give monochromatisation. One disadvantage of the counter methods is the time taken to collect data, but in the past few years this has been overcome by the introduction of automatic diffractometers.

The accuracy of data obtained from photographic techniques is likely to be less than that from methods involving counters. The calculation of interfilm scale factors introduces errors into the data. Also, most counter diffractometers employ a diffraction geometry which allows all the reciprocal lattice points to pass through the reflecting sphere. This avoids the need to remount, or select a new crystal to collect the full intensity data. Both photographic and counter techniques will suffer systematic errors due to physical factors such as absorption, extinction and multiple reflections.

3.2. Absorption

During the passage of an X-ray beam through a crystal, radiation is absorbed. The decrease in the intensity of an X-ray beam, dI, after passing through a thickness, dx, of a crystal is given by the equation:

$$-dI = \mu.I.dx$$

where I is the initial intensity of the X-ray beam and μ is the linear absorption coefficient for the crystal. For a finite crystal, if I_o is the intensity of the incident beam, x the path length for the beam and I is the intensity of the emergent beam, integration of the above equation gives

$$I = I_o e^{-\mu x}$$

The linear absorption coefficient is defined by the equation

$$\mu = d\Sigma\rho\mu_m$$

where d is the crystal density,

ρ is the fractional weight of each element in the crystal,

μ is the mass absorption coefficient for each element in the crystal.

A table of mass absorption coefficients is given in International Tables for X-Ray Crystallography[32]. Buerger[33] showed that the X-ray reflections with the longest path through the crystal reach their maximum intensity when the crystal diameter is $2/\mu$, and suggested that this value should be taken as the optimum thickness.

Methods for the correction of intensities for absorption have been studied for a number of ideal shapes[34]. Jeffery and Rose[35] have shown that small deviations from the exact shape can result in large errors in the corrected intensities.

3.3. Extinction

Extinction is the attenuation of the incident beam which results from Bragg reflection. The extinction which occurs in a perfect crystal is known as primary extinction. The majority of crystals however are imperfect, because of dislocations and are considered as to be made up of a large number of mosaic blocks (perfect crystals at slightly different orientations). Blocks which are close to the surface of the crystal will shield blocks of the same orientation beneath, giving rise to secondary extinction.

Primary and secondary extinction can occur together and both depend upon the intensity of the diffracted beam, the wavelength of the incident beam and the size and shape of the crystal. The effect of extinction can be reduced by the use of small crystals which have had a thermal shock, to increase the mosaicity.

No theoretical procedures have yet been produced which are completely satisfactory in the correction of extinction. International Tables for

X-Ray Crystallography[36] briefly outline a number of procedures which have been used to correct for these effects.

3.4. Multiple Reflections

The condition for Bragg reflection can occur simultaneously for more than one set of planes and thus give rise to an overestimate of the integrated intensity. The phenomenom was first studied by Renniger[37] and is most likely to occur when the reciprocal lattice points are closely spaced. Burbank[38] has shown that multiple reflection is most likely to occur, when using the "symmetrical-A setting"*, if the crystal is mounted with a symmetry axis parallel to the ϕ axis. In reflection geometrics that allow careful choice of the azithmal angle will avoid this problem. Coppens[39] has described a method for the elimination of multiple reflections on the four-circle diffractometer.

* See 12.2 for description.

4. STRUCTURE FACTORS

4.1. Atomic Scattering Factor

X-rays are scattered by extranuclear electrons in an atom. The amplitude of the scattered radiation from a free electron is independent of the angle of scattering, since the volume of an electron is insignificant in comparison with the dimensions of the wavelength of X-rays. The volume occupied by electrons in an atom however, is such that X-rays scattered from electrons in different positions in an atom, will destructively interfere with one another. This reduces the resultant amplitude of the scattered radiation. At low scattering angles the phase differences between electrons in different positions will be small, and the scattering factor will be equal to the number of electrons in the atom. For high scattering angles the phase differences are greatest, and the amplitude of the scattered radiation is lowest.

The atomic scattering factor for an atom at rest, ${}^{o}f_i$, gives a measure of the scattering power of the atom, and is the ratio of the amplitude of the radiation scattered by the atom to the amplitude scattered from an electron under the same conditions. Tables of scattering factors for different atoms and ions are given as a function of $\sin\theta/\lambda$ in International Tables for Crystallography[40].

Thermal motion possessed by atoms in a structure effectively increases their volume. This requires the modification of the theoretical scattering factors with the introduction of a temperature factor, B.

i.e. $$f_i = {}^{o}f_i \exp(-B \sin^2\theta/\lambda^2)$$

The isotropic temperature factor, B, is related to the mean-square vibrational amplitude, $\bar{u}^2$, of the atom by the equation

$$B = 8\pi^2 \bar{u}^2$$

In the later stages of refinement, anisotropic temperature factors are used for the atoms, which enables the thermal motion to be represented by an ellipsoid of vibration. In this case, the expression for the atomic scattering factor becomes

$$f_i = {}^{o}f_i.\exp-(b_{11}\,h^2 + b_{22}\,k^2 + b_{33}\,l^2 + 2b_{12}hk + 2b_{13}hl + 2b_{23}kl)$$

where b_{11}, b_{22}, b_{33}, b_{12}, b_{13} and b_{23} are constants which define the principal axes of the vibrational ellipsoid.

4.2. The Structure Factor

The structure factor, F_{hkl}, of a set of planes (hkl), is a complex quantity which requires both amplitude and phase to express it fully. The amplitude of each structure factor can be determined experimentally from the observed intensity, I_{hkl}, by means of the equation

$$I_{hkl} = K.Lp.|F_{hkl}|^2$$

where Lp is the Lorentz-polarisation factor and K is the scale factor required to bring the relative intensities to an absolute scale.

The general equation for the structure factor is

$$F_{hkl} = \sum_{j=1}^{n} f_j.\exp\left[2\pi i(hx_j + ky_j + lz_j)\right]$$

where x_j, y_j and z_j are the fractional co-ordinates (co-ordinates expressed as a fraction of the relevant cell dimension) of the atoms in a structure containing n atoms. The expression can be rewritten:

$$F_{hkl} = \sum_{j=1}^{n} f_j.\cos 2\pi(hx_j + ky_j + lz_j) + i\sum_{j=1}^{n} f_j.\sin 2\pi(hx_j + ky_j + lz_j)$$

which separates the factor into its real and imaginary parts.

In a centrosymmetric structure, the expression can be simplified to

$$F_{hkl} = 2 \sum_{j=1}^{n/2} f_j \cos 2\pi(hx_j + ky_j + lz_j)$$

the summation being taken over the atoms not related by a centre of symmetry in the unit cell. Symmetry elements other than a centre can be used to amend the general expression, which allows the structure factor to be calculated for a plane in the unit cell from the atomic positions in the asymmetric unit only.

The methods for the determination of the phases of the structure factors are discussed in Chapter 5.

4.3. The Lorentz-Polarisation Factor

As stated in 4.2 the structure amplitude is derived from the observed intensity, after the latter has been corrected for Lorentz-polarisation. This factor comprises two parts, p, the polarisation factor corrects for the polarisation of the incident unpolarised X-ray beam caused by diffraction. It is related to the Bragg angle, θ, by the equation

$$p = (1 + \cos^2 2\theta)/2$$

The Lorentz factor, L, is a geometrical correction applied to normalise the different angular velocities with which the different reciprocal lattice points pass through the sphere of reflection. The factor is a function of the diffraction geometry used in the collection of intensity data.

4.4. The Scale Factor

Lipson and Cochran[41] have stressed the importance of the use of absolute intensities in the determination of crystal structures. Wilson[42]

has described a statistical method for the determination of the scale factor, the method also gives a value for the overall isotropic temperature factor.

The method depends upon the approximation that

$$\langle |F_{hkl}|^2 \rangle = \langle \sum_{i=1}^{n} f_i^2 \rangle$$

where $\langle |F_{hkl}|^2 \rangle$ is the averaged absolute intensity

since $$I_{hkl} \alpha |F_{hkl}|^2$$

where I_{hkl} is the intensity of the hkl plane corrected for Lorentz-polarisation factors

then $$\langle I_{hkl} \rangle = K \langle |F_{hkl}|^2 \rangle$$

$$K = \frac{\langle I_{hkl} \rangle}{\langle |F_{hkl}|^2 \rangle} = \frac{\langle I_{hkl} \rangle}{\sum_{i=1}^{n} (f_i)^2} .$$

Correction of the scattering factors for thermal motion gives

$$K = \frac{\langle I_{hkl} \rangle}{\sum_{i=1}^{n} {}^{o}f_i^{\,2} \exp(-2B \sin^2\theta/\lambda^2)} ,$$

rearranging and taking logarithms the equation becomes

$$\ln \left(\frac{\langle I_{hkl} \rangle}{\sum_{i=1}^{n} {}^{o}f_i^{\,2}} \right) = \ln K - \frac{2B \sin^2\theta}{\lambda^2} .$$

A graph of $\ln \left(\frac{\langle I_{hkl} \rangle}{\sum_{i=1}^{n} {}^{o}f_i^{\,2}} \right)$ against $\sin^2\theta$ should give a straight line

of intercept $\ln K$, and gradient $-2B/\lambda^2$.

For the averaging of intensities the reciprocal lattice is divided into a number of equal zones of $\sin^2\theta$ and the averages for each zone found. Rogers[43] has recommended that, when averaging, the systematic absences should be omitted and each intensity corrected to its reduced intensity to allow for symmetry.

The Wilson method often gives a statistical scatter of points about the 'best straight line', which increases the probable error in the scale and temperature factor estimates. Rogers[44] suggests the auxiliary plot of $\ln\left(\frac{\langle I_{hkl}\rangle}{\sum_{i=1}^{n} \sigma_i^2}\right)$ against $\sin^2\theta$ where σ_i is the atomic scattering factor for the ith atom at zero theta. The auxiliary plot should be straighter than the Wilson plot and both graphs should extrapolate to the same value.

Karle and Hauptmann[45] introduced the 'K-curve' method, which gives values for the scale and temperature factors, to generate unitary structure amplitudes. Mellor[46] lists a program using this method and claims superior results to those obtained by the Wilson plot.

4.5. Tests for Centricity

Friedel's law[47] which states that hkl and $\bar{h}\bar{k}\bar{l}$ reflections have the same intensity (which is obeyed, provided that the wavelength of the X-rays does not lie near to the absorption edge of the atoms in the crystal) gives an inherent centre of symmetry to X-ray photographs. This centre of symmetry makes distinguishing between centrosymmetric and non-centrosymmetric structures difficult.

A non-centrosymmetric structure is indicated by the presence, but not precluded by the absence, of the pyro- or piezo-electric effect.

Wilson[48] has devised a statistical method for solving the problem. The method is based upon the different intensity distributions of centro- and non-centrosymmetric structures. He has shown that the ratio of the

square of the mean structure amplitude to the mean square structure amplitude should be $\pi/4$ for an acentric distribution and $2/\pi$ for a centric distribution. Frequently the result of this test is not conclusive and Howells, Phillips and Rogers[49] in 1950 devised a better statistical method in which the cumulative distribution is used. An acentric distribution is represented by the function:

$$N(z) = 1 - \exp(-z)$$

where N(z) is the proportion of the intensities which are less than or equal to the fraction, z, of the local intensity average. The function which gives the centric distribution is

$$N(z) = \mathrm{erf}(z/2)^{\frac{1}{2}}$$

where "erf" is the error function and is given by the relationship:

$$\mathrm{erf}(x) = \int_0^x e^{-a^2}\, da$$

Theoretical values of these distributions for various values of z have been tabulated[50]. The method does not allow for variations caused by the fall off in atomic scattering factors with increase in θ. Thus an intensity must always be compared with the local average to determine the appropriate z. The derivation of local intensity averages is similar to that used in the Wilson plot.

The method can be applied to both two and three dimensional data and depends upon the random distribution of atoms in the unit cell. Collin[51] and Hargreaves[52] have modified the distribution function for structures with heavy atoms in special positions. It has also been noticed[53] that other distributions occur with hypercentric structures.

5. SOLUTION OF THE PHASE PROBLEM

As stated in Section 4.2 the collection of intensity data gives a value of the structure amplitude for each plane within the crystal, but gives no information as to the value of the phase angle. The assignment of a phase angle to each amplitude can be approached in a number of ways, the route taken being governed by the type and number of atoms which constitute the unit cell.

5.1. Trial and Error Methods

A structure factor calculation, using a set of trial atomic co-ordinates, enables a direct comparison of the observed and calculated structure amplitudes. It has been found useful to express the overall agreement in terms of the mean discrepancy, usually called the 'residual',

$$R = \frac{\Sigma||F_o|-|F_c||}{\Sigma|F_o|}$$

the summation being taken over all the observed planes. The residual is a useful indication for following the refinement of a trial structure, although it does not give a quantitative measure of the accuracy. Wilson[54] has shown that for an incorrect structure of 'similar' atoms, the most probable value of the residual is 0.828 for a centrosymmetric structure and 0.586 for a non-centrosymmetric structure.

Information which may be of use in the initial stages of a structure determination, can be gained from a number of sources. Physical and spectral properties of the crystal, along with a general survey of the intensities, have all been used[55] to provide valuable indications as to the overall arrangement of the atoms. Use of these general indications with usual bond lengths and angles is, in favourable cases, able to provide enough information for a postulate of the structure to be made. This

structure, providing the value for the residual is encouraging, can be refined by one of the methods described in Chapter 6.

Recourse to these methods is usually made when the structure being determined is not over complicated. A group of atoms with known conformation (e.g. aromatic rings) if present, effectively reduces the number of trial parameters and may dominate the packing in the structure.

Success using these methods is very dependent upon the resourcefulness of the researcher, and structure determinations are now more frequently being undertaken using improved Patterson or Direct methods.

5.2. The Patterson Function and the Heavy Atom Method

Patterson[56] showed that if a Fourier summation is carried out using the phaseless $|F_{hkl}|^2$ as coefficients, the resulting synthesis reveals information of the orientation and magnitudes of interatomic vectors. The Patterson function,

$$P(u,v,w) = \frac{1}{V} \sum_{h}^{\rightarrow\infty} \sum_{k}^{\rightarrow\infty} \sum_{l}^{\rightarrow\infty} |F_{hkl}|^2 . \cos 2\pi(hu + kv + lw)$$

exhibits vectors whose distances from the origin, equal the distances between pairs of maxima in the electron density. The height of a peak in the function is proportional to the product of the scattering factors of the atoms producing the maximum. A cell containing N atoms will therefore give rise to N(N-1) Patterson peaks, other than those which coincide at the origin of the vector cell. In structures containing many light atoms, the Patterson function will generate a large number of vectors of similar height, many of which will coincide or overlap. As a result, individual interatomic vectors will be difficult to identify and the crystal structure will be insoluble by this method.

A number of sharpening procedures have been proposed[57], which enhance the amplitudes of planes with high Bragg angles. The resulting

function shows better resolution of peaks. Serious series termination effects however lead to the formation of spurious peaks, using these methods, and may make the interpretation of the function no easier.

Greatest use of the Patterson function is made when an atom of relatively high atomic number, 'heavy', is present in the structure. The structure factor can then be subdivided into heavy atom, (H), and light atom, (L) contributions,

$$F_{hkl} = f_H \exp\left[2\pi i(hx_H + ky_H + lz_H)\right] + \sum_{j=1}^{N-1} f_{Lj} \exp\left[2\pi i(hx_j + ky_j + lz_j)\right]$$

where f_H and f_{Lj} are the scattering factors of the heavy and light atoms respectively.

If f_H is very much greater than f_L, the heavy atom contribution will tend to dominate the right hand side of the equation above, except in the relatively rare cases when all the atoms scatter in phase to give a contribution greater than that of the heavy atom. In the case of a centrosymmetric crystal, the result is specially useful as the signs of a high proportion of F_{hkl} are determined solely from the heavy atom contribution. Allocating the phases so determined to the observed structure amplitudes allows an electron density synthesis to be calculated. In favourable circumstances this synthesis will reveal some, if not all, of the remaining light atoms. The fraction of structure factors having the same sign as the heavy atom contribution can be assessed using the relationships derived by Sim[58].

The basic principles of the heavy atom method, when used with non-centrosymmetric structures, are the same as those described for centrosymmetric structures. There is, however, a range of errors between the correct phases of the structure factors, and the phases as calculated from the heavy atom positions. An electron density synthesis using the

'heavy atom phases' is likely to be less well resolved than the corresponding centrosymmetric synthesis, although the positions of a number of lighter atoms may be indicated. For any specific example, the fraction of structure factors, $N(\Delta)$, for which the phase calculated from the heavy atom positions is within $\pm \Delta$ of its true value has been calculated by Sim[59].

When the right hand side of the structure factor equation is not greatly dominated by the heavy atom contribution, a higher fraction of the structure factors will have phases different from those determined from the heavy atoms. An initial electron density synthesis, based on the heavy atom phases, will therefore, be less well resolved and contain less useful information about the light atom positions. When this is the case, information about the positions of the light atoms can often be found by reverting back to a sharpened Patterson function and using the vector convergence method[60], or computing the Buerger minimum function[61].

5.3. Isomorphous Replacement Method

Data from two or more isomorphous crystals can be combined to give information about different atoms which are in corresponding positions in the two structures. The replaced atoms are usually chosen to be heavy so that the heavy atom method or the delta F^2 Patterson synthesis[62], can be used to determine the heavy atom co-ordinates. In theory, the phase problem can be solved, if two heavy atom derivatives can be obtained, by drawing Argand diagrams. This method has been applied successfully for a number of protein structures.

5.4. Direct Methods

Direct methods are so called because of their attempt to determine the phases of the structure factors without previously postulating any atomic positions.

Harker and Kasper[63] derived some inequality relationships between structure factors, using the Cauchy inequality. The relationships were applied by Gillis[64] to determine the signs of about forty structure factors for the oxalic acid dihydrate crystal. Inequality relationships appropriate to a given space group can be derived from symmetry considerations. Karle and Hauptman[65] have demonstrated that all inequalities are a consequence of the electron density function, $\rho(xyz)$, never being zero. Owing to the decreased maximum structure amplitude with increasing Bragg angle, most direct methods use normalised structure amplitudes.

Sayre[66], using one of the inequality relationships, devised a sign relationship for structure factors which can be expressed symbolically as:

$$S(h + h^1) = S(h)\, S(h^1)$$

where $S(h)$, $S(h^1)$ and $S(h + h^1)$ are the signs of the structure factors $F_{h,k,l}$, F_{h^1,k^1,l^1} and $F_{h+h^1,\ k+k^1,\ l+l^1}$ respectively. Once a few signs have been determined, the above equation can be used to generate more signs, and these, in turn, can be combined to produce even more. Providing that reflections with large normalised structure amplitudes are considered, the generated signs will probably be correct, and these large structure factors are the ones required to produce a recognisable Fourier synthesis of the structure. Probability formulae for evaluating the reliability of a sign determined using the above equation have been derived by Hauptman and Karle[67] and also by Cochran and Woolfson[68]. These methods have been used to great effect in the determination of large, light atom structures.

6. REFINEMENT OF A STRUCTURE

A "satisfactory" model proposed by use of one or more of the methods described in the previous chapter, can be refined by a number of methods if the model is sufficiently close to the true structure.

6.1. The Fourier Synthesis

The three dimensional periodicity of a crystal allows the electron density within the crystal to be represented by a Fourier series. The coefficients of the series are the structure factors. The electron density, $\rho(X,Y,Z)$, at a point in the unit cell whose co-ordinates are X, Y and Z expressed as fractions of the unit cell translations, may be evaluated as the Fourier series

$$\rho(X,Y,Z) = \frac{1}{V} \sum_h \sum_k \sum_l F_{hkl} . \exp\left[-2\pi i(hX + kY + lZ)\right]$$

where V is the volume of the unit cell. The above equation can be modified for use with two and one dimensional data, both suffer from overlap of atoms in projection, the latter far more seriously than the former.

The electron density, formed using the phases calculated from a trial model and the observed structure amplitudes, will be intermediate between the trial and true structures. The positioning of atoms to peaks of electron density will provide a better model, and successive Fourier syntheses will cause refinement towards the true structure. In non-centrosymmetric structures the n-shift rule[69] is used which speeds up the refinement. Practical methods for the summing of Fourier syntheses have been described by Buerger[70].

Refinement by "Observed Fourier" methods ceases when two successive syntheses are identical, this rarely happening at low values of the residual.

In the later stages of refinement the results of series termination effects[71] and incorrect estimates of the temperature factor and positional parameters are difficult to separate. These disadvantages may be overcome by the use of one or more of the methods following.

6.2. Difference Synthesis

Series termination effects may be removed from a Fourier refinement process by the use of $F_o - F_c$ as Fourier coefficients in a difference synthesis. Wide application of this method has been found in the location of atoms not included in the structure factor calculation. Incorrect estimates of thermal and positional parameters also give rise to characteristic features in this synthesis, although refinement of these parameters is usually achieved by least-squares methods.

6.3. Least-Squares Method

The simultaneous refinement of all the structure parameters is most effectively achieved by the method of least-squares. The method consists of the systematic variation of the atomic parameters so as to minimise the quantity $\Sigma w(|F_o|-|F_c|)^2$, where the sum is taken over all the independent structure amplitudes and w is a weighting factor. The weighting factor for a particular reflection should be taken as proportional to the reciprocal of the square of the standard deviation of the observed structure amplitude.

If $u_1, u_2, \ldots\ldots u_n$ are the n parameters to be refined, the quantity $\Sigma w(|F_o|-|F_c|)^2$, (R_1), is a minimum when, $\partial R_1/\partial u_i = 0$ where $i = 1,2,\ldots\ldots n$

Thus the condition is

$$\Sigma\, w\, \Delta\, \frac{\partial \Delta}{\partial u_i} = 0$$

where $i = 1,2,\ldots\ldots n$ and $\Delta = |F_o|-|F_c|$. The corrections, ε_i, to be applied to the values of u_i are given by the n simultaneous equations[72]:

$$\sum_{j}^{n} \epsilon_i \left(\Sigma w \frac{\partial \Delta}{\partial u_i} \cdot \frac{\partial \Delta}{\partial u_j}\right) = - \sum_{j}^{n} w\Delta \frac{\partial \Delta}{\partial u_i}$$

where $i = 1,2,.....n$

The values of $\partial\Delta/\partial u_i$ are calculated for the trial structure and are given by:

$$\frac{\partial \Delta}{\partial u_i} = - \frac{\partial |F_c|}{\partial u_i}$$

Approximations to the Least-squares method are often made in the early stages of refinement. Disregard of all but the diagonal terms allows the solutions to the normal equations to be simplified to:

$$\epsilon_i = \frac{\Sigma w\Delta \frac{\partial F_c}{\partial u_i}}{\Sigma w \left(\frac{\partial F_c}{\partial u_i}\right)^2}$$

where $i = 1,2,.....n.$

6.4. Parameter Shift Method

The methods outlined so far for the refinement of structures do not lead to convergence in unfavourable cases. These cases usually have in common heavy overlapping of atoms in projection. Fourier and least-squares methods are difficult to apply in such circumstances and, indeed, even in three dimensions where overlap is no problem the refinement process will rarely converge unless the trial co-ordinates are close to the correct positions.

A method of refinement that does not appear to be affected by heavy overlapping in projection is the "Parameter-Shift Method" which has been described by Bhuiya and Stanley[73,74]. The method has been used with success in a number of structure refinements where other refinement methods have failed.

The method uses a structure which can be defined in terms of n parameters, whose initial values u_1, u_2 ..... u_n give a value for the residual, R:

$$R(u_1,u_2,.....u_n) = \frac{\Sigma||F_o|-|F_c||}{\Sigma|F_o|}$$

In the Parameter-Shift method the first parameter is varied in steps of Δu_1 from $u_1-k\Delta u_1$ to $u_1+k\Delta u_1$, and the 2K+1 values of R are calculated for each. In the initial stages of refinement the steps, Δu_1, are quite large. The parameter is set equal to the value which gave the lowest R, the other parameters are treated, in turn, similarly. The values of the residual are calculated directly, as in a structure factor calculation and not by

$$R(u_1 + p\Delta u_1,u_2,.....u_n) = R(u_1,u_2.....u_n) + \frac{\partial R}{\partial u_1} p\Delta u_1$$

which would not be valid for the large shifts which may be used.

The advantage of this method is that it will move atoms away from false positions which give a local minimum of R whereas this is not usually the case with least-squares methods.

The time for a cycle by this method is proportional to the product of the number of increments, k, for each parameter, the number of reflections, and the number of parameters. The residual, albeit not the most desirable index to the accuracy of a structure is a good indication in the early stages of refinement.

PART 2

THE CRYSTAL STRUCTURE OF MONOCHLOROACETAMIDE

7. PRELIMINARY X-RAY WORK

7.1. Physical Properties

Chloroacetamide* was crystallised from benzene, water and water/ethanol solutions predominantly as small plates. The major face exhibited was {100}, using the axial description given below. Some long needles were obtained from the water solution, exhibiting the faces {100}, {001}, the b-axis being parallel to the needle. The high vapour pressure of the crystal, which caused total sublimation of a 0.2 x 0.3 x 0.2 mm crystal in ten days after mounting necessitated the use of crystals mounted in Lindemann glass tubes for all photographs including those used for the collection of intensity data.

7.2. X-Ray Equipment

This portion of the work was carried out using a Phillips X-Ray generator, operated at 35KV and 20 mA; nickel filtered copper radiation was used throughout. The recording device used for the measurement of the unit cell was a Leeds Weissenberg goniometer. A Nonius integrating Weissenberg goniometer was used in the collection of photographs for intensity measurement. Ilford Industrial G X-Ray film was used, being processed at 20°C with Ilford "Phen-X" developer and Ilford "Ilfofix" acid-hardening fixer.

7.3. Unit Cell Dimensions and Space Group

Oscillation, rotation and Weissenberg photographs showed the crystal to be monoclinic. Unit cell dimensions were measured for crystals obtained from water and benzene solutions, the determinations agreeing with those published by Dejace†. Inspection of photographs from benzene and water derived crystals showed them to be identical. A number of crystallisations

* B.D.H. ANALAR Grade
† See Introduction for previous determinations

from water were performed in an attempt to prepare the "Unstable Modification"†, however hOl photographs of all crystals were the same.

The unit cell dimensions were determined more accurately from sets of zero level photographs calibrated with aluminium powder lines. A least-squares refinement was used[75].

$a = 10.275_6$ Å

$b = 5.152_2$ Å

$c = 7.499_0$ Å

$\beta = 98.8_2°$

Volume = 392.3 Å^3

The following systematic absences were noted on zero and equi-inclination photographs:

hkl	-	no general absences
hOl	-	absent for l = 2n + 1
OkO	-	absent for k = 2n + 1

The space group $P2_1/c$ was therefore assigned.

7.4. Crystal Density

The crystal density was measured by floatation in benzene and iodobenzene mixtures at room temperature. The density of the liquid mixture in which the crystals remained suspended was found by use of a specific gravity bottle. The average value for the density was found to be 1.57 g cm^{-3}.

7.5. The Number of Molecules per Unit Cell

The number of molecules per unit cell is related to the density by the equation:

† See Introduction for previous determinations

$$Z = \frac{d_{meas.} \times V}{1.66 \times M}$$

where $d_{meas.}$ = the crystal density (g cm^{-3}),

V = volume of unit cell ($\mathring{A}^3$),

M = Molecular weight of chloroacetamide.

Using $d_{meas.}$ = 1.57 g cm^{-3}

V = 392.3 $\mathring{A}^3$

M = 93.5

the calculated value of Z = 3.98. Thus Z, the number of molecules per unit cell, is 4.

8. COLLECTION OF 3-D INTENSITY DATA

8.1. Optimum Crystal Size

Using the mass absorption coefficients for the atoms present in the chloroacetamide crystal the calculated value for μ, the linear absorption coefficient was calculated to be 70.0 cm^{-1}. The optimum thickness*, t, for chloroacetamide was found to be 0.28mm. All crystals used were chosen as near as possible to this optimum size and no attempt was made to correct for X-Ray absorption errors.

8.2. Integrating Weissenberg Goniometer

The action of the integrating Weissenberg goniometer was similar to that described by Wiebenga and Smits[76]. Integration was possible in two directions, rotatory (of shift 'a') and translatory (of shift 'b'). A pin wheel and eccentric, which was turned by stops at the end of the traversal through each reflection in a record, acted as the integrator control. Fourteen traversals through a record were required for the rotatory integrator to reach its original position, during this time the translatory integrator passed through 1/30th. of its total motion.

When using the integrating mechanism care was taken to start the apparatus with the translatory integrator at its maximum or minimum displacement, and to finish at a similar position. This ensured complete integration of the Weissenberg photograph. The collection of an integrated photograph therefore took an integral number of (14 x 30 x t) minutes, where t = the number of minutes for traversal through one record. For a 200° record at a rate of 100° per minute, the total time required would be an integral number of 14 hours. It was observed that the rotatory integrator sometimes remained fixed in its maximum position and hence spoiled

* See Chapter 3.2.

the photograph. The weight of the tongue attached to the camera was not enough to engage the integrating pin to the pin wheel and eccentric. A lead weight fitted to the tongue prevented this occurring.

The displacement of the integrators were determined by first taking the non-integrated photograph and measuring the maximum spot size. Integrator settings of greater than twice this spot size, in the relevant directions, produced a plateau region within each reflection. The density of the plateau was taken to be proportional to the integrated intensity.

8.3. Microdensitometer

The plateau heights of the reflections were measured using a "Joyce, Loeble & Co. Ltd. Mk.III B" double-beam recording microdensitometer. The instrument balances the density of the measured spot with an optical wedge. A pen attached to the optical wedge allowed the display of the spot density on a linear scale. Before the measurement of each reflection the pen recorder was zeroed using background intensity adjacent to the reflection. Initial experiments to test the precision of the measurements, showed poor correlation between remeasured intensities. It was thought that the plateau region was too small to be accurately traversed by the microdensitometer beam. To reduce this problem the displacement of the translatory integrator was set at its maximum to produce a streak. Traversal of this type of integrated reflection was easier and gave better correlation between remeasured intensities.

8.4. Collection of 3-Dimensional Intensity Data

Three dimensional intensity data were collected using the equi-inclination Weissenberg method[77]. To ensure that the intensity data recorded, came within the linear range of the microdensitometer, the multifilm technique was employed[31]. Thus, a pack of four films interleaved with aluminium foil (0.001 inches thick) was used for each exposure.

The integrated intensity for each reflection was measured on the microdensitometer.

Crystals were mounted about the y and z axes and two series of photographs were recorded, h0l to h4l, and hk0 to hk5. For each layer the intensity of each reflection was measured on all four films of the pack. An average film factor was determined and the average intensity for each plane calculated.

The intensity data for reflections common to different photographs, were corrected for Lorentz and polarisation factors using the graphical method devised by Cochran[78]. These corrected intensities were placed on the same arbitary scale by comparing intermediate values of $|F_{hkl}|^2$, the h0l film being taken as the arbitary reference standard. The routes by which this inter-layer scaling was achieved is shown in Figure 8.1.

8.5. Absolute Scaling and Overall Temperature Factor

The intensity data, now on an arbitary scale, were placed on an approximation to the absolute scale by the method due to Wilson[42].

The h0l zone was divided into five ranges, each containing approximately equal number of reflections. $\ln\left(\frac{\langle|F_o|^2\rangle}{\langle\sum_{i=1}^{N} {}^{o}f_i{}^2\rangle}\right)$ was calculated and plotted against the average $(\sin\theta/\lambda)^2$ for each range. The resultant plot is shown in Figure 8.2 from which the scale factor (with respect to $|F_o|^2$, $\{\equiv 1/K\}$) was found to be 1.49, and 2.8 Å^2 for the overall temperature factor, B.

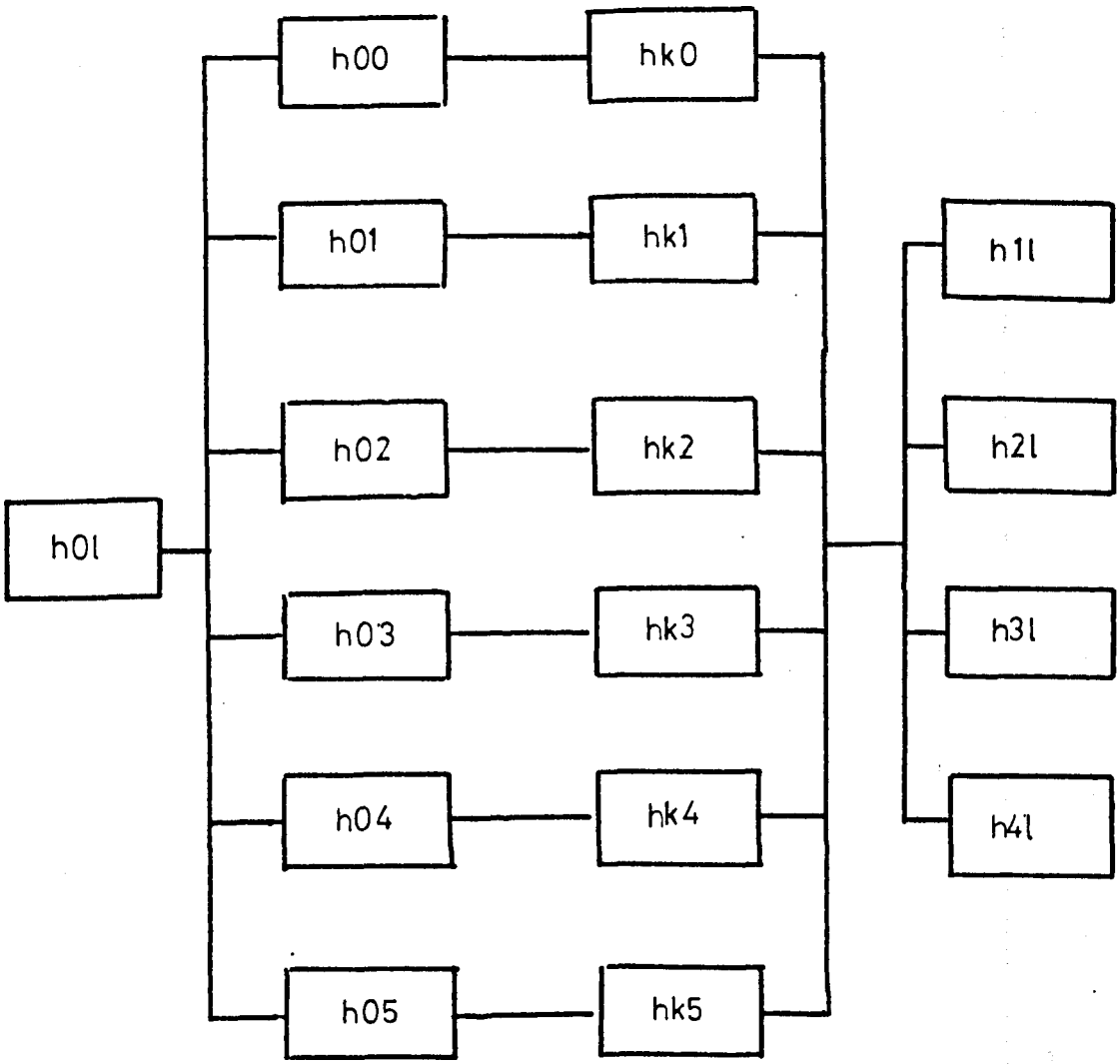

figure 8.1. Routes for Inter-film Scaling

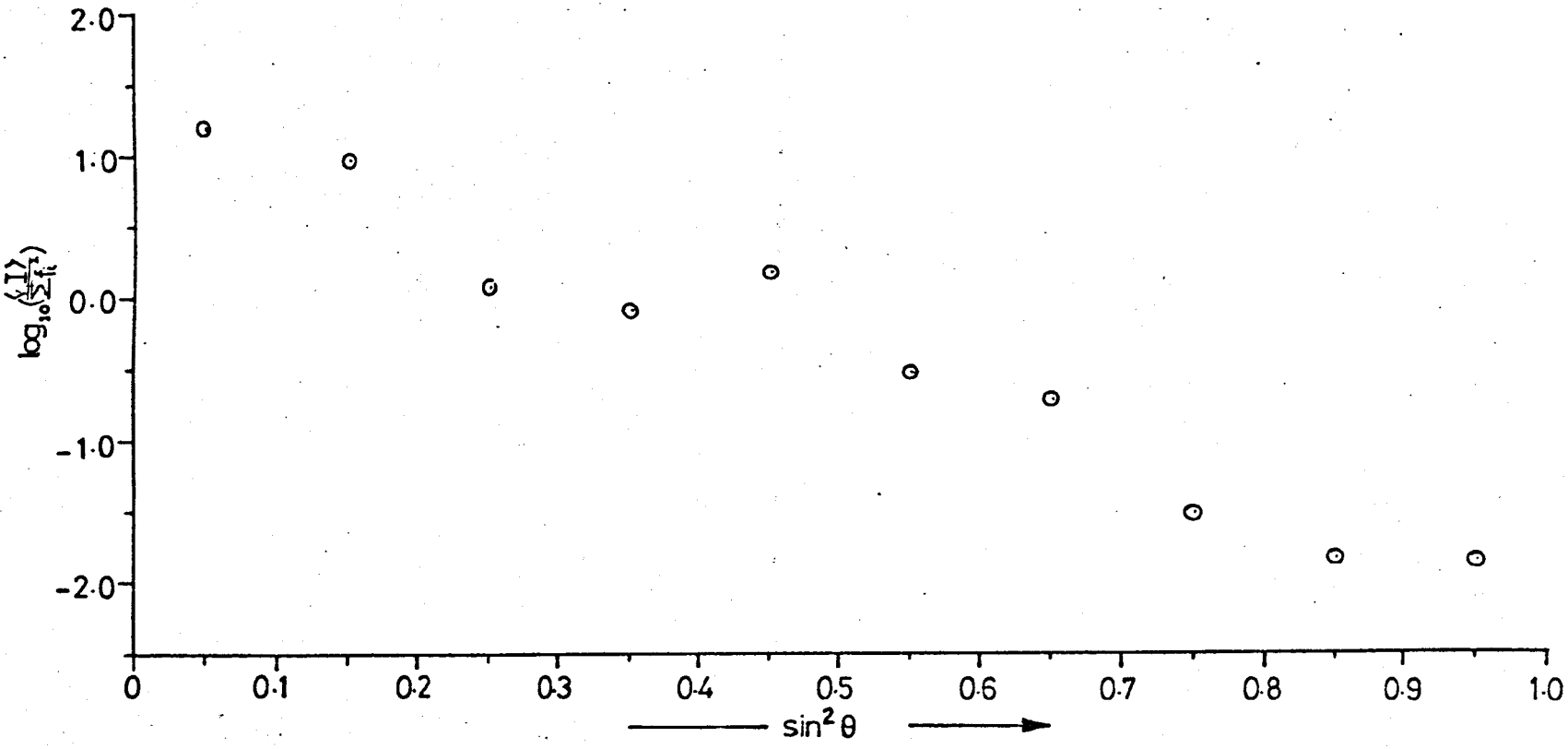

Figure 8.2. Wilson Plot of the h0l Zone

9. THE DETERMINATION AND REFINEMENT OF THE STRUCTURE

9.1. The Patterson Function

The three dimensional Patterson function was computed for one quarter of the unit cell. The volume was defined by $0.0 \leq u \leq 0.5$; $0.0 \leq v \leq 1.0$ and $0.0 \leq w \leq 0.5$ in intervals of 1/50, 1/25 and 1/40 of u, v and w respectively. The F_{hkl}^2 data were used with the inclusion of F_{ooo}^2 in the ATLAS X-Ray 63 program.

The space group $P2_1/c$, in which the amide crystallises, requires the atoms of the four molecules in the unit cell to be in the equivalent positions: (x, y, z), $(\bar{x}, \bar{y}, \bar{z})$, $(x, \frac{1}{2}-y, \frac{1}{2}+z)$ and $(\bar{x}, \frac{1}{2}+y, \frac{1}{2}-z)$. Peaks in the Patterson function which represent the chlorine-chlorine vectors will therefore be found at:

1. $\pm (2x, 2y, 2z)$
2. $\pm (2x, \overline{2y}, 2z)$
3. $\pm (0, \frac{1}{2}-2y, \frac{1}{2})$
4. $\pm (2x, \frac{1}{2}, \frac{1}{2}+2z)$

The largest peaks in the function were found on the Harker section $(u, \frac{1}{2}, w)$ and the Harker line $(0, v, \frac{1}{2})$ at $(0.24, \frac{1}{2}, 0.37)$ and $(0, 0.64, \frac{1}{2})$. The peaks $(0.24, 0.36, 0.36)$ and $(0.24, 0.64, 0.36)$ were also prominent which further indicated a chlorine position at $(0.12, 0.32, 0.185)$.

9.2. Structure Factor Calculations and Three-Dimensional Electron Density Syntheses

For the space group $P2_1/c$, the calculated structure factors are given by:[78]

$$k+l = 2n) \quad F_c = 4 \sum_{i=1}^{N} f_i \left[\cos 2\pi(hx + lz)\right] \cos 2\pi\, ky_i$$

$$k+l = 2n+1) \quad F_c = -4 \sum_{i=1}^{N} f_i \left[\sin 2\pi(hx + lz)\right] \sin 2\pi\, ky_i$$

where N is the number of atoms in the asymmetric unit.

Structure factors for the three-dimensional data were calculated using the chlorine atom position and the overall temperature factor ($3.2\ \mathring{A}^2$) obtained from the Wilson plot. The initial value of the reliability index was 0.51.

The expression for the electron density for the space group $P2_1/c$ becomes:[79]

$$\rho_{XYZ} = \frac{4}{V_c}\left\{\sum_{o}^{\infty}\sum_{o}^{\infty}\sum_{o}^{\infty}\left[\begin{matrix}k+l=2n\\ F_{hkl}\end{matrix}\cos 2\pi(hX+lZ) + F_{\bar{h}kl}\cos 2\pi(-hX+lZ)\right]\cos 2\pi kY - \sum_{o}^{\infty}\sum_{o}^{\infty}\sum_{o}^{\infty}\left[\begin{matrix}k+l=2n+1\\ F_{hkl}\end{matrix}\sin 2\pi(hX+lZ) + F_{\bar{h}kl}\sin 2\pi(-hX+lZ)\right]\sin 2\pi kY\right\}$$

The series was summed for the same quarter of the unit cell and with the same intervals as the Patterson function. The phases of the structure factor calculation were applied to the observed structure amplitudes and used as the Fourier coefficients. Atoms in the amide group were clearly resolved in the resulting electron density map. Peaks at the oxygen and nitrogen atoms were significantly different in height and allowed the oxygen atom to be assigned trans to the chlorine atom. The methylene carbon atom was not as well formed as the other peaks although a definite centre was found which gave a reasonable model.

The co-ordinates of the model were used for a further structure factor calculation (R = 0.29). Two cycles of successive Fourier syntheses and structure factor calculation resulted in a reduction of the reliability index to 0.27. A Fourier synthesis from the final structure factor calculation gave peaks in the electron density map which were coincident with the atoms of the model. The atomic co-ordinates at this stage of

the refinement are listed in Table 9.1, and agreed well with those found by Dejace.

Atom	x/a	y/b	z/c
Cl	0.1120	0.3201	0.1751
C1	0.1915	0.0000	0.1580
C2	0.3210	0.0208	0.0895
$\bar{O}$	0.3660	0.8125	0.0562
N	0.3875	0.2300	0.0790

TABLE 9.1

Fractional Co-ordinates after Fourier Refinement

The refinement was continued using ORFLS, a full matrix least-squares program. One cycle of least-squares refinement varying all the positional parameters and an overall temperature factor (R = 0.21), followed by two cycles with individual atom isotropic temperature factors reduced the residual to 0.178. A three dimensional difference synthesis showed anisotropy of the chlorine atom. Two cycles, using ORFLS, with the chlorine atom refining anisotropically gave R = 0.137. A further two cycles with all the atoms refining anisotropically (R = 0.126) gave a maximum of 0.1 as the ratio of the parameter change to its associated standard deviation.

In the former least-squares refinement unit weights were applied to all the observations. An analysis of the distribution of $(|F_o|-|F_c|)$ with F_o and $\sin\theta$ indicated that a different weighting scheme would be more suitable. The analysis, with respect to $\sin\theta$ showed an even distribution of $(|F_o|-|F_c|)^2$, Δ^2, over the whole range. With respect to F_o the largest Δ^2 were found with weak and very intense reflections. A weighting scheme

available with ORFLS, "The University of Washington Scheme", applies a weighting function

$$W = |Q1/(J)|^2$$

where Q1 is a constant and W is the weight applied by the program. (J) is whichever of the three functions SIGMA, $Q2|F_o| + Q3$ and $Q4|F_o|_{min} + Q5$ is a maximum. SIGMA is the standard deviation of the structure amplitude $|F_o|$ and $|F_o|_{min}$ is the minimum observable structure amplitude; Q2, Q3, Q4 and Q5 are constants.

The values used in the new weighting scheme were:

Q1 = 1.1

Q2 = 0.1

Q3 = -2.5

Q4 = 0.0

Q5 = 1.1

the majority of observations using this scheme had weights which were inversely proportional to the square of the standard deviation of the observed structure amplitude.

When the weighting function was used in two cycles of least-squares refinement, the parameters of the methylene carbon atom changed most, the x co-ordinate by 0.3 of its standard deviation. The value of the residual did not change and, as all the parameters were changing by less than 0.1 of their associated standard deviations, the refinement of the heavier atoms was assumed to have ceased.

A three dimensional weighted difference synthesis was computed for the quarter of the unit cell previously defined. Three significant, well resolved peaks were found which corresponded closely to the expected hydrogen atom positions of the amide group and one of the methylene group. The position expected for the remaining methylene hydrogen atom showed a

broad ridge of electron density in the ab plane. A composite map showing the peaks is given in Figure 9.1.

The three well resolved hydrogen atoms were included in the model and were given the isotropic temperature factors of the atoms to which they were bonded. Two cycles of least-squares refinement reduced the residual to 0.105, without the refinement of any of the hydrogen atom parameters. A three dimensional difference synthesis, in the region of the remaining hydrogen atom showed no further resolution. A hydrogen atom bonded tetrahedrally to the methylene carbon atom, with a bond length of 1.07Å, was generated using the program BONDAT of the X-RAY 63 system. The inclusion of this atom, and a modification of the hydrogen atoms to have the anisotropic temperature factors of the atom to which they were bonded gave R = 0.104. After two cycles of least-squares all the parameter changes were below 0.05 of their respective standard deviations.

A three dimensional difference synthesis showed no significant features in the regions of the atomic centres and it was concluded that the limit of refinement had been reached. The final values of the atomic co-ordinates are given in Table 9.2 and the vibrational parameters of the heavier atoms in Table 9.3. The standard deviations for the positional and vibrational parameters, as output by ORFLS on the last cycle, are given in Table 9.4 and Table 9.5 respectively. A list of the observed and calculated structure factors is shown in Appendix II.

FIGURE 9.1. Composite Difference Fourier Synthesis Projected onto 010

Contour lines are drawn at intervals of 0.1 e $\mathring{A}^{-3}$, starting at 0.1 e $\mathring{A}^{-3}$

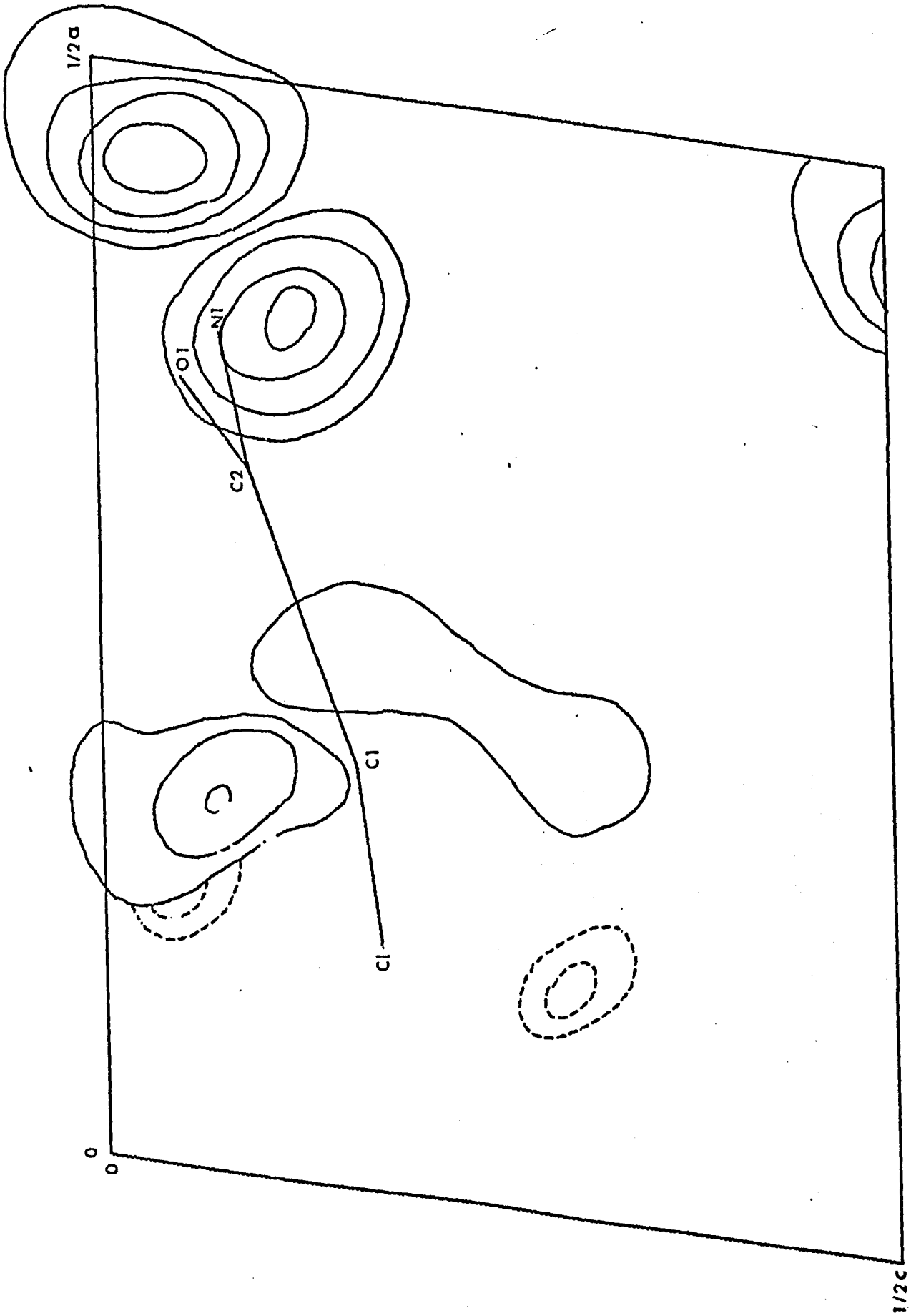

Atom	x/a	y/b	z/c
Cl1	.11245	.31685	.17435
C1	.18847	.00259	.16172
C2	.32049	.01111	.09556
O1	.36212	.79653	.05512
N1	.38111	.23030	.07945
H1	.20830	-.04166	.29791
H2	.16250	-.16667	.06458
H3	.45833	.21040	.03541
H4	.38750	.39583	.16041

TABLE 9.2.

Final Atomic Co-ordinates.

Atom	U_{11}	U_{22}	U_{33}	U_{12}	U_{13}	U_{23}
Cl1	.037805	.040478	.051137	.008503	.022195	.001729
C1	.037914	.039320	.047226	-.007562	.022143	-.003197
C2	.041338	.032198	.036465	.008115	.014430	.001294
O1	.047542	.036720	.072817	.002477	.023303	.000594
N1	.050686	.025542	.057753	-.005126	.029427	-.004757

TABLE 9.3.

Final Vibrational Parameters.

Atom	$\sigma(x/a)$	$\sigma(y/b)$	$\sigma(z/c)$
C11	.00019	.00041	.00028
C1	.00039	.00082	.00059
C2	.00040	.00081	.00055
O1	.00031	.00058	.00045
N1	.00035	.00059	.00050

TABLE 9.4.

Estimated Standard Deviations of Atomic Co-ordinates.

Atom	$\sigma(U_{11})$	$\sigma(U_{22})$	$\sigma(U_{33})$	$\sigma(U_{12})$	$\sigma(U_{13})$	$\sigma(U_{23})$
C11	0.00134	0.00126	0.00161	0.00119	0.00110	0.00128
C1	0.00542	0.00497	0.00582	0.00489	0.00496	0.00548
C2	0.00521	0.00437	0.00527	0.00449	0.00427	0.00441
O1	0.00429	0.00360	0.00547	0.00381	0.00393	0.00409
N1	0.00524	0.00389	0.00586	0.00373	0.00458	0.00389

TABLE 9.5

Estimated Standard Deviations of the Thermal Parameters.

10. DESCRIPTION OF THE STRUCTURE

10.1. Molecular Dimensions

The fractional monoclinic co-ordinates (x/a, y/b, z/c) given in Table 9.2 were converted to orthogonal angstrom co-ordinates (x_o, y_o, z_o) with respect to the axes x, y, z´ by the matrix transformation[80]:

$$\begin{vmatrix} x_o \\ y_o \\ z_o \end{vmatrix} = \begin{vmatrix} a & 0 & c\cos\beta \\ 0 & b & 0 \\ 0 & 0 & c\sin\beta \end{vmatrix} \begin{vmatrix} x/a \\ y/b \\ z/c \end{vmatrix}$$

Bond lengths, AB, were calculated from the orthogonal co-ordinates of the atoms A and B using the equation

$$AB^2 = \Delta x_o^{\,2} + \Delta y_o^{\,2} + \Delta z_o^{\,2}$$

where $\Delta x_o = x_o(A) - x_o(B)$ etc.

The standard deviation of a bond length is given by[81]

$$\sigma^2(AB) = \frac{\Delta x_o^{\,2}.\sigma^2(\Delta x_o) + \Delta y_o^{\,2}.\sigma^2(\Delta y_o) + \Delta z_o^{\,2}\,\sigma^2(\Delta z_o)}{AB^2}$$

The bond lengths and standard deviations calculated using the above equations are shown in Table 10.1.

Bond angles between atoms were calculated using the cosine rule, and their estimated standard deviations were calculated using the equation[82]

$$\sigma^2(\cos A\hat{B}C) = \left(\frac{AC}{AB.BC}\right)^2 \sigma^2(AC) + \left(\frac{BC^2-AB^2-AC^2}{2.AB^2.BC}\right)^2 \sigma^2(AB) + \left(\frac{AB^2-AC^2-BC^2}{2.AB.BC^2}\right)^2 \sigma^2(BC)$$

Bond (AB)	Length (AB) (Å)	σ (AB) (Å)	Bond (AB)	Length (AB) (Å)	σ (AB) (Å)
Cl-C(1)	1.806	.005	C(1)-C(2)	1.515	0.009
C(2)-O	1.240	.008	C(2)-N	1.304	0.008
*C(1)-H(1)	1.07	-	C(1)-H(2)	1.10	-
N-H(3)	0.91	-	N-H(4)	0.91	-

(* Atom H(1) was generated as indicated in Chapter 9)

TABLE 10.1

Bond Lengths and Standard Deviations

Angle (ABC)	Bond Angle (ABC)	σ (ABC)
Cl-C(1)-C(2)	114.0°	0.5°
C(1)-C(2)-O	114.5°	0.6°
C(1)-C(2)-N	121.3°	0.6°
O-C(2)-N	124.2°	0.6°

TABLE 10.2

Bond Angles and Standard Deviations

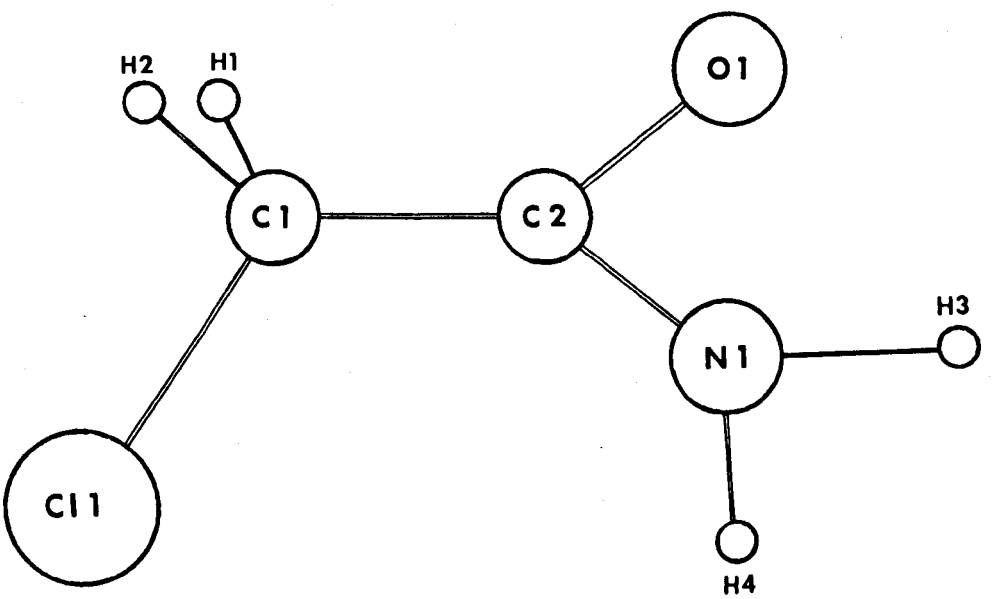

Table 10.2 shows the bond angles and estimated standard deviations for the chloroacetamide molecule.

The equations for the best planes through a selected number of atoms were calculated from the orthogonal co-ordinates by the least-squares method. The form of the perpendicular equation for a plane is[83]

$$lx_o + my_o + nz_o = p$$

where p is the perpendicular distance of the plane from the origin, and l, m and n are the direction cosines between the perpendicular and the positive directions of the x, y and z axes respectively. The least-squares plane through the N points (x_i, y_i, z_i), with respect to the orthogonal axes is given by the solution of the equations[84]

$$\sum_{i=1}^{N} x_i (lx_i + my_i + nz_i - p) = 0$$

$$\sum_{i=1}^{N} y_i (lx_i + my_i + nz_i - p) = 0$$

$$\sum_{i=1}^{N} z_i (lx_i + my_i + nz_i - p) = 0$$

$$l^2 + m^2 + n^2 = 1$$

The equation of the best plane through the carbo-amide group was calculated to be:

$$0.33214\ x_o - 0.10052\ y_o + 0.93786\ z_o = 1.70650$$

Within the limits of this determination the carbo-amide group is planar, the amide carbon atom shows the maximum displacement from the plane (0.009Å). The chlorine atom is displaced by -0.34Å from the carbo-amide plane, corresponding to a rotation of 11.9° about the carbon-carbon bond. The chlorine atom was trans to the oxygen atom.

10.2. The Crystal Structure

Monochloroacetamide has a crystal structure similar to many primary amides, forming centrosymmetrically related hydrogen bonded pairs (dimers). These dimers are further hydrogen bonded to axis related dimers, producing ribbons of associated molecules parallel to the b axis. The maximum number of hydrogen bonds is achieved. Neighbouring molecular ribbons, related by the screw axis, give parallel hydrogen bonded systems.

Projections of the final structure onto 010 and 001 are given in Figure 10.2 and Figure 10.3 respectively. Stereoscopic views of the structure are shown in Figure 10.4.

The equation of the least-squares plane through the centrosymmetrically related amide groups was calculated to be:

$$0.33313x_o - 0.10036y_o + 0.93752z_o = 1.71164$$

which, within the limits of the determination is coplanar with the carboamide plane. The plane makes an angle of 1.4° with the amide group of the asymmetric unit.

Table 10.3 summarises the geometry of the hydrogen bonds.

Bond	(Å) N - H	(Å) N ..... O	C - $\hat{O}$ ... N	N - $\hat{H}$ ... O
Across the centre of symmetry	0.91	2.97	119.3°	174.1°
Parallel to the b axis	0.91	2.93	148.2°	146.7

TABLE 10.3

The Hydrogen Bonding

One of the hydrogen bonds (N - H3 ... O) is nearly linear while the axis translation hydrogen bond deviates by more than 30° from linearity.

FIGURE 10.2. Structure Projected onto 010

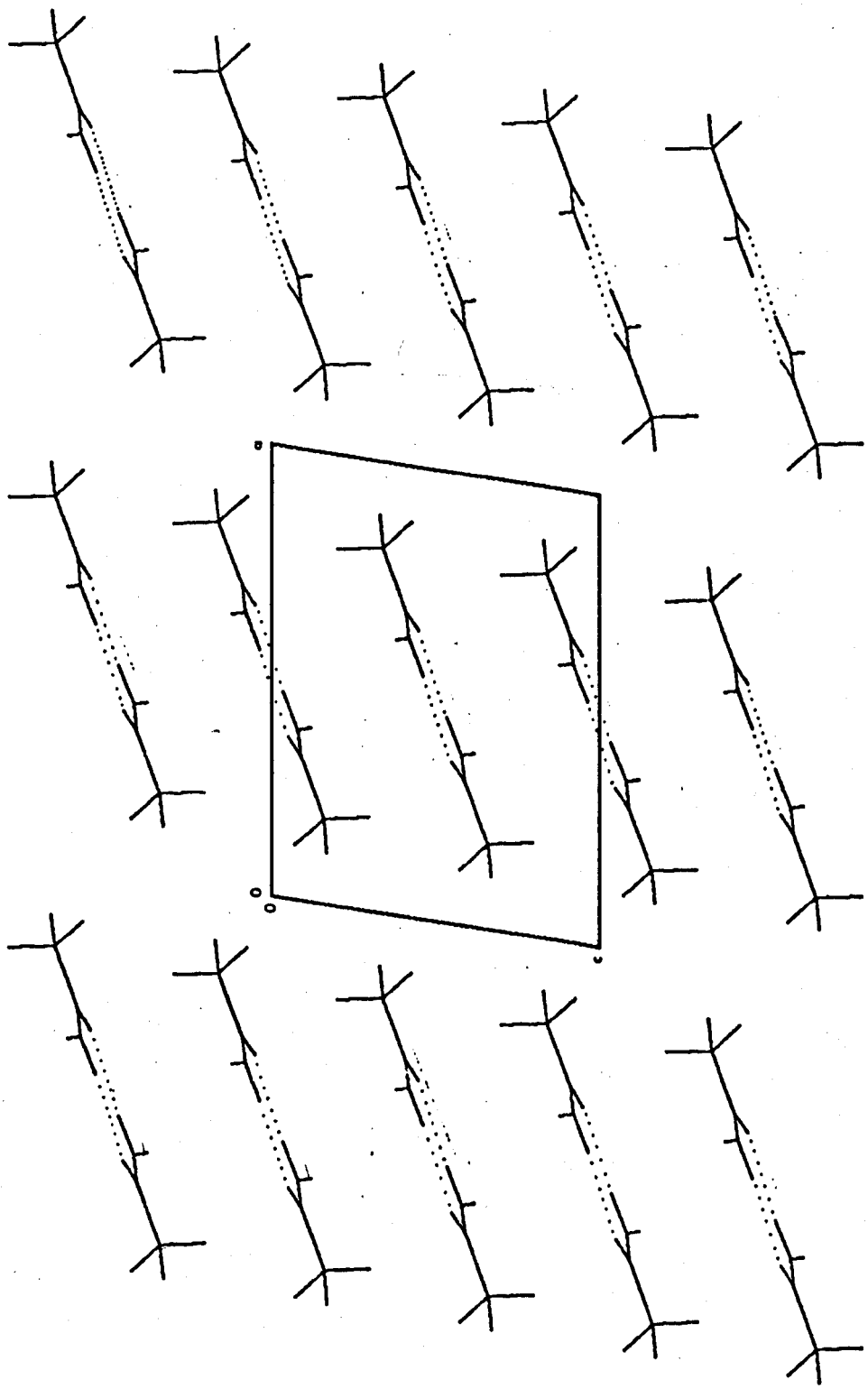

FIGURE 10.3. Structure Projected onto 001

(c glide related molecules have been omitted for clarity)

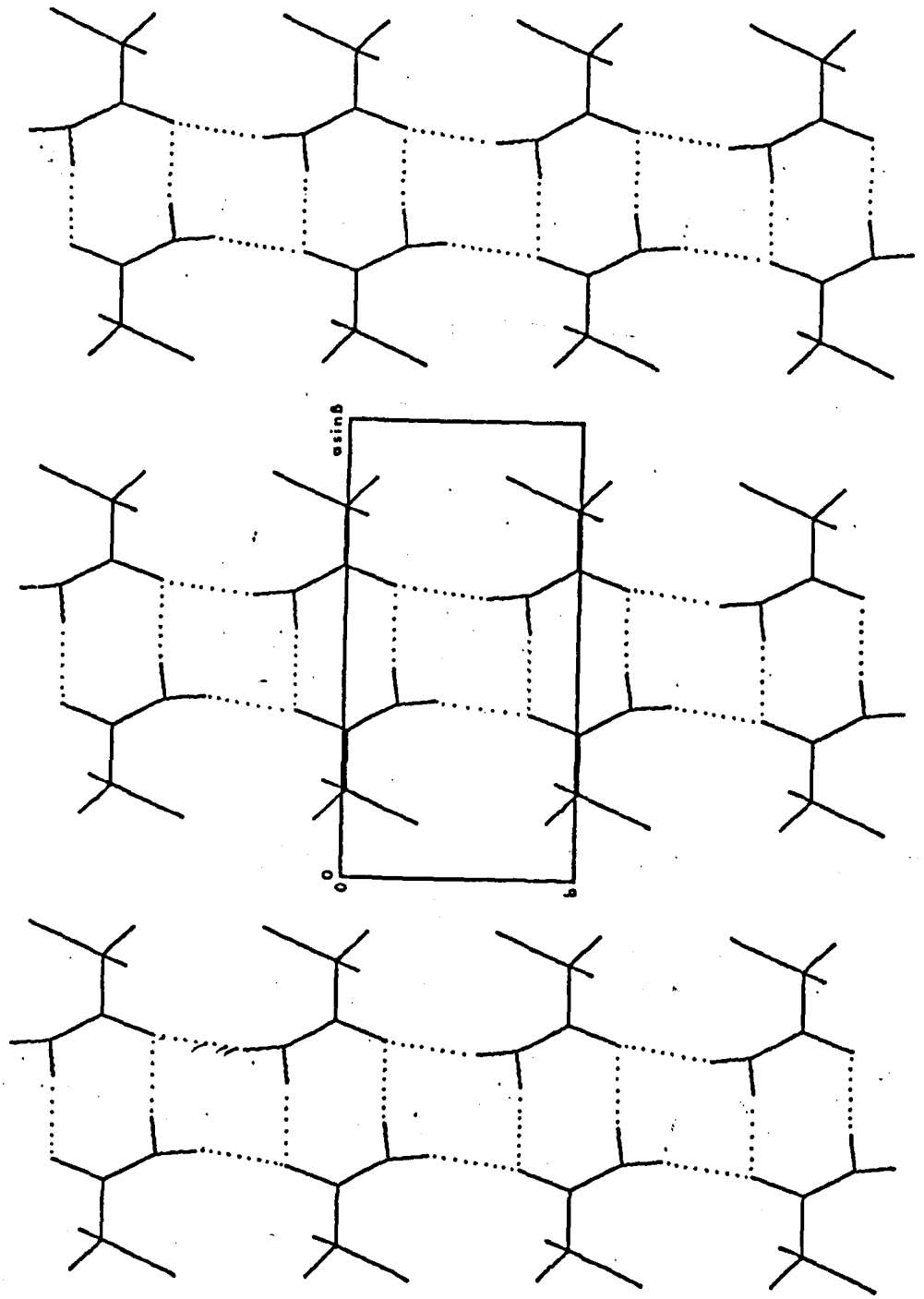

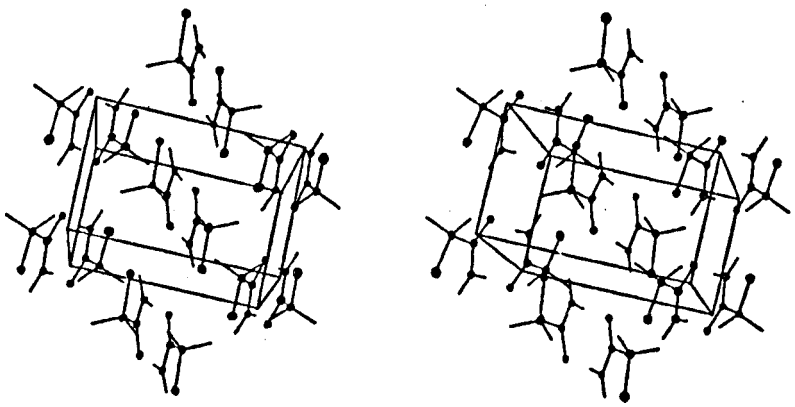

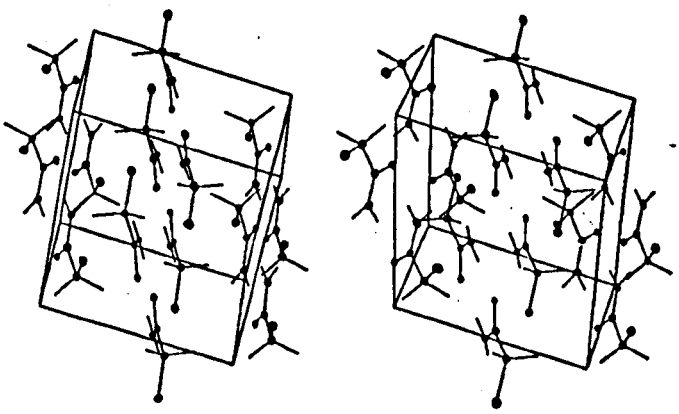

FIGURE 10.4. Stereoscopic views.

Donohue[85] has suggested that 30° is the maximum bend a hydrogen bond should exhibit.

There are no abnormally short contact distances between atoms in any of the equivalent positions. The closest approach to a Van der Waals contact, other than those involving the chlorine atoms, is 2.79 Å (between H1 and H2 of glide related molecules). The chlorine atoms only approach Van der Waals distances between themselves, the distances are shown in Table 10.4.

Symmetry Operation	Contact Distance
Centre of Symmetry	3.72 Å
Glide plane	3.81 Å
Screw axis	3.75 Å

TABLE 10.4

Contact Distances between Chlorine Atoms

10.3. Comparison with related Compounds

The crystal structures of a large number of primary amides have been determined. The carbo-amide group dimensions of a number of these analyses are shown in Table 10.5 for comparative purposes.

Carbon-nitrogen and carbon-oxygen bond lengths in these related structures generally fall into the ranges 1.31 - 1.33 Å and 1.24 - 1.25 Å respectively. The carbon-nitrogen bond length in chloroacetamide is below the usual range, but the difference is not significant. In most of the structures, however, a short carbon-nitrogen bond is associated with a long carbon-oxygen bond; attributable to increased and decreased double bond character respectively. The carbon-oxygen bond in this determination is also lower than the mean.

TABLE 10.5

Comparison of Amide Groups

Compound	C-C(Å)	C-N(Å)	C-O(Å)	C-C-O(°)	C-C-N(°)	O-C-N(°)	Ref.
Acetamide (rhombohedral)	1.530 (0.005)	1.338 (0.007)	1.258 (0.006)	120.7 (0.5)	116.7 (0.5)	122.6 (0.5)	4
Acetamide (orthorhombic)	1.505 (0.013)	1.334 (0.017)	1.260 (0.011)	119.6 (1.1)	117.2 (1.5)	123.1 (0.5)	3
Adipamide	1.49 (0.01)	1.33 (0.01)	1.23 (0.01)	121 -	115.5 -	123 -	5
6-amido-3-pyridazone	1.46 (∿0.014)	1.33 (∿0.014)	1.25 (∿0.014)	119 -	118 -	123 -	86
Ammonium Oxamate	1.564 (0.002)	1.324 (0.002)	1.248 (0.002)	120.2 (0.2)	115.5 (0.2)	124.2 (0.3)	87
Benzamide	1.501 (0.004)	1.342 (0.003)	1.249 (0.003)	120.5 (0.2)	117.5 (0.2)	122.1 (0.2)	10
N-N diphenyl acetamide	1.502 (0.003)	1.336 (0.003)	1.217 (0.003)	121.7 (0.2)	117.2 (0.2)	121.0 (0.2)	88
Ethyl Carbamate	- -	1.345 (0.003)	1.221 (0.003)	- -	- -	124.7 (0.3)	14

Table 10.5 continued

Compound	C-C(Å)	C-N(Å)
Ammonium Carbamate	- -	1.361 (0.005)
Glutaramide	1.52 (0.01)	1.34 (0.01)
m-Hydroxybenzamide	1.501 (0.020)	1.302 (0.018)
Terephthalimide	1.494 (0.005)	1.309 (0.006)
o-Nitrobenzamide	1.503 (0.008)	1.339 (0.008)
Dilactylamide	1.515 (0.004)	1.314 (0.005)
Nicotinamide	1.524 (0.017)	1.336 (0.019)
Oxamide	1.542 (0.006)	1.315 (0.004)

C-O(Å)	C-C-O(°)	C-C-N(°)	O-C-N(°)	Ref.
1.289	-	-	118.7	89
(0.005)	-	-	(0.3)	
1.22	121	117	122	90
(0.01)	-	-	-	
1.247	119.0	116.6	124.4	91
(0.016)	-	-	-	
1.257	119.8	118.0	122.2	92
(0.006)	(0.7)	(0.7)	(0.9)	
1.225	116	121.4	122.3	93
(0.008)	-	-	-	
1.240	119.2	117.6	123.2	94
(0.003)	(0.3)	(0.2)	(0.3)	
1.217	118.2	116.8	125.0	7
(0.014)	-	-	-	
1.243	119.5	114.8	125.7	95
(0.004)	(0.3)	(0.3)	(0.3)	

Table 10.5 Continued

Compound	C-C(Å)	C-N(Å)
Picolinamide	1.515 (0.008)	1.330 (0.007)
α-pyrazinamide	1.503 (0.008)	1.312 (0.008)
Sorbamide	1.478 (0.002)	1.343 (0.002)
Suberamide	1.522 (0.01)	1.322 (0.01)
Succinamide	1.512 (0.002)	1.333 (0.002)
Monofluoroacetamide	1.533 (0.005)	1.319 (0.005)
Difluoroacetamide	1.543 (0.007)	1.334 (0.008)
Monochloroacetamide	1.48 -	1.33 -
Monochloroacetamide	1.515	1.304

C-O(Å)	C-C-O(°)	C-C-N(°)	O-C-N(°)	Ref.
1.241 (0.007)	119.5 (0.5)	115.5 (0.5)	125.0 (0.5)	96
1.244 (0.008)	119.1 (0.6)	117.5 (0.6)	123.1 (0.6)	97
1.261 (0.002)	122.4 (0.18)	115.9 (0.18)	121.7 (0.18)	98
1.248 (0.01)	120.5 -	116.5 -	123.0 -	99
1.238 (0.002)	122.4 (0.2)	115.6 (0.2)	122.0 (0.2)	16
1.254 (0.005)	117.3 (0.4)	118.7 (0.4)	124.0 (0.4)	13
1.247 (0.008)	118.0 (0.5)	115.2 (0.5)	126.7 (0.4)	100
1.23 -	110.8 -	119.1 -	130.1 -	11
1.240	114.5	121.3	124.2	-

Of the compounds in Table 10.4 only the aromatic primary amides show similar trends (m-hydroxybenzamide in particular). In aromatic amides the bond lengths are short because of the effects of conjugation between the benzene ring and the amide group, resulting in resonance stabilisation. Chloroacetamide also has a short carbon-carbon bond similar to the aromatic amides, although formally the methylene carbon atom is $\underline{sp}^3$ hybridised compared with $\underline{sp}^2$ of the aromatic carbon. This shortening could be explained if the methylene carbon bonding orbital (to the amide group) had increased $\underline{s}$ character, which could be seen as a result of hyperconjugation.

Most of the hydrogen bonding systems shown by primary amides, show nitrogen-oxygen distances across the dimer to be shorter than that of the glide plane-, screw axis- or translation related hydrogen bonds. In chloroacetamide the opposite is true, albeit marginally so. The angle, nitrogen-hydrogen-oxygen, of 145° deviates too far from linearity, and the strength of the hydrogen bond between $\underline{b}$ axis related molecules will be significantly less than that across the dimer, with an angle of 175°.

PART 3

THE CRYSTAL STRUCTURE OF BENZANILIDE

11. PRELIMINARY X-RAY WORK

11.1. Physical Properties

A sample of N-benzoylaniline (benzanilide) was prepared by the benzoylation of aniline with benzoyl chloride in benzene solution. Crystals suitable for examination were obtained by recrystallisation from an aqueous solution of ethyl alcohol. Prism crystals were found exhibiting the general faces {100}, {001} and {011}. Elongation of the crystals was sometimes observed parallel to the b-axis. An elemental analysis of the crystals followed by an Infra-Red spectrum confirmed the crystals to be of benzanilide.

11.2. X-Ray Equipment

Studies of the unit cell and space group were carried out using a Leeds Weissenberg goniometer. Nickel filtered copper radiation, from a Phillips 1009/30 X-ray generator was used throughout. Ilford "Industrial G" X-ray film was used, and was processed at 20°C with Ilford "Phen-X" developer and Ilford "Ilfofix" acid hardening fixer.

11.3. Unit Cell Dimensions and Space Group

Oscillation, rotation and Weissenberg photographs showed the crystal to be monoclinic. Unit cell dimensions were measured from zero level Weissenberg photographs about the b and c axes. The interaxial angles were calculated by the method of triangulation.

The following systematic absences were noticed on zero, first and second order Weissenberg photographs:

hkl - absent for $h + k + l = 2n + 1$
h0l - absent for $h = 2n + 1$; $(l = 2n + 1)$
0k0 - absent for $(k = 2n + 1)$

The conditions enclosed in parentheses arise as a consequence of the

first condition. The first condition results from a unit cell which is body centred and the second condition shows that there is an axial glide plane (Ø1Ø) with a glide component of c/2. The space group was therefore be either Ia or I2/a.

11.4. Determination of Accurate Cell Dimensions

Corrected cell dimensions were obtained from measurements using the three circle diffractometer* used to collect the intensity data. A method devised by Bond[101] was employed to correct the "Bragg 2θ" measurements for each plane. Families of planes, having the same direction cosines for their normals (hence producing a row in the reciprocal lattice) were considered together. The value of θ, observed for each reflection, was used in an extrapolation method[102] to eliminate zero-errors in the value of θ and errors resulting from mis-setting the φ circle.

For each set of planes the φ and χ circles were set to bring the reciprocal lattice row into the equatorial plane. The various orders of diffraction were located using the θ and 2θ-circles only.

If θ_o is the observed value for θ for a particular plane and α is the zero error, then the actual value of θ, θ_t, is given by the equation:

$$\theta_t = \theta_o + \alpha$$

The observed spacing for the planes is given by the Bragg equation:

$$d_o = n\lambda/2 \sin \theta_o$$

and the actual spacing, d_t, by

$$d_t = n\lambda/2 \sin(\theta_o + \alpha)$$

* See Chapter 12 for description

Thus,
$$\frac{d_o}{d_t} = \frac{\sin(\theta_o + \alpha)}{\sin \theta_o}$$

if α is small the equation can be rewritten in the form

$$d_o = d_t + \alpha d_t \cot\theta_o$$

Thus, for a set of planes, a graph of d_o against $\cot\theta_o$ should give a straight line of intercept d_t and gradient αd_t. Graphs were plotted for the 00l, 0k0, h00, 0kk, $h0\bar{h}$, hh0 and hhh sets of reflections and the values of α were used to correct the values of θ_o.

The corrected θ values were then used as data to a computer program written by Bracher[75] to refine the unit cell dimensions by the method of least-squares.

The final unit cell dimensions given by the program were

$a = 23.3834 \pm 0.0030$ Å

$b = 5.3345 \pm 0.0025$ Å

$c = 8.0270 \pm 0.0070$ Å

$\beta = 91.993 \pm 0.083^\circ$

Unit Cell Volume = 1000.67 Å^3

11.5. Measurement of Crystal Density

The density of benzanilide crystals was found by floatation in mixtures of benzene and iodobenzene. The average density was found to be 1.326 g cm^{-3}.

11.6. Number of Molecules in the Unit Cell

Using the expression given in Chapter 7, the number of molecules in the unit cell was calculated to be 3.998.

12. COLLECTION OF 3-D INTENSITY DATA

12.1. 4-Circle Diffractometer

Small and Travers[103] have constructed a semi-automatic diffractometer which is based upon the geometry of a counter diffractometer system described by Furnace and Harker[104], the nomenclature being that of Arndt and Phillips[105].

The system was the normal beam equatorial method, the detector and incident beam being in the equatorial plane. The θ and 2θ circles are also in the equatorial plane and rotate about the ω axis which is perpendicular to this plane. The χ-circle is mounted vertically on the θ-circle with its axis perpendicular to the ω-axis. A standard goniometer head, which holds the crystal rotates about the ϕ axis, which is attached to the χ-circle. The ϕ circle moves about the χ-circle by means of a manually operated worm and wheel. The proportional counter is mounted on the 2θ-circle, and can be moved independently of the θ-circle. A detector collimator reduces the amount of background radiation received and the detector is also shielded by a lead screen. A schematic diagram of the apparatus is shown in Figure 12.1.

Rotation of the θ-circle is achieved by a motor at the base of the diffractometer. The motor rotates the θ-circle in steps of $1\frac{1}{2}'$. The timing between the steps is governed by a signal generator, which outputs a square wave of frequency 600 Hz. Accumulation of 1000 pulses from the signal generator, by the control unit, causes the suspension of counting at the proportional counter and activates a magnetic clutch. An angular rotation of the θ-circle through $1\frac{1}{2}'$ operates a microswitch which deactivates the magnetic clutch, switches on the proportional counter and recommences the timing of pulses from the generator.

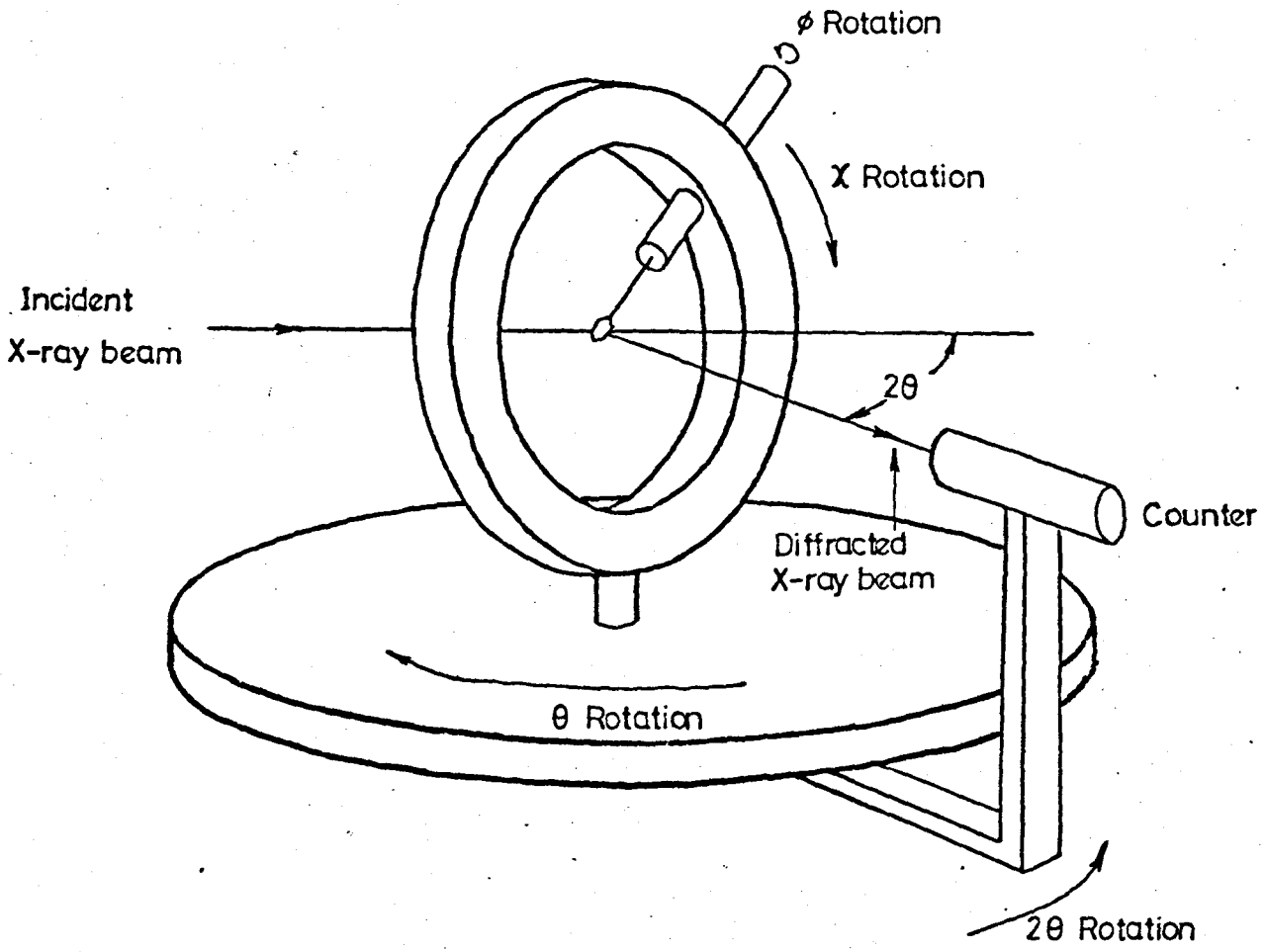

figure 12.1. Schematic diagram of the four circle diffractometer

12.2. Collection of 3-D Intensity Data

A crystal of benzanilide was mounted with its b axis coincident with the ϕ axis of the diffractometer. Alignment of the crystal on the goniometer axis was done initially by eye and more accurately by observing the count maxima for the 0k0 reflections. With the unique b axis parallel to the ϕ axis of the diffractometer, the χ angle required to bring the 0k0 reciprocal lattice points into the equatorial plane was 90°, in this position only the θ- and 2θ- values need be set to observe the reflection. A method similar to that of "double oscillation" was used to correct the setting of the goniometer axis. The crystal was considered properly aligned when rotation of the ϕ axis, with the θ- and 2θ- circles set to the calculated values for the particular reflection, produced the minimum difference in the diffracted beam counting rate at the detector.

A computer program was written by the author which calculated the setting values for the θ-, 2θ-, χ and ϕ circles for the unique set of reflections. The symmetrical-A setting was employed[106], in which the χ-circle plane is symmetrical with respect to the incident and diffracted beams and contains the scattering vector at the reflecting position. How the angular settings bring a reciprocal lattice point to the reflecting position on the surface of the Ewald Sphere is shown in Figures 12.2 and 12.3. Figure 12.2 shows the Ewald sphere and a smaller sphere (drawn through the reciprocal lattice point P) with its centre at the origin of the reciprocal lattice. A ϕ rotation brings P to position Q in the χ plane, and a χ rotation moves it to position R in the equatorial plane. Figure 12.3 is a plan view of the equatorial plane. The reciprocal lattice point, now at R, is brought to the surface of the Ewald sphere by rotating about the ω-axis through the angle θ, the detector being positioned at 2θ to receive the diffracted beam.

The method used to collect the intensities could have been any of the

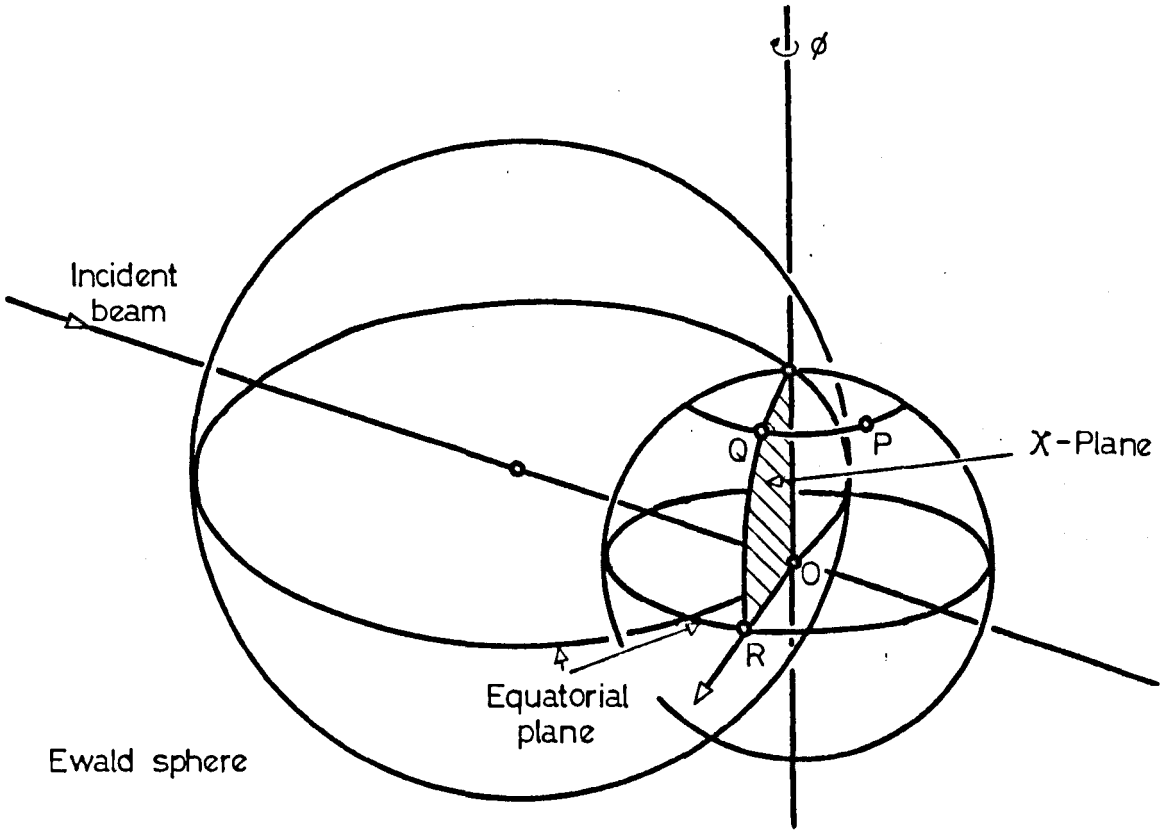

FIGURE 12.2 NORMAL BEAM EQUATORIAL GEOMETRY

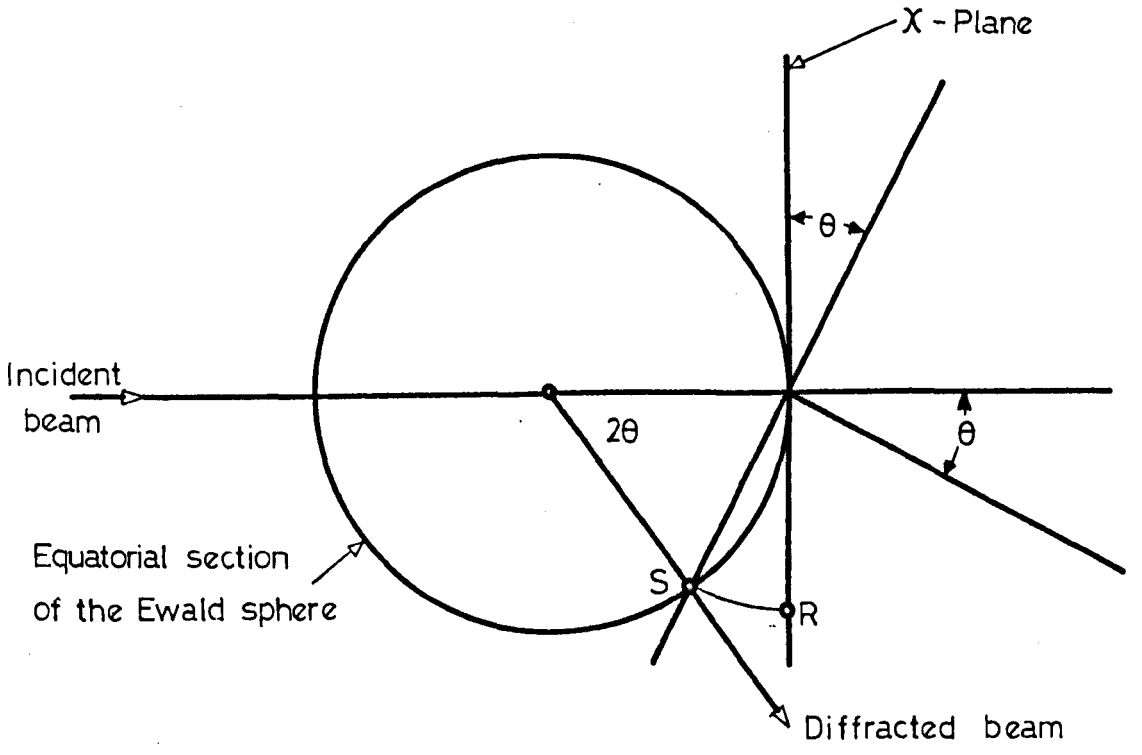

FIGURE 12.3 THE SYMMETRICAL - A SETTING

"stationary crystal-stationary detector", "moving crystal-stationary detector" or "moving crystal-moving detector" methods. The "stationary crystal-stationary detector" method although the fastest of the three, suffers the disadvantage of unreliable results if the incident X-ray beam is not uniform and convergent. Of the remaining two methods, Cobbledick[107] suggests that the latter (2θ-scan) is more accurate than the former (ω scan). The ω-scan, in which the θ- and 2θ- circles are not coupled during the motor driven scan of the reflection includes much of the background radiation thus giving a systematic overestimation of the integrated peak intensity.

For a particular reflection the circles were set to the calculated values and were individually adjusted to locate the peak of the reflection. The θ- and 2θ- circles were linked together for a 2θ- scan and the θ- circle was wound back from the position of maximum peak intensity by either 1° or 2° depending upon the magnitude of scan required. For reflections with $\theta < 60^{\circ}$, the circle was wound back through 1° and the scan through the reflection consisted of $\frac{1}{2}^{\circ}$, 1° and $\frac{1}{2}^{\circ}$ respectively. If the counts recorded on the scaler after each separate scan were I_1, I_2 and I_3 respectively, then the integrated intensity, I, was given by $I = I_2 - I_1 - I_3$. For reflections with $\theta > 60^{\circ}$ and with intense reflections with $\theta > 55^{\circ}$ the θ-circle was turned back through 2° and separate scans of 1°, 2° and 1° were used. This larger scan angle of 4° enabled any resolution of the $K\alpha_1$, $K\alpha_2$ doublet to be included in the peak scan. Cobbledick[108] advises the omission of reflections with $\theta > 80^{\circ}$ because of the uncertainty caused by the reflection of X-rays from the goniometer axis.

The linearity of counting rate for the proportional counter on the Small-Travers diffractometer has been reported[109] to have an upper limit of 4000 counts per second. For very intense reflections with counting rates greater than this the X-ray tube current was reduced to a suitable

value, for three of these reflections it was also found necessary to insert aluminium absorbers (0.001mm thick) to bring the counting rate into the linear range.

The 712 reflection, a reflection with a medium sized integrated intensity, was chosen as the 'standard' and its measurement at regular intervals enabled the integrated intensities to be corrected by a scale-factor for any 'drift' in the electronics and radiation damage to the crystal. The standard was always measured before and after any adjustments were made to either counter or generator settings.

The collection of data for all the very intense reflections was done at the same time to reduce the number of errors in the scale factors at reduced current and with absorbers.

12.3. Counting Statistics

The diffraction of X-rays is a random process and this leads to a statistical uncertainty in the intensities. The counting rate will follow the Gaussian law of distribution. If the number of counts, N, recorded in equal times follow a Gaussian distribution about the mean value, $\bar{N}$, the standard deviation of the distribution, $\sigma(N)$ is approximately

$$\sigma(N) = \bar{N}^{\frac{1}{2}}$$

The integrated intensity, I, is obtained by subtracting the background count, I_{back}, from the peak count, I_{peak}, and the standard deviation of the integrated intensity, $\sigma(I)$, is given by the expression:

$$\sigma(I) = (\sigma^2_{(I_{back})} + \sigma^2_{(I_{peak})})^{\frac{1}{2}}$$

where $\sigma_{(I_{back})}$ and $\sigma_{(I_{peak})}$ are the standard deviations of the background and peak counts respectively, since the amounts of time spent measuring the peak and background are equal.

12.4. Absolute Scaling of Intensities

The integrated intensity and standard deviation of the intensity of each reflection were calculated as described in the previous sections using a program written by the author. The intensity of 1086 unique reflections were measured, of these 243 had an integrated intensity less than their corresponding standard deviation, the values of $\sigma(I)$ and I were retained but the reflection was termed unobserved. Two of the unobserved reflections had a negative or zero intensity, in these cases $\sigma(I)$ was retained and the background corrected intensity was given a value of one count.

The intensities were corrected for 'drift' in the electronics and brought onto a relative scale by application of Lorentz polarisation factor. Scale and overall temperature factors were calculated using a program, 'POSCALE', written by M. T. G. Powell[110] of Portsmouth Polytechnic for the Elliott 4130. POSCALE uses the Wilson method to calculate the scale and temperature factors, the values output being 0.516 and 4.17 Å^2 respectively. The Wilson plot obtained is shown in Figure 12.4.

Table 12.1 shows the predicted accuracy using Cruickshank's expression[111], in each of the three axial directions for all the data available.

12.5. Statistical Test for Centricity

The systematic absences noted in Section 11.3 indicated the space group to be either the centrosymmetric I2/a or the non-centrosymmetric Ia.

With four molecules in the unit cell the space group Ia was preferred to I2/a as the latter would require the benzanilide molecule to possess a two fold axis.

The 'N(z) test' was carried out on the three dimensional data, using a program written by the author. The hypercentric distribution obtained is shown in Figure 12.5. The test has been used successfully on projection

Figure 12·4 The Wilson Plot

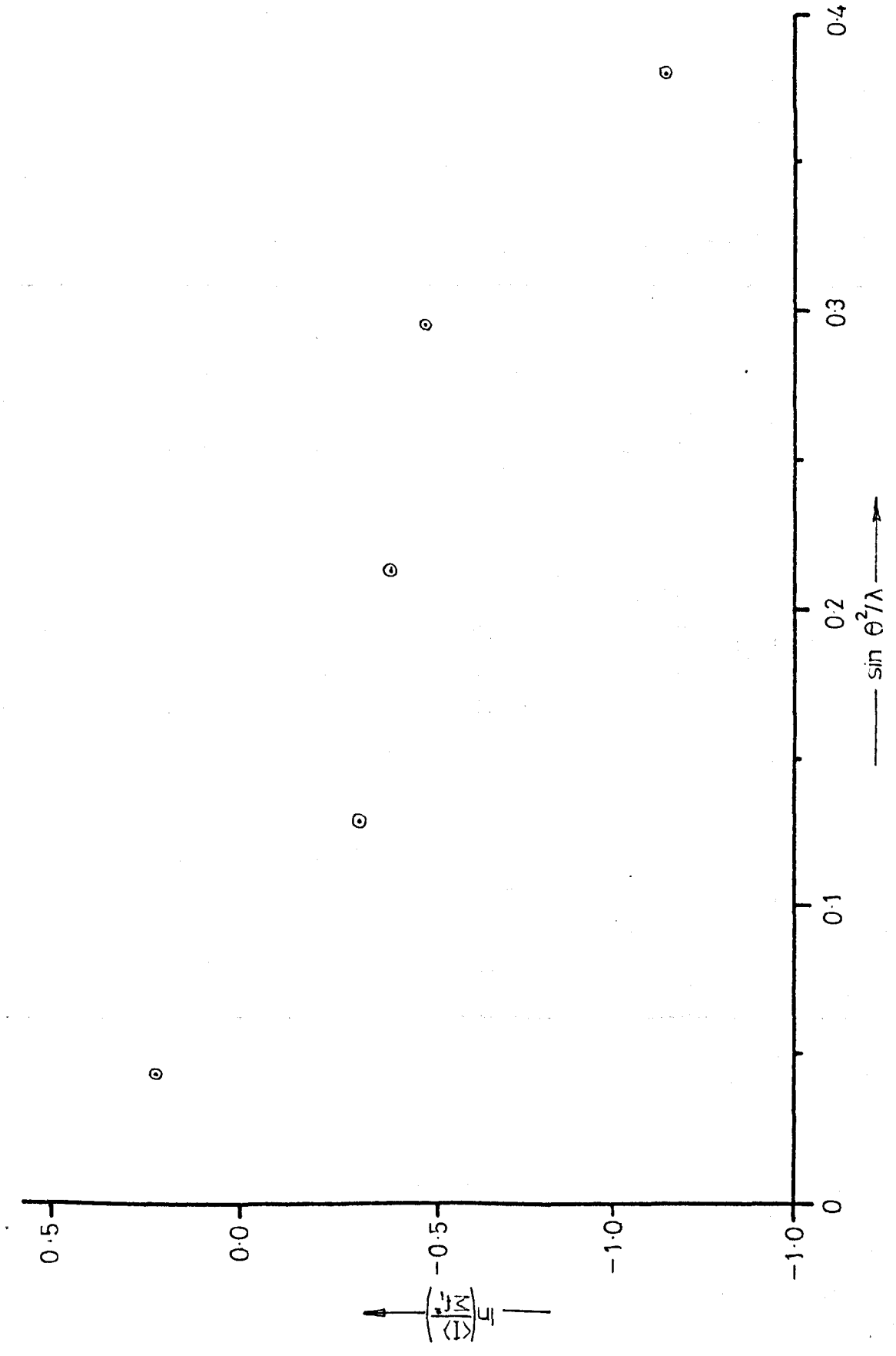

	ISOTROPIC		ANISOTROPIC		
	CENTRIC	NON-CENTRIC	CENTRIC	NON-CENTRIC	
Carbon	0.0015	0.0021	0.0016	0.0022	
Nitrogen	0.0013	0.0018	0.0014	0.0019	σ_x (Å/10%R)
Oxygen	0.0011	0.0015	0.0011	0.0016	
Hydrogen	0.034	0.049	0.037	0.052	
Carbon	0.0051	0.0072	0.0054	0.0077	
Nitrogen	0.0039	0.0056	0.0043	0.0060	σ_y (Å/10%R)
Oxygen	0.0031	0.0043	0.0033	0.0046	
Hydrogen	0.064	0.090	0.068	0.096	
Carbon	0.0033	0.0046	0.0035	0.0049	
Nitrogen	0.0026	0.0036	0.0027	0.0039	σ_z (Å/10%R)
Oxygen	0.0020	0.0028	0.0021	0.0030	
Hydrogen	0.041	0.058	0.044	0.062	

TABLE 12.1

Estimated Positional Errors

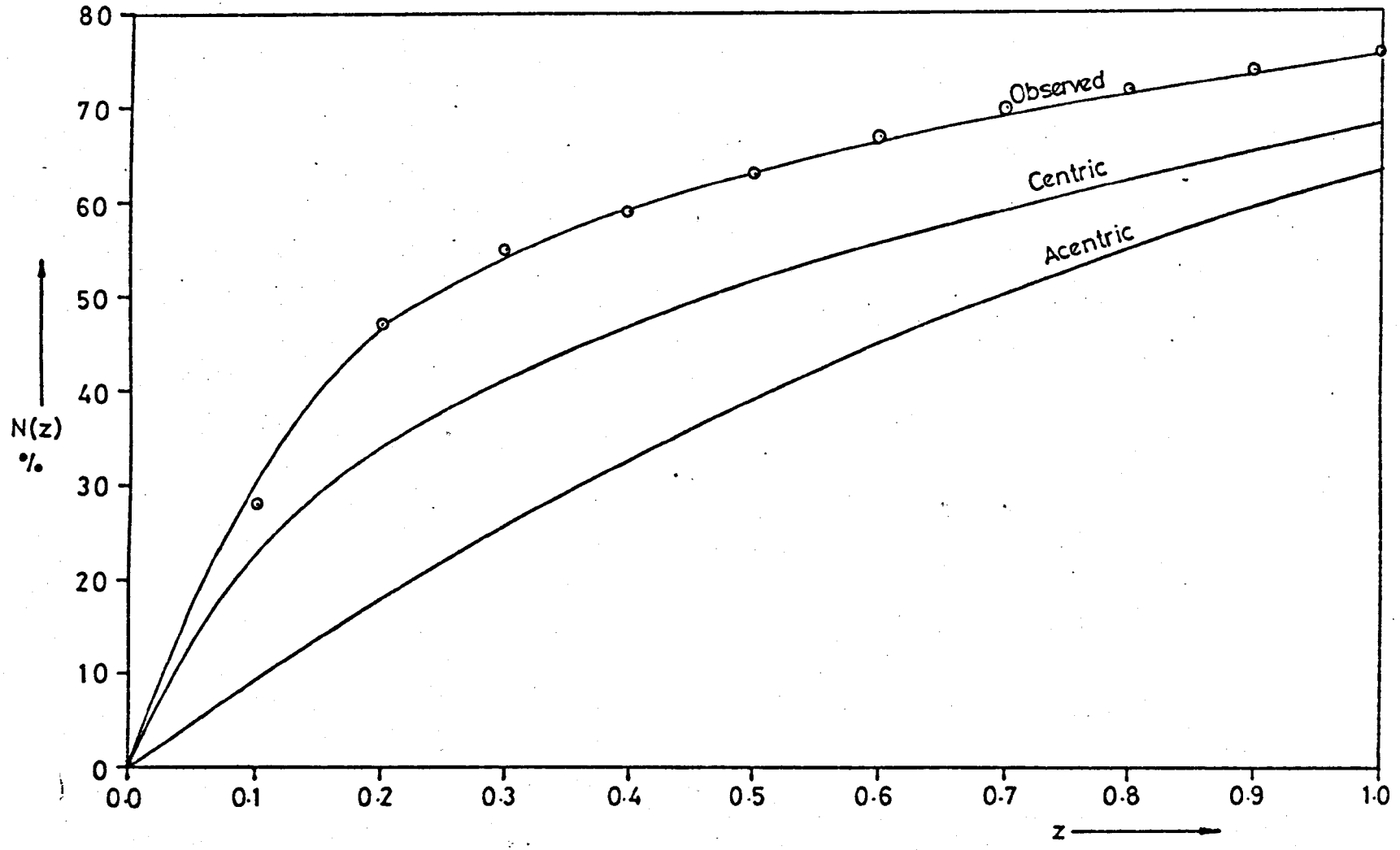

fig.12.5 N(z) test with benzanilide 3-D (hkl) data.

data and it was thought that the intensity distributions of the h0l or hk0 data may have been centric. The distribution in the two projections was found to be hypercentric, similar to the three dimensional data.

The presence of a hypercentric distribution has usually been associated with centrosymmetric molecules related to one another by a non-crystallographic centre of symmetry. It was assumed that the space group was Ia and that the molecules were in a conformation which approximated to them having a centre of symmetry. A further possibility would be for the molecule to be also related to other molecules by an approximate centre of symmetry.

13. THE DETERMINATION AND REFINEMENT OF THE STRUCTURE

13.1. The Patterson Function

The two dimensional Patterson function projected onto (010) and (001) was computed using the X-RAY 63 program FOURR. The maps were divided into $1/88^{ths}$, $1/23^{rds}$ and $1/30^{ths}$ of u, v and w respectively. The vector maps obtained are shown in Figures 13.1 and 13.2. Interpretation of these maps was limited to an indication that the benzanilide molecule lay with its long axis approximately parallel to the $10\bar{1}$ plane. This was substantiated by the large observed structure factor for the plane $20\bar{2}$.

A three dimensional Patterson synthesis, with the same intervals used for the two dimensional syntheses, was computed in an attempt to give information about the y co-ordinates of the atoms. The map was dominated by a diffuse peak parallel to $10\bar{1}$, similar to that shown by the projection onto 010. The assignment of vectors within this peak was not successful. The Harker lines 0, y, ½ and ½, y, 0 did show well resolved peaks at 0, 0.128, ½ and ½, 0.124, 0; from which it was calculated that the 'centre of the benzene rings' were 1.3Å from the c-glide plane. The presence of only one peak on each of these lines was taken to indicate that the centre of each ring was the same distance from the c-glide plane.

13.2. Two Dimensional Trial Structures

Using the dimensions of the unit cell, and benzene ring dimensions displayed by similar molecules, e.g. Acetanilide[112], it was calculated that the benzene rings must be inclined by at least 30° to the b-axis. This angle was required to prevent unfavourable interactions between b-axis translation related rings. The interactions between c-glide related benzene rings was both a function of the inclination of the ring to the b-axis and the distance of the ring from the c-glide plane. A program was written to vary the orientation of a benzene ring in the benzanilide unit

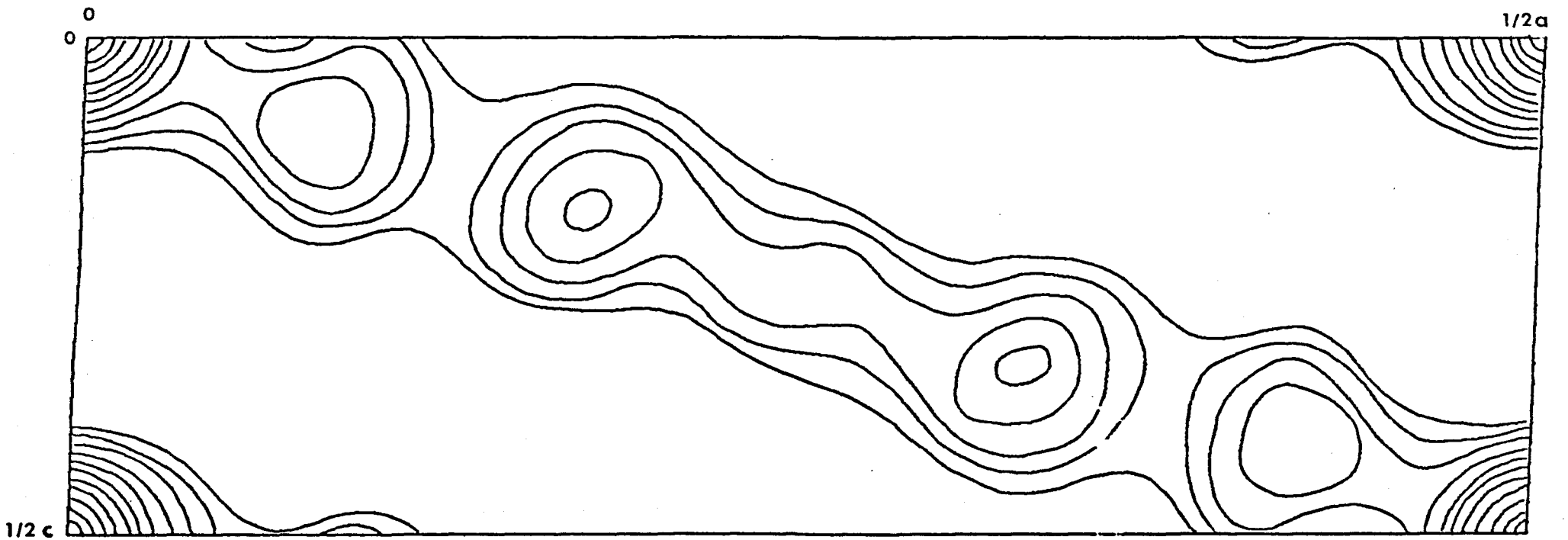

FIGURE 13.1. Patterson Projection onto 010

Contoured at arbitary intervals

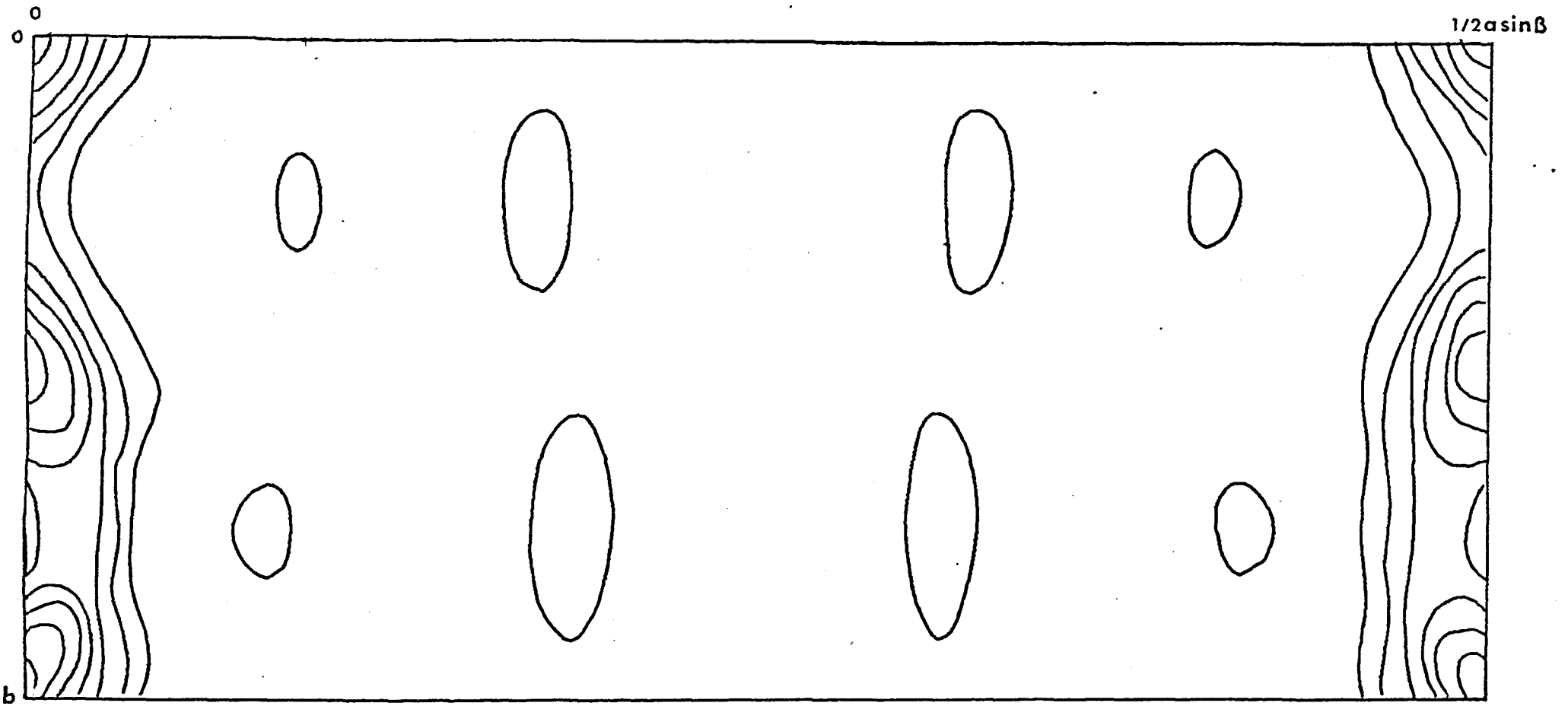

FIGURE 13.2. Patterson Projection onto 001

Contoured at arbitary intervals

cell. The analysis showed that the most favourable packing was obtained with the benzene rings inclined by 30°-35° to the b-axis, and the ring mid-way between the c-glide planes (∿ 1.3Å).

Orientation of the amide group, using the arguments of Leiserowitz and Schmidt[2], appeared to be parallel to the b-axis. The unit cell dimension of the b-axis was only slightly longer than the usual dimension for an axis containing a translation hydrogen bond.

A model was proposed with the long axis of the molecule in the $10\bar{1}$ plane, with rings inclined at 30° to the b-axis. The h0l projection was studied using the co-ordinates shown in Table 13.1 and atomic numbering scheme shown in Figure 13.3.

For the space group Ia the calculation of the structure factors is simplified by consideration of the space group symmetry. The structure factor can be considered as being composed of a real component, A, and an imaginary component, B, where for the space group Ia, these components can be written as:

$$\left.\begin{aligned} A^i_{hkl} &= 4 \cos 2\pi(hx_i + lz_i) \cos 2\pi ky_i \\ B^i_{hkl} &= 4 \sin 2\pi(hx_i + lz_i) \cos 2\pi ky_i \end{aligned}\right\} \quad \text{for } l = 2n \ (h + k + l = 2n)$$

and

$$\left.\begin{aligned} A^i_{hkl} &= -4 \sin 2\pi(hx_i + lz_i) \sin 2\pi ky_i \\ B^i_{hkl} &= 4 \cos 2\pi(hx_i + lz_i) \sin 2\pi ky_i \end{aligned}\right\} \quad \text{for } l = 2n+1 \ (h + k + l = 2n)$$

The structure amplitude, $|F_{hkl}|$, and the phase, α_{hkl}, are given by the expressions:

$$|F_{hkl}| = (A^2 + B^2)^{\frac{1}{2}}$$

$$\alpha_{hkl} = \tan^{-1} \frac{B}{A}$$

Atom	x/a	z/c
C11	.210	.210
C12	.190	.250
C13	.135	.185
C14	.100	.100
C15	.120	.060
C16	.175	.115
N1	.260	.260
C1	.285	.285
O1	.270	.270
C21	.345	.345
C22	.365	.305
C23	.420	.360
C24	.455	.455
C25	.435	.495
C26	.380	.440

TABLE 13.1

Initial HOl Model for Benzanilide

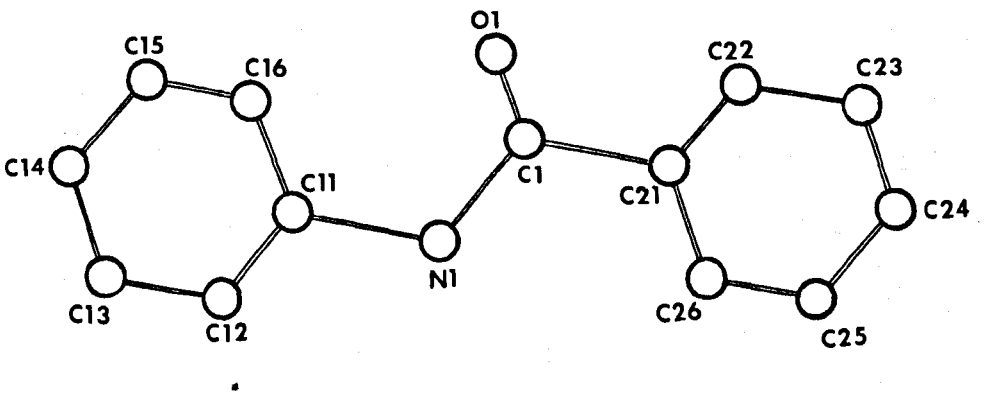

FIGURE 13.3

The Atomic Numbering Scheme

where $A = \sum_i f_n A^i_{hkl}$

and $B = \sum_i f_n B^i_{hkl}$

and the summation is over the atoms in the asymmetric unit.

Structure factors were calculated using the co-ordinates of the trial model, together with an overall temperature factor found from the Wilson plot. The initial value of the residual was 0.48.

For the space group Ia the equation for the electron density becomes:

$$\rho_{XYZ} = \frac{4}{V_c} \left\{ \sum_0^\infty \sum_0^\infty \sum_0^\infty \left\{ \sum_{h=2n} \left\{ |F_{hkl}| \cos\left[2\pi(hX + lZ) - \alpha_{hkl}\right] + |F_{\bar{h}kl}| \cos\left[2\pi(hX + lZ) - \alpha_{hkl}\right] \right\} \cos 2\pi kY \right.$$

$$\left. - \sum_0^\infty \sum_0^\infty \sum_0^\infty \left\{ \sum_{h=2n+1} \left\{ |F_{hkl}| \sin\left[2\pi(hX + lZ) - \alpha_{hkl}\right] + |F_{hkl}| \sin\left[2\pi(-hX + lZ) - \alpha_{hkl}\right] \right\} \sin 2\pi kY \right\}$$

Phases from the structure factor calculation were applied to the observed structure amplitudes and an electron density synthesis onto 010 was computed. New atomic positions were estimated using the double shift rule[69]. Three successive cycles using this process gave R = 0.38. A difference map showed features in the region of each atomic centre which were thought to indicate an overestimate of the overall isotropic temperature factor obtained from the Wilson plot. The overall temperature factor for this projection was reduced to 3.9 $\mathring{A}^2$ giving, R = 0.36.

The hk0 projection was studied using the x co-ordinates from the h0l projection and y co-ordinates were proposed to obtain a reasonable model.

Electron density syntheses onto 001 showed heavy overlapping of atoms owing to the c-glide related molecules. Refinement was achieved by translating the whole of the molecule parallel to the b-axis in 0.001 fractional co-ordinates (y/b). The residual dropped to 0.32 and the two dimensional refinement was considered to be complete.

A program, FCLS, was written to refine the structure by the method of least-squares. In the initial stages of refinement the off-diagonal terms of the normal equations were ignored, and only the positional parameters were varied. The partial derivative of F_c with respect to the positional parameter u, is given by the expression:

$$\frac{\partial F_c}{\partial u} = \frac{\partial A}{\partial u} \cos \alpha + \frac{\partial B}{\partial u} \sin \alpha$$

Thus the partial differentials for the space group Ia are:

$$\frac{\partial F_c}{\partial x_i} = -8 \sum_{i=1}^{N} \left\{ \pi h f_i \sin\left[2\pi(hx_i + lz_i)\right] \cos 2\pi ky_i \right\} \cos \alpha$$

$$+ 8 \sum_{i=1}^{N} \left\{ \pi h f_i \cos\left[2\pi (hx_i + lz_i)\right] \cos 2\pi ky_i \right\} \sin \alpha$$

$$\frac{\partial F_c}{\partial y_i} = -8 \sum_{i=1}^{N} \left\{ \pi k f_i \cos\left[2\pi(hx_i + lz_i)\right] \sin 2\pi ky_i \right\} \cos \alpha$$

$$- 8 \sum_{i=1}^{N} \left\{ \pi k f_i \sin\left[2\pi(hx_i + lz_i)\right] \sin 2\pi ky_i \right\} \sin \alpha$$

and $$\frac{\partial F_c}{\partial z_i} = -8 \sum_{i=1}^{N} \{\pi l f_i \sin[2\pi(hx_i + lz_i)] \cos 2\pi ky_i\} \cos \alpha$$

$$+ 8 \sum_{i=1}^{N} \{\pi l f_i \cos[2\pi(hx_i + lz_i)] \cos 2\pi ky_i\} \sin \alpha$$

for $l = 2n$ and

$$\frac{\partial F_c}{\partial x_i} = -8 \sum_{i=1}^{N} \{\pi h f_i \cos[2\pi(hx_i + lz_i)] \sin 2\pi ky_i\} \cos \alpha$$

$$- 8 \sum_{i=1}^{N} \{\pi h f_i \sin[2\pi(hx_i + lz_i)] \sin 2\pi ky_i\} \sin \alpha$$

$$\frac{\partial F_c}{\partial y_i} = -8 \sum_{i=1}^{N} \{\pi k f_i \sin[2\pi(hx_i + lz_i)] \cos 2\pi ky_i\} \cos \alpha$$

$$- 8 \sum_{i=1}^{N} \{\pi k f_i \cos[2\pi(hx_i + lz_i)] \cos 2\pi ky_i\} \sin \alpha$$

and $$\frac{\partial F_c}{\partial z_i} = -8 \sum_{i=1}^{N} \{\pi l f_i \cos[2\pi(hx_i + lz_i)] \sin 2\pi ky_i\} \cos \alpha$$

$$- 8 \sum_{i=1}^{N} \{\pi l f_i \sin[2\pi(hx_i + lz_i)] \sin 2\pi ky_i\} \sin \alpha$$

for $l = 2n + 1$, where N is the number of atoms in the asymmetric unit.

The initial residual value using this program with the complete data was 0.47. After two cycles the residual had risen to 0.61 and the parameter shifts were becoming larger. The program was altered to allow damping factors to be applied to the shifts. The model did not refine below R = 0.44.

A three dimensional Fourier synthesis using this model showed broad peaks in the region of each atom. The carbon and nitrogen atoms bridging the two phenyl groups were so broad as to produce an ovoid of electron density encompassing both atoms. The three atoms of the amide group were removed from the model in an attempt to detect their positions in a difference synthesis. The resulting map produced a cylinder of electron density over the whole volume expected to contain the three atoms. The residual electron density also extended toward the expected amide hydrogen position. As the benzene rings were not in the same orientation, with respect to the c-glide planes, the carbon and nitrogen atoms were interchanged. The oxygen atom was repositioned accordingly. Refinement using this model was abandoned when the hk0 projection would not refine by Fourier methods below 0.41 (other than by interchanging benzene rings).

Three dimensional refinement using the full matrix least-squares programs ORFLS (in X-RAY 63) and FMLS[113] failed, the solutions oscillated and rapidly diverged. Correlation matrices, output by both these programs, showed positive correlation ($\sim$0.4) between all x co-ordinates and between all z co-ordinates. Atoms related by a pseudo-two-fold axis parallel to the b-axis had correlation coefficients, for x and z parameters, of about 0.8. Atoms related by a pseudo-centre of symmetry, about the centre of the carbon-nitrogen bond, had coefficients of about 0.65. Parameters corresponding to y co-ordinates showed negative correlation ($\sim$ -.40), between atoms related by the pseudo-centre, and positive correlation between pseudo 2-fold axis related atoms of about 0.25. It was decided to refine the model by a blocked diagonal matrix least-squares method, to avoid the interatomic correlations. The program BLOKLS in the X-RAY 63 suite was used. After two cycles (R = 0.27) the expected symmetry, and dimensions, of the molecule were destroyed. The refinement ceased at R = 0.26. A series of two and three dimensional refinements were tried using this model,

without success. A number of techniques were used including Bunn error syntheses[114] in projection, and low angle reflections in three dimensions.

The failure of Fourier and least-squares methods to refine the model prompted the writing of a program using the parameter-shift method.

The h0l and hk0 projections with residual values 0.36 and 0.32 respectively were used in the refinement. After two cycles onto 010, the residual dropped to 0.23, with little change in the model. The refinement onto 001, refining the y co-ordinates only gave R = 0.28 after one cycle. The model was effectively the same. (Three of the atoms did move considerably, but only to c-glide related positions). The x co-ordinates were allowed to vary, in addition to the y co-ordinates. Two cycles moved the nitrogen and carbon atoms towards one another to produce a bond length of 0.91Å and reduced the residual to 0.18. Observed and difference Fourier syntheses were difficult to interpret, owing to the superimposition of c-glide related atoms in the projection.

13.3. Three Dimensional Refinement of the Structure

The program used to minimise the residual was altered to accept the full three dimensional data. After six cycles, varying only the positional parameters, the residual was 0.23 (from 0.45).

The X-RAY 72 program package was released and was available, as a development program, via the link to the 'University of Manchester Regional Computer Centre'. Three dimensional refinement was continued using CRYLSQ, the full matrix least-squares program.

After two cycles, varying the positional parameters and the scale and overall temperature factors, the residual dropped to 0.193. The parameters for each atom were put into separate blocks to prevent oscillation of the solution and parameter shifts were damped by a factor of 0.8. The atoms were allowed to refine with individual isotropic temperature factors for

two cycles (R = 0.18) followed by anisotropic temperature factors for four cycles (R = 0.148). Refinement of the model was slowing down and a three dimensional difference synthesis was computed for the volume containing the asymmetric unit. Figure 13.3 shows the composite difference map obtained projected onto 001.

The map shows a number of peaks corresponding closely to expected hydrogen atom positions. In addition, the map showed two distinct peaks which were images of the amide carbon and nitrogen atoms. The positions of these peaks were related to the original atomic positions by a two fold axis parallel to the b-axis through the oxygen atom. An image molecule was generated, related to the model by the two fold axis described above. Many of the atoms of the image were found to correspond with atoms in the model. Where co-ordinates differed significantly, a large anisotropic temperature factor was found in the least-squares parameters.

13.4. Evidence of Disorder

Further evidence of disorder was found on close inspection of Weissenberg photographs. Diffuse scattering effects, formally thought to be due to thermal disorder, were observed parallel to a* in reciprocal space and to a lesser extent parallel to c*. The equi-inclination Weissenberg photographs h0l and h1l are shown in Plate 13.1. The presence of this evidence also re-inforced the assumption that the disorder mostly affected reciprocal lattice points parallel to the a*c* plane. The symmetry relationship between the model and 'image' is also consistent with the twinning conditions required by monoclinic space groups.[115]

13.5. Refinement of the Disordered Structure

From the heights of the peaks found in the difference Fourier synthesis it was estimated that the disordered structure represented 25% of the population. The site occupancy parameters (G) of the model were set to

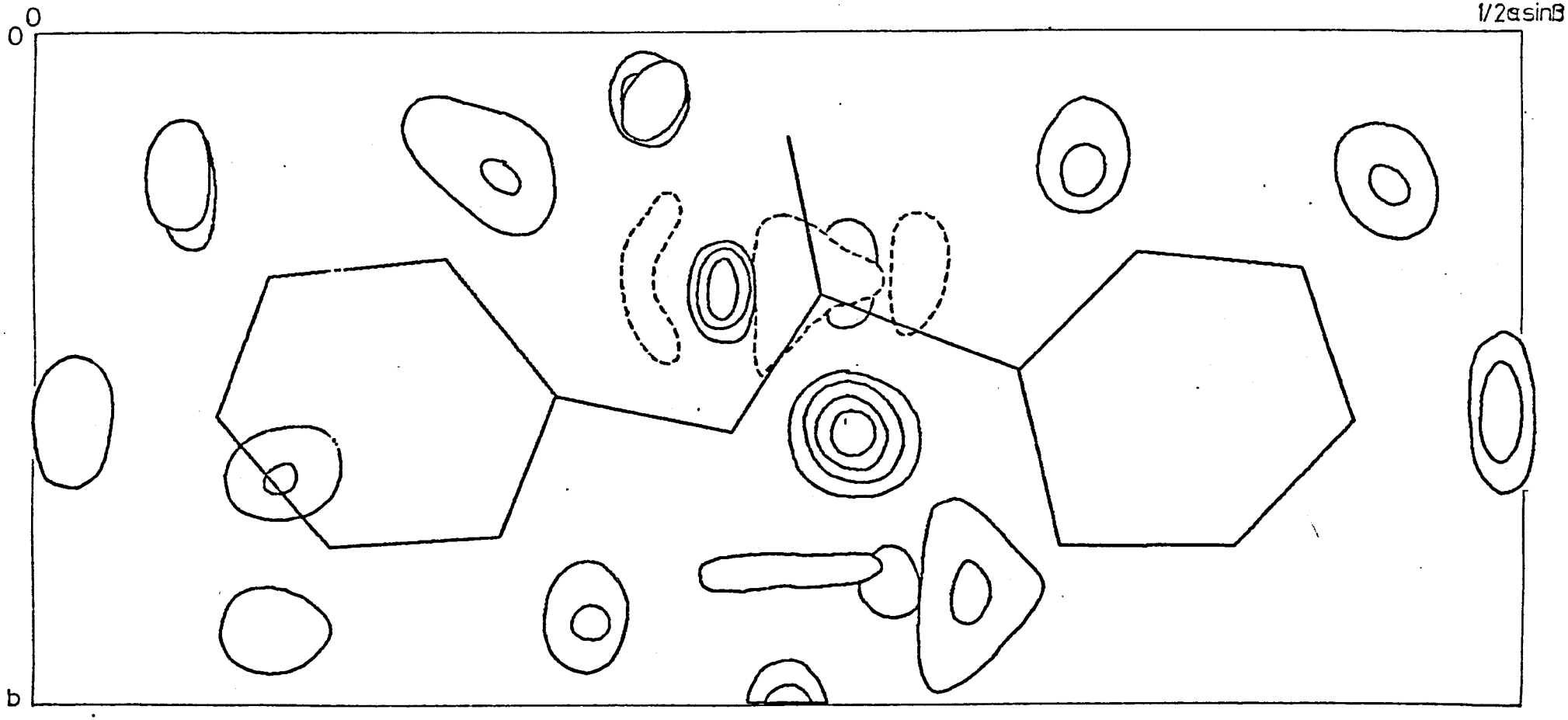

FIGURE 13.3. Composite Difference Fourier Synthesis showing Hydrogen Atoms and Disorder

Contours are drawn at intervals of 0.1 e $Å^{-3}$ starting at 0.1 e $Å^{-3}$

PLATE 13.1.

0.75 and a disordered image (G = 0.25) was generated about the postulated two fold axis. In previous least-squares refinements the x and z co-ordinates of the oxygen atom had not been refined in order to fix the origin of the unit cell. In the refinement of the disordered structure, the x and z co-ordinates of the oxygen atom were allowed to refine, in order that the position of the two fold axis was not biased.

The model with an overall temperature factor (R = 0.193) was chosen as the starting point.

Attempts to constrain positional parameters of the 'image' as functions of the model (as formally allowed by CRYLSQ) failed. The non-trivial constraining of parameters in the program only works for constraints imposed by the space group. Constraints were achieved by making the program CRYLSQ write the least-squares parameters on a file at the end of a cycle. A program was written, which read the parameters from the file and generated the 'image' from the 'model'. Output from the program was in a form suitable for input to the program LOADAT of X-RAY 72.

After eight cycles the refinement had slowed down (R = 0.15). A difference Fourier still showed an underestimate of the site occupancy of the 'image'. The site occupancy of each atom of the 'model' was allowed to refine for four cycles, in addition to the positional parameters. The program which constrained the 'image' was amended to average the site occupancies of the 'model' atoms and generate the 'image' with a related site occupancy. After three cycles the 'model' site occupancy had fallen to 60%. At this stage the co-ordinates of C14 and C24 were interchanged with the 'image' co-ordinates of C24 and C14 respectively, as the site occupancies of C14 and C24 were consistently refining to values below 0.5.

The site occupancy of the 'model' stabilised at 61% after two further cycles (R = 0.14), and a difference Fourier synthesis did not reveal any peaks in the 'image' nitrogen and carbon atom positions. A composite projection of the difference Fourier synthesis is shown in Figure 13.4.

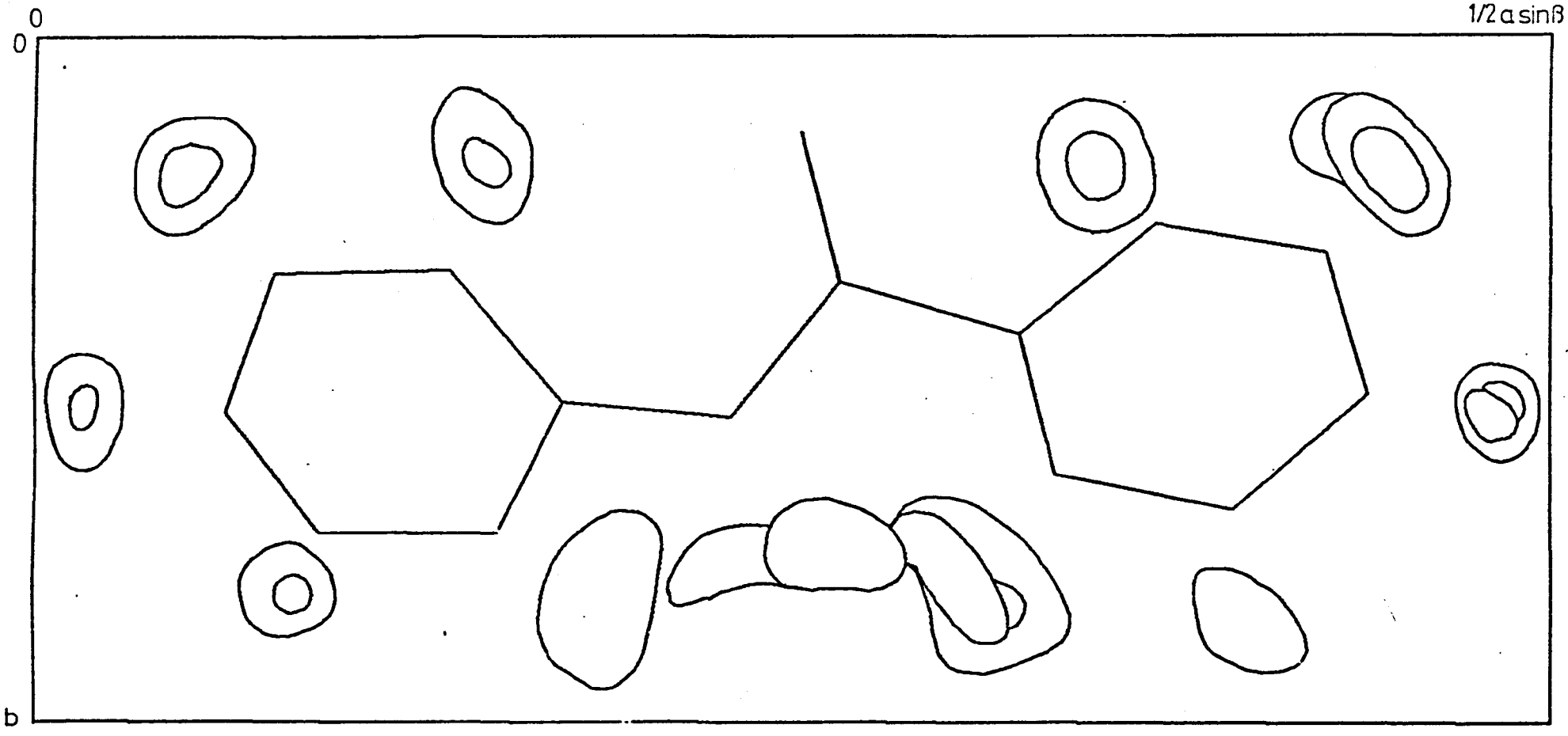

FIGURE 13.4. Composite Difference Fourier Synthesis for Ia Refinement Projected onto 001

Contours are drawn at intervals of 0.2 e $\mathring{A}^{-3}$, starting at 0.1 e $\mathring{A}^{-3}$

The clearly resolved peaks in the map correspond to the expected hydrogen atom positions. It was decided to enter the hydrogen atoms into the model to account for all the known electron density. The positional co-ordinates of the non-hydrogen atoms of the 'model' were refined as described above for four cycles (R = 0.119). The heavier atoms of the 'model' were allowed to refine anisotropically for two cycles (R = 0.084). The 'image' was constrained after each cycle and the hydrogen atoms were given the anisotropic temperature factors of the atom to which they were bonded.

As the populations of the 'model' and 'image' were not the same, the 'image' was allowed to refine independently of the 'model'. Two cycles of least-squares resulted in a reduction in the residual to 0.078. Parameter shifts were still large despite blocking the matrix for every atom. Tables 13.2 and 13.3 list the positional parameters and their standard deviations on the final cycle. The vibrational parameters and standard deviations are shown in Tables 13.4 and 13.5 respectively.

13.6. Refinement of the Disordered Structure in the Space Group I2/a

A comparison of the intermolecular contact distances between 'image' and 'model' related molecules did not reveal any unfavourable interactions to explain clearly why the populations of the 'model' and 'image' were different.

A refinement was undertaken with the population parameters of the 'model' and 'image' set to 50%. In this equal proportion, given that the disorder does relate the molecules by a two fold axis parallel to the b-axis, the structure can be refined as though the space group was I2/a. The cell was considered to contain eight benzanilide molecules, each molecule having a population parameter of 0.5.

The non-disordered model, with an overall temperature factor (R = 0.193)

Atom	x/a	y/b	z/c
C11	-.07731	.52275	-.06950
C12	-.09887	.71381	-.16734
C13	-.15438	.70818	-.22285
C14	-.18735	.52832	-.17822
C15	-.17061	.33266	-.06947
C16	-.11191	.32988	-.01434
N 1	-.01875	.54307	-.01433
C 1	.01653	.34864	.01187
O 1	.00573	.13006	-.01625
C21	.07668	.42417	.06671
C22	.12109	.26379	.02477
C23	.17559	.31042	.06659
C24	.19288	.51939	.15237
C25	.14915	.69067	.22287
C26	.08928	.63152	.16047
H12	-.07038	.87451	-.19813
H13	-.15945	.80417	-.33690
H14	-.23674	.55327	-.21358
H15	-.20496	.21666	-.01608
H16	-.10191	.20398	.07194
H 1	.01230	.73067	-.01449
H22	.10825	.13507	-.03371
H23	.19363	.16666	.05924
H24	.22755	.54355	.16704
H25	.16109	.88264	.23855
H26	.05987	.75008	.20012

TABLE 13.2.

Final Atomic Co-ordinates for Ia Refinement.

('model')

Atom	x/a	y/b	z/c
C112	.07728	.52577	.06720
C122	.09867	.71517	.16811
C132	.15428	.71038	.20390
C142	.18750	.52406	.17800
C152	.17061	.33280	.06852
C162	.11194	.33267	.01482
N 12	.01833	.54353	.01346
C 12	-.01669	.35161	-.01169
O 12	-.00562	.13148	.01927
C212	-.07782	.41898	-.06632
C222	-.12054	.26501	-.02472
C232	-.17563	.30591	-.06502
C242	-.19165	.51513	-.14995
C252	-.14927	.68959	-.20258
C262	-.08907	.63288	-.16070
H122	.07038	.87451	.19813
H132	.15945	.80417	.33690
H142	.23674	.55327	.21358
H152	.20496	.21666	.01608
H162	.10191	.20398	-.07194
H 12	-.01230	.73067	.01449
H222	-.10825	.13507	.03371
H232	-.19363	.16666	-.05924
H242	-.22755	.54355	-.16704
H252	-.16109	.88264	-.23855
H262	-.05987	.75008	-.20012

TABLE 13.2.

Continued

Final Atomic Co-ordinates for Ia Refinement.

('image')

Atom	σ x/a	σ y/b	σ z/c
C11	.00045	.00253	.00140
C12	.00049	.00249	.00154
C13	.00063	.00334	.00182
C14	.00058	.00302	.00155
C15	.00055	.00268	.00170
C16	.00055	.00277	.00162
N 1	.00037	.00182	.00137
C 1	.00045	.00216	.00167
O 1	.00062	.00142	.00256
C21	.00047	.00259	.00150
C22	.00049	.00255	.00155
C23	.00051	.00277	.00162
C24	.00047	.00284	.00165
C25	.00059	.00281	.00159
C26	.00054	.00272	.00168
C112	.00064	.00363	.00204
C122	.00079	.00398	.00241
C132	.00096	.00503	.00257
C142	.00082	.00492	.00219
C152	.00082	.00415	.00260
C162	.00075	.00412	.00230
N 12	.00056	.00284	.00208
C 12	.00061	.00316	.00226
O 12	.00085	.00216	.00330
C212	.00068	.00388	.00210
C222	.00072	.00390	.00222
C232	.00078	.00419	.00246
C242	.00068	.00409	.00273
C252	.00087	.00405	.00242
C262	.00079	.00395	.00244

TABLE 13.3.

Estimated Standard Deviations of Atomic Co-ordinates for Ia Refinement. ('image' atoms have numbers <xx>2).

Atom	U_{11}	U_{22}	U_{33}	U_{12}	U_{13}	U_{23}
C11	.038067	.060227	.045590	-.004336	-.005343	-.000104
C12	.043361	.052992	.056749	.001947	-.004796	-.001348
C13	.060954	.082260	.065067	-.001526	-.000535	.000855
C14	.063270	.074320	.048354	.022832	-.013227	-.005121
C15	.055871	.056603	.066338	-.019375	.013549	-.008893
C16	.052528	.058926	.059146	.002985	-.011151	.008549
N 1	.037314	.043177	.062822	-.003215	-.007494	-.000485
C 1	.042974	.043059	.055147	.001057	-.006958	-.009773
O 1	.035341	.042206	.090368	.001524	-.001042	-.007876
C21	.038574	.063229	.049565	-.000996	.004749	-.001451
C22	.041853	.060562	.053372	.002720	-.003537	-.000531
C23	.043982	.069344	.060374	.007925	-.011070	.012667
C24	.029021	.073925	.063555	-.013811	-.003132	.014761
C25	.062147	.068505	.049149	-.001282	-.001386	-.002777
C26	.050838	.060177	.064879	.005984	.002019	-.004471
C112	.028534	.058748	.039576	.001921	-.001646	-.003311
C122	.043492	.057229	.055454	-.008850	-.003775	-.000916
C132	.061802	.086765	.053250	.005641	.010226	.007550
C142	.050324	.094813	.034586	.012007	-.009691	-.000420
C152	.051776	.057844	.065083	-.001609	.016392	-.010092
C162	.043964	.061612	.051732	.003007	-.012851	.009710
N 12	.037938	.047097	.059416	-.001721	.002063	-.000864
C 12	.031945	.036120	.046849	.001567	-.005964	-.003850
O 12	.034087	.041548	.078518	.000188	.005725	.002096
C212	.034042	.058921	.041756	.006251	.000452	-.008912
C222	.037174	.060580	.047373	-.001762	-.003513	-.000927
C232	.042439	.066235	.055154	.009193	-.010662	-.000529
C242	.025957	.060516	.084696	-.006061	.011774	.011078
C252	.058230	.057255	.054519	.001312	-.001892	-.004312
C262	.042589	.050413	.060998	-.000231	-.001415	-.003889

TABLE 13.4.

Final Vibrational Parameters for Ia Refinement.

(Atoms numbered <xx>2 are of the 'image')

Atom	$\sigma(U_{11})$	$\sigma(U_{22})$	$\sigma(U_{33})$	$\sigma(U_{12})$	$\sigma(U_{13})$	$\sigma(U_{23})$
C11	0.00683	0.00941	0.00722	0.00685	0.00561	0.00701
C12	0.00757	0.00902	0.00852	0.00696	0.00651	0.00730
C13	0.01028	0.01386	0.01079	0.01010	0.00845	0.01024
C14	0.00996	0.01179	0.00852	0.00946	0.00759	0.00856
C15	0.00877	0.00976	0.00979	0.00790	0.00766	0.00854
C16	0.00832	0.00974	0.00891	0.00757	0.00690	0.00794
N 1	0.00560	0.00645	0.00708	0.00471	0.00566	0.00603
C 1	0.00831	0.00749	0.00820	0.00573	0.00761	0.00735
O 1	0.00636	0.00474	0.00939	0.00611	0.00586	0.00804
C21	0.00706	0.00966	0.00757	0.00696	0.00582	0.00749
C22	0.00732	0.00966	0.00816	0.00723	0.00625	0.00761
C23	0.00787	0.01112	0.00921	0.00789	0.00693	0.00849
C24	0.00603	0.01112	0.00904	0.00713	0.00595	0.00854
C25	0.00959	0.01097	0.00824	0.00882	0.00701	0.00814
C26	0.00870	0.01028	0.00974	0.00781	0.00739	0.00875
c112	0.00902	0.01367	0.00991	0.00958	0.00755	0.01026
C122	0.01154	0.01500	0.01336	0.01098	0.00981	0.01165
C132	0.01530	0.02158	0.01453	0.01555	0.01203	0.01456
C142	0.01299	0.02132	0.01058	0.01461	0.00946	0.01277
C152	0.01346	0.01531	0.01515	0.01192	0.01159	0.01298
C162	0.01219	0.01491	0.01294	0.01143	0.00995	0.01208
N 12	0.00920	0.01026	0.01110	0.00746	0.00928	0.00988
O 12	0.00981	0.01023	0.01041	0.00740	0.00946	0.00934
C 12	0.01003	0.00734	0.01542	0.00885	0.00857	0.01070
C212	0.00995	0.01394	0.01048	0.00994	0.00811	0.01010
C222	0.01041	0.01457	0.01162	0.01044	0.00907	0.01119
C232	0.01190	0.01669	0.01312	0.01163	0.01009	0.01259
C242	0.00969	0.01482	0.01752	0.01034	0.01043	0.01384
C252	0.01406	0.01521	0.01357	0.01258	0.01112	0.01225
C262	0.01110	0.01368	0.01403	0.01051	0.00999	0.01194

TABLE 13.5

Estimated Standard Deviations of the Thermal Parameters for Ia Refinement.

('image' atoms have numbers <xx>2)

was again used as the starting point*. After two cycles, using CRYLSQ, the residual was 0.14. All the atoms were then allowed to refine anisotropically. Initially a full matrix refinement was employed. The shifts were large and unreliable owing to high correlation between atoms related by the 'pseudo centre of symmetry'. As in the non-centrosymmetric refinement the matrix was blocked to avoid these correlations. After six cycles of blocked refinement (R = 0.112) the changes in the parameters became small and a difference Fourier synthesis was computed. The composite difference map obtained, projected onto 001 is shown in Figure 13.5.

The hydrogen atoms indicated in the difference Fourier map were included in the next structure factor calculation (R=0.111). Least-squares refinement of the non-hydrogen atoms for two cycles resulted in a value of 0.090 for the residual. The hydrogen atoms were given the isotropic temperature factors of the atoms to which they were bonded. Two cycles of refinement (R = 0.089) produced shifts in the parameters of less than 10% of their estimated errors. The positional parameters from the final cycle and their respective standard deviations are shown in Tables 13.6 and 13.7. Tables 13.8 and 13.9 show the vibrational parameters and standard deviations of the heavier atoms.

* The two fold axis used to generate the 'image' from the 'model' when refining with the space group Ia was repositioned to correspond with a two fold axis at ($\frac{1}{4}$, y, 0) in the space group I2/a.

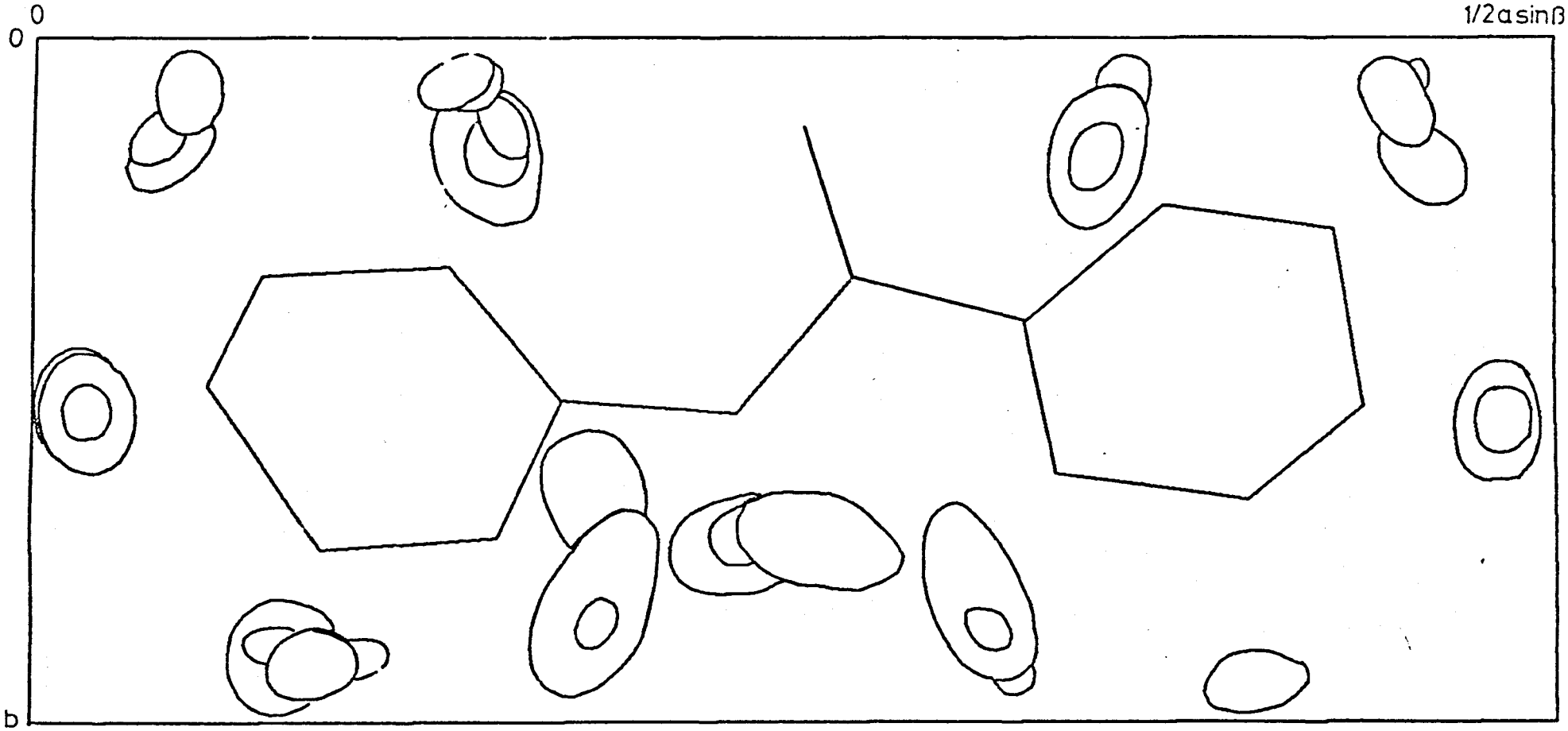

FIGURE 13.5. Composite Difference Fourier Synthesis for I2/a Refinement Projected onto 001

Contours are drawn at intervals of 0.1 e $Å^{-3}$, starting at 0.1 e $Å^{-3}$

Atom	x/a	y/b	z/c
C11	.17272	.52487	-.06913
C12	.15093	.71760	-.17012
C13	.09351	.73141	-.20774
C14	.05737	.49741	-.14908
C15	.07747	.33824	-.07596
C16	.13687	.33029	-.01731
N 1	.23092	.54423	-.01366
C 1	.26651	.35011	.01174
O 1	.25188	.13051	-.02700
C21	.32746	.42033	.06656
C22	.37082	.25609	.02067
C23	.42504	.29035	.05646
C24	.43809	.54304	.17779
C25	.39818	.67850	.21937
C26	.33942	.63447	.16010
H12	.18295	.86087	-.20333
H13	.08864	.83913	-.33333
H14	.01477	.54783	-.20000
H15	.04318	.16522	-.04333
H16	.15114	.16087	.07667
H 1	.24432	.72609	.02667
H22	.34659	.17391	-.07000
H23	.45795	.15217	.04333
H24	.48636	.54783	.19667
H25	.40909	.84783	.32667
H26	.31591	.85217	.20667

TABLE 13.6.

Final Atomic Co-ordinates for I2/a Refinement.

Atom	σ x/a	σy/b	σz/c
C11	.00028	.00147	.00089
C12	.00035	.00158	.00107
C13	.00039	.00206	.00119
C14	.00034	.00184	.00113
C15	.00029	.00137	.00091
C16	.00032	.00156	.00095
N 1	.00023	.00121	.00090
C 1	.00028	.00143	.00107
O 1	.00147	.00092	.00180
C21	.00032	.00155	.00093
C22	.00034	.00181	.00108
C23	.00040	.00193	.00113
C24	.00030	.00157	.00089
C25	.00033	.00151	.00095
C26	.00033	.00155	.00099

TABLE 13.7.

Estimated Standard Deviation of Atomic Co-ordinates for I2/a Refinement.

Atom	U_{11}	U_{22}	U_{33}	U_{12}	U_{13}	U_{23}
C11	.031672	.048193	.045160	-.003654	-.000392	-.001934
C12	.055268	.043693	.061738	.008657	-.003784	.006486
C13	.057205	.078555	.066300	.009054	.006232	-.007878
C14	.042646	.062702	.068426	-.009445	.003714	.008742
C15	.038987	.033594	.051173	-.009979	.004545	.007899
C16	.044052	.049089	.051430	-.001676	-.005516	.012747
N 1	.039144	.043539	.063741	-.002183	-.002299	.000086
C 1	.037329	.043489	.051157	-.000289	-.007456	-.004466
O 1	.052575	.042590	.053060	.003841	-.008906	-.002821
C21	.043756	.050221	.045079	-.005150	-.001028	.003046
C22	.046462	.063545	.060952	.004489	.000849	-.001039
C23	.065814	.066970	.059062	-.003199	-.006393	-.006326
C24	.039203	.053104	.043290	-.006207	-.008356	-.007231
C25	.049544	.044139	.049514	-.012364	-.006113	.000363
C26	.047082	.045802	.054904	.001560	-.005212	-.006811

TABLE 13.8.

Final Vibrational Parameters for I2/a Refinement.

Atom	$\sigma(U_{11})$	$\sigma(U_{22})$	$\sigma(U_{33})$	$\sigma(U_{12})$	$\sigma(U_{13})$	$\sigma(U_{23})$
C11	0.00397	0.00526	0.00459	0.00388	0.00342	0.00422
C12	0.00577	0.00565	0.00612	0.00473	0.00474	0.00479
C13	0.00628	0.00840	0.00697	0.00617	0.00528	0.00646
C14	0.00508	0.00695	0.00667	0.00506	0.00467	0.00578
C15	0.00432	0.00442	0.00498	0.00374	0.00374	0.00417
C16	0.00478	0.00548	0.00516	0.00428	0.00398	0.00451
N 1	0.00394	0.00431	0.00489	0.00309	0.00418	0.00414
C 1	0.00511	0.00477	0.00516	0.00344	0.00506	0.00461
O 1	0.00582	0.00302	0.01190	0.00518	0.01160	0.00368
C21	0.00483	0.00552	0.00473	0.00437	0.00383	0.00439
C22	0.00534	0.00682	0.00631	0.00509	0.00466	0.00551
C23	0.00691	0.00771	0.00637	0.00607	0.00529	0.00586
C24	0.00443	0.00575	0.00466	0.00429	0.00367	0.00438
C25	0.00523	0.00519	0.00509	0.00441	0.00416	0.00434
C26	0.00506	0.00541	0.00548	0.00436	0.00422	0.00461

TABLE 13.9

Estimated standard Deviations of the Thermal Parameters for I2/a Refinement.

14. DESCRIPTION OF THE STRUCTURE

The analysis of the crystal structure of benzanilide has yet to reach a satisfactory conclusion. The general features of the structure have been determined, but the results shown below have a number of unreasonable features. Taken individually, these features reflect the uncertainty in the parameters. Taken as a whole, it can be seen that unusual bond lengths and angles between atoms in one part of the molecule, have equally unusual counterparts in a pseudo symmetry related position. Undoubtedly there is a compromise solution which will cancel these features.

14.1 Molecular Dimensions

All the results given in this section were calculated using the X-RAY 72 program package. The bond lengths for the molecules defined in Tables 13.2 and 13.6 are shown in Table 14.1. Estimated standard deviations, in the least two significant figures, are given in parentheses.

Bond	Bond Lengths (A)		
	Ia Refinement		I2/a Refinement
	'model'	'image'	
C11 - C12	1.372 (16)	1.378 (19)	1.395 (11)
C12 - C13	1.358 (16)	1.322 (19)	1.368 (12)
C13 - C14	1.289 (18)	1.283 (19)	1.275 (13)
C14 - C15	1.407 (15)	1.395 (17)	1.406 (11)
C15 - C16	1.427 (16)	1.424 (17)	1.451 (10)
C16 - C11	1.391 (13)	1.385 (15)	1.407 (11)
C11 - N1	1.429 (14)	1.433 (16)	1.420 (09)
N1 - C1	1.337 (14)	1.322 (17)	1.345 (10)
C1 - O1	1.213 (16)	1.226 (19)	1.256 (13)
C1 - C21	1.514 (14)	1.524 (16)	1.522 (10)
C21 - C22	1.396 (15)	1.344 (17)	1.400 (12)
C22 - C23	1.330 (15)	1.335 (18)	1.304 (13)
C23 - C24	1.364 (17)	1.354 (19)	1.388 (14)
C24 - C25	1.497 (17)	1.434 (18)	1.540 (12)
C25 - C26	1.504 (16)	1.467 (18)	1.456 (11)
C26 - C21	1.364 (15)	1.390 (19)	1.394 (12)

TABLE 14.1

Bond Lengths and Estimated Standard Deviations

The bond angles and estimated standard deviations output by the program BONDLA are shown in Table 14.2.

Angle	Bond Angle (°)		
	Ia Refinement		I2/a Refinement
	'model'	'image'	
C11 - Ĉ12 - C13	120.0 (1.2)	116.6 (1.7)	120.3 (8)
C12 - Ĉ13 - C14	119.9 (1.3)	125.2 (1.8)	119.1 (9)
C13 - Ĉ14 - C15	124.6 (1.1)	120.6 (1.9)	125.7 (7)
C14 - Ĉ15 - C16	116.3 (1.4)	116.1 (1.7)	115.8 (7)
C15 - Ĉ16 - C11	117.2 (1.1)	118.4 (1.6)	117.2 (7)
C16 - Ĉ11 - C12	121.7 (1.0)	121.3 (1.5)	120.4 (6)
C16 - Ĉ11 - N1	121.3 (1.0)	121.6 (1.4)	122.5 (5)
C12 - Ĉ11 - N1	116.8 (1.2)	117.0 (1.6)	117.0 (7)
C11 - N̂1 - C1	124.7 (1.4)	125.4 (1.6)	125.0 (6)
N1 - Ĉ1 - O1	126.4 (1.7)	125.8 (1.9)	121.4 (9)
N1 - Ĉ1 - C21	113.6 (1.3)	115.5 (1.7)	115.1 (6)
O1 - Ĉ1 - C21	119.7 (1.6)	118.3 (2.0)	122.9 (9)
C1 - Ĉ21 - C22	117.3 (1.5)	118.8 (1.7)	116.7 (7)
C21 - Ĉ22 - C23	122.6 (1.6)	124.0 (1.6)	124.2 (9)
C22 - Ĉ23 - C24	123.0 (1.5)	120.3 (1.7)	119.9 (9)
C23 - Ĉ24 - C25	119.7 (1.4)	120.1 (1.6)	120.3 (7)
C24 - Ĉ25 - C26	112.7 (1.4)	117.8 (1.6)	115.0 (7)
C25 - Ĉ26 - C21	122.3 (1.5)	117.1 (1.7)	118.4 (7)
C26 - Ĉ21 - C22	118.8 (1.4)	120.6 (1.7)	121.6 (7)
C26 - Ĉ21 - C1	123.8 (1.5)	120.6 (1.7)	121.8 (7)

TABLE 14.2

Bond Angles and Estimated Standard Deviations

Least-squares planes and the angles between these planes were calculated using the program LSQPL. The planes were the first benzene ring (defined by the atoms C1<x>), the amide group and the second benzene ring. The coefficients of the equations defining each of these planes*

* See Section 10.1.

for each refinement are shown in Table 14.3.

Plane	Coefficients l	m	n	p	Refinement
1st ring	-0.22480	0.50096	0.83577	0.01739	Ia 'model'
Amide Group	0.39010	0.13148	-0.91133	2.58959	
2nd ring	-0.15142	-0.54379	0.82545	-1.94290	
1st ring	-0.26528	-0.51717	0.81373	-1.50071	Ia 'image'
Amide Group	0.37384	-0.11504	-0.92033	-0.27412	
2nd Ring	-0.11554	0.50845	0.85330	0.87301	
1st ring	-0.26435	0.50162	0.82371	-0.08563	I2/a
Amide Group	0.39058	0.13281	-0.91094	2.59592	
2nd ring	-0.23440	-0.54924	0.80212	-2.70299	

TABLE 14.3

Least-Squares Plane Coefficients

The maximum displacement of an atom, from a plane to which it contributed was 0.06Å (atom C14 of the Ia 'image'). This value, compared with the standard deviations of the co-ordinates, is significant; but it is doubtful at this stage whether any conclusion can be drawn from this deviation from planarity. Within the limits of the planarity of the benzene rings the carbon and nitrogen atoms of the amide group are in the plane of the benzene ring to which they are bonded.

The angles between these planes are shown in Table 14.4.

Planes	Angle between planes (°)		
	Ia Refinement 'model'	'image'	I2/a Refinement
Ring 1 & Amide Group	38.4°	37.9°	38.1°
Ring 1 & Ring 2	63.1°	62.5°	63.4°
Amide Group & Ring 2	28.0°	27.5°	26.5°

TABLE 14.4

Angles between Planes

14.2. The Crystal Structure

Benzanilide, in each of the refinements, shows the same basic crystal structure. The structure is very similar to many primary amides, if it is considered that the benzanilide molecule replaces the usual primary centrosymmetrically related dimer. Hydrogen bonds between axis translation related molecules produce ribbons of associated molecules parallel to the b-axis. Neighbouring molecular ribbons are related by glide planes, with a and c components respectively, to give parallel hydrogen bonded systems.

Projections of the final structure, obtained from the Ia 'model', onto 010 and 001 are shown in Figures 14.1 and 14.2 respectively.

The hydrogen bond is, as was expected from the length of the b-axis*, rather long. An interesting feature is a comparison of the hydrogen bonding, observed between axis translation related molecules and rotated translation related molecules. This sort of interaction, although not necessarily present in the proposed disordered structure, could give an indication as to how favourable such contacts would be. Table 14.5 summarises these interactions. The table shows that the hydrogen bonding geometry is only slightly affected by the disorder. With the exception of

* See Section 1.1.

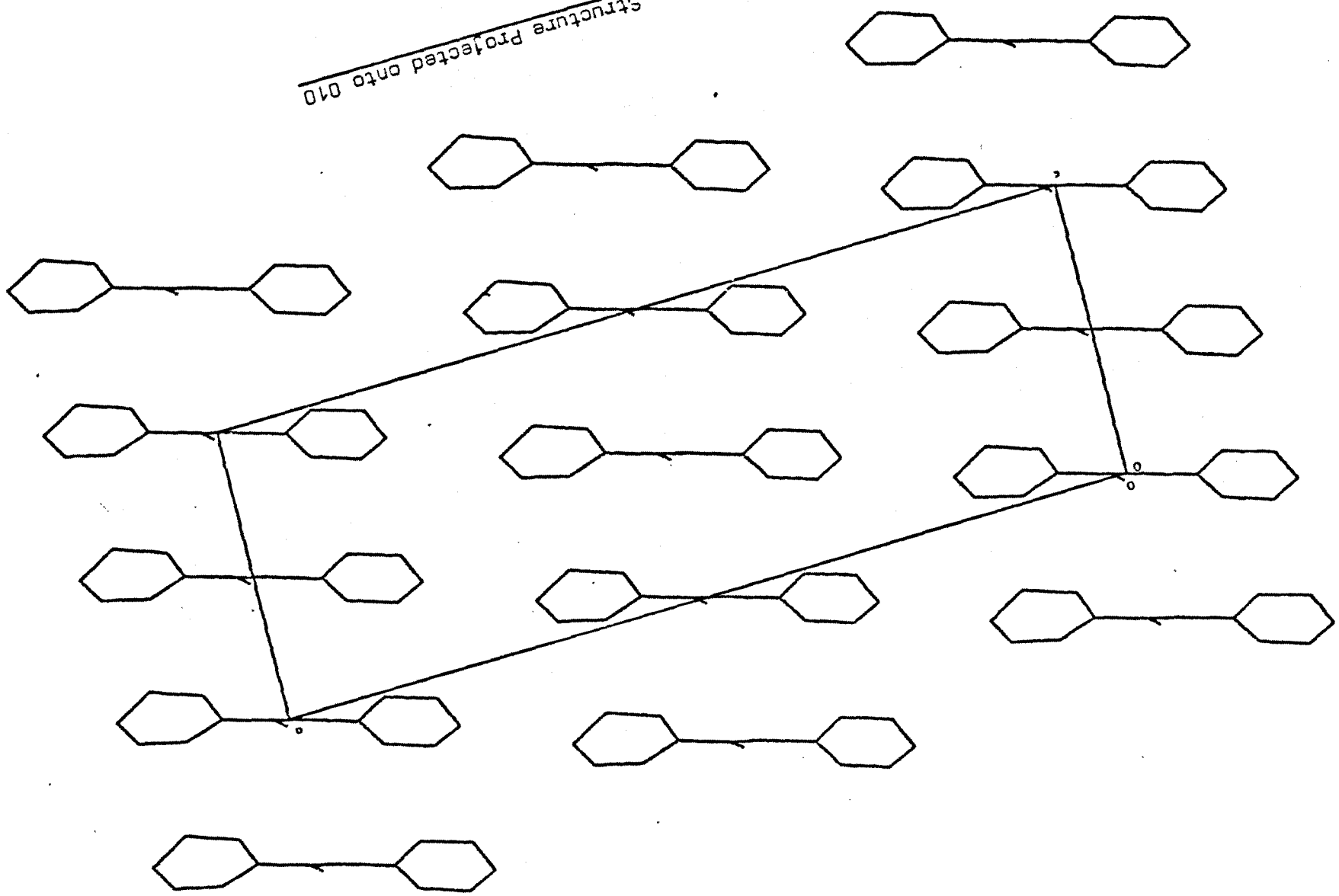

FIGURE 14.1. Structure Projected onto 010

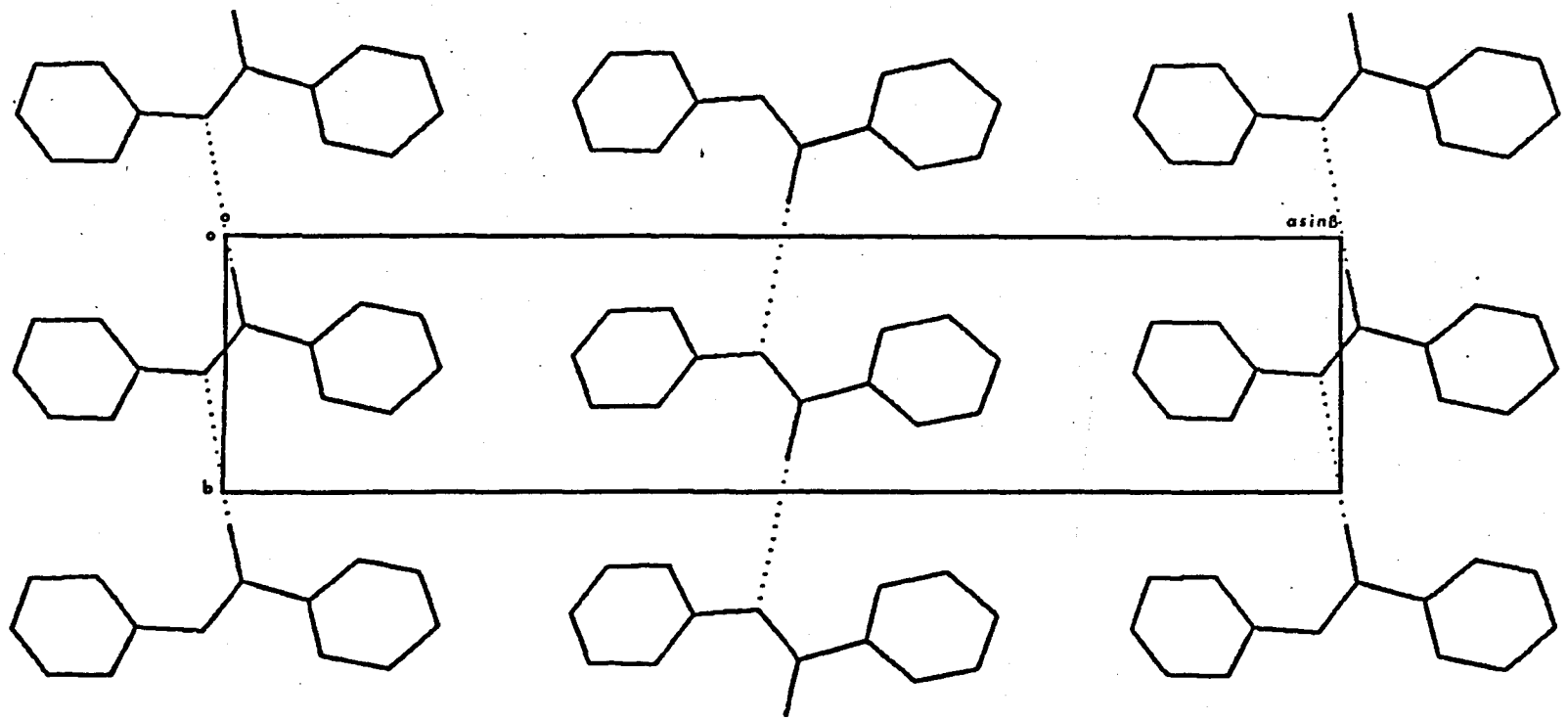

FIGURE 14.2. Structure Projected onto 001

(c glide related molecules have been omitted for clarity)

b-axis Hydrogen Bond	N-H(Å)	N...O(Å)	H...O(Å)	N-Ĥ...O(°)	C11-N̂...O(°)	C1-N̂1...O	C-Ô...N1
'model' (Ia)	1.13	3.18	2.14	171.8	104.1	130.8	168.9
'image' (Ia)	1.13	3.18	2.14	167.3	103.2	131.0	167.3
'model' (I2/a)	1.07	3.16	2.21	169.9	102.1	132.2	162.4
'image' to 'model' (I2/a)	1.07	3.17	2.16	157.1	102.8	132.2	149.6

TABLE 14.5

Comparison of Hydrogen Bonding Dimension between Models

dimensions which involve the hydrogen atom, the only change in the geometry is shown in the C-$\hat{O}$...N angle between disordered b-axis related molecules.

14.3. Comparison with Related Compounds

In contrast to the numerous primary amide structures which have been published, there are few aromatic secondary amides with which to compare the benzanilide structure. Table 14.6 shows the dimensions of the amide group in three related structures. The ranges of related bond lengths and angles shown in Table 14.6 are wider than for the corresponding ranges shown by the primary amides. With the exception of acetanilide however, the accuracy of the results are significantly less.

A point worthy of note in Table 14.6 is the greatly different angle between the amide plane and the plane of the benzene ring attached to the nitrogen. The isostructural p-chloro- and p-bromo-acetanilides show what is probably the minimum angle between these planes to avoid close intramolecular contact between the oxygen atom and the ortho hydrogen atom. The significantly greater angles between the planes showed by acetanilide and benzanilide must be a consequence of the molecular packing.

Compound	C-C(Å)*	C-N(Å)	C-O(Å)	C-C-O(°)	C-C-N(°)	O-C-N(°)	Amide-(N)-Phenyl Planes-(°)	Ref.
Acetanilide	1.495 (0.003)	1.354 (0.003)	1.219 (0.003)	121.6 (0.2)	115.3 (0.2)	123.1 (0.2)	17.6	112
p-Bromo-acetanilide	1.53 (0.01)	1.30 (0.01)	1.22 (0.01)	118.3 (0.8)	117.7 (0.7)	123.8 (0.8)	5.0	116
p-Chloro-acetamide	1.60 (0.01)	1.43 (0.01)	1.22 (0.01)	126 (1)	114 (1)	121 (1)	5.8	117
Benzanilide (Ia 'model')	1.51 (0.01)	1.34 (0.01)	1.21 (0.02)	120 (2)	114 (1)	126 (2)	38	-
Benzanilide (Ia 'image')	1.52 (0.02)	1.32 (0.02)	1.23 (0.02)	118 (2)	115 (2)	126 (2)	38	-
Benzanilide (I2/a)	1.52 (0.01)	1.35 (0.01)	1.26 (0.01)	123 (1)	115 (1)	121 (1)	38	-

TABLE 14.6

Comparison of Amide Groups - Related Compounds

* In benzanilide the non-amide carbon atom is in a benzene ring. *The others have a carbon (amide) - carbon* (methyl) bond.

PART 4

DISCUSSION

15. DISCUSSION

Arguments have frequently been put forward suggesting reasons for both the packing of molecules, and the conformation of molecules in the unit cell.

The crystal structures of both chloroacetamide and benzanilide appear to be dominated by intermolecular forces. Although it would be inadvisable to consider Van der Waals and hydrogen bonding forces to the exclusion of any other, the structures described underline the importance of the former. In the chloroacetamide structure, the intermolecular chlorine-chlorine vectors predominate to such an extent that there are no Van der Waals contacts between the amide group dimers. The tilt of the amide group to the b-axis, along which a hydrogen bond is formed, is probably caused by the lack of amide group Van der Waals contacts. The molecule, in order to produce a more dense structure, is forced out of the orientation which would form an ideal hydrogen bonding geometry. Van de Waals contacts between benzene rings dominate the benzanilide structure, and the resonance stabilisation of a more planar conformation is lost. The extent to which Van der Waals forces govern the benzanilide structure is indicated by the observed disorder. Molecules which are rotated through 180° have Van der Waals contacts similar to the unrotated molecule; and there seems to be little difference in energy between associations of molecules in each orientation.

It has been suggested[100], that the planar molecule displayed in the monofluoroacetamide structure is due to repulsion between the fluorine and oxygen atoms, whereas in the difluoroacetamide structure, with both fluorine atoms on the same side of the amide plane, the repulsion is between the $-CHF_2$ group and the amide plane. If the reasoning for the monofluoroacetamide conformation is correct, it would be expected that in the difluoroacetamide structure, the fluorine atoms would be staggered to the

amide plane and cis to the nitrogen atom. In this conformation, both fluorine atoms would be remote from the oxygen atom, and further from the plane of the amide group than was observed.

In the monofluoroacetamide structure a non-planar molecule (in the same unit cell) would result in closer fluorine-fluorine contacts between neighbouring hydrogen bonded ribbons. In a larger unit cell, Van der Waals contacts between ribbons would become longer. The structure observed, shows that the loss in conformational energy due to the fluorine atom eclipsing the nitrogen atom is made up by a gain in the energy associated with Van der Waals contacts and a more dense structure. Difluoroacetamide shows a significant change in the relation of neighbouring hydrogen bonded ribbons to one another. Rather than have parallel hydrogen bonded ribbons which would need to be far enough apart to accommodate the intermolecular fluorine-fluorine contacts; the ribbons are staggered, allowing the two fluorines to fit between.

The arguments used above are retrospective, as are most arguments regarding crystal structures, and the prediction of a structure without reference to crystallographic data is still in the realm of fiction. If such predictions are to be made, Van der Waals forces will play a major role, but these forces will need to be quantified more than is currently possible. Sakurai et.al.[118] have summarised a series of structures showing intermolecular chlorine-chlorine approaches of 3.3Å and suggest that these approaches are normal Van der Waals contacts. They further suggest that Van der Waals radii are not constant, but are functions of the direction of approach with respect to the atoms and bonds.

REFERENCES

1. Donohue, J., J. Phys. Chem., (1952) , 56 , 502.
2. Leiserowitz, L. & Schmidt, G.M.S., J.Chem.Soc. (A), (1969), 2372.
3. Hamilton, W.C., Acta Cryst., (1965) , 18 , 866.
4. Denne, W.A., Ph.D. Thesis, University of Lancaster , (1966).
5. Hospital, M. & Housty, J., Acta Cryst., (1966) , 20 , 626.
6. Bryden, J.H., Acta Cryst., (1961) , 14 , 61.
7. Wright, W.B. & King, G.S.D., Acta Cryst., (1954) , 7 , 283.
8. Katayama, M., Acta Cryst., (1956) , 9 , 986.
9. Structure Reports, vol.V, ed. W.B.Pearson, N.V.A. Oosthoek's Uitgevers Mij., Utrecht, (1963) , p. 498.
10. Blake, C.C.F., Ph.D. Thesis, University of Birmingham , (1959).
Penfold, B.R. & White, J.C.B., Acta Cryst., (1959) , 12 , 130.
11. Dejace, J., Acta Cryst., (1955) , 8 , 851.
12. Penfold, B.R. & Simpson, W.S. Acta Cryst., (1956) , 9 , 832.
13. Hughes, D.O., Ph.D. Thesis, University of Birmingham , (1961).
Hughes, D.O. & Small, R.W.S., Acta Cryst., (1962) , 15 , 933.
14. Bracher, B.H., Ph.D. Thesis, University of Birmingham , (1964).
Bracher, B.H. & Small, R.W.S., Acta Cryst., (1967) , 23 , 410.
15. Ladel, J. & Post, B., Acta Cryst., (1954) , 7 , 559.
16. Davies, D.R. & Pasternaak, R.A., Acta Cryst., (1956) , 9 , 334.
17. Leiserowitz, L. & Schmidt, G.M.S., J.Chem.Soc. (A), (1969), 2374.
18. Brathovde, J.R. & Lingafelter, E.C., Acta Cryst., (1958) , 11 , 729.

19. Turner, J.D. & Lingafelter, E.C., Acta Cryst., (1955) , 8 , 551.
20. Hughes, D.O., Tetrahedron, (1968) , 24 , 6423.
21. Bartell, L.S., J.Am. Chem. Soc., (1959) , 81 , 3497.
22. Bartell, L.S., J.Chem.Phys, (1960) , 32 , 827.
23. Bartell, L.S., Tetrahedron, (1962) , 17 , 177.
24. Mulliken, R.S., Tetrahedron, (1959) , 6 , 68.
25. Dejace, J., Acta Cryst., (1957) , 10 , 240.
26. Aihara, A., Bull. Chem. Soc. Japan ,(1960) , 33 ,1188.
27. Takagi, S., Shintani, R., Chihara, H. & Seki, S., Bull. Chem. Soc. Japan , (1959) ,32 , 127.
28. Aihara, A., Bull. Chem. Soc. Japan ,(1960) , 32 , 1242.
Aihara, A., Bull. Chem. Soc. Japan ,(1960) , 33 , 194.
29. Brown, C.J. & Cobridge, D.E.C.,Acta Cryst., (1954) , 7 , 711.
30. Bragg, W.H., Proc.Roy.Soc. (London) , (1913) , 88A , 428.
31. de Lange, J.J., Robertson, J.M. & Woodward, I., Proc.Roy.Soc. (London) , (1939) , A171 , 398.
Iball, J., J.Sci.Instr. , (1954) , 31 , 71.
32. International Tables for X-ray Crystallography, Kynoch Press , (1962) , 3 , 162.
33. Buerger, M.J., "X-ray Crystallography", J. Wiley & Sons, Inc., New York, N.Y. (1940) , p.180.
34. International Tables for X-ray Crystallography, Kynoch Press , (1959) , 2 , 292.
35. Jeffery, J.W. & Rose, K.M., Acta Cryst., (1964) , 17 , 343.
36. International Tables for X-ray Crystallography, Kynoch Press (1959) , 2 , 313.
37. Renniger, M., Z.Phys., (1937) , 106 , 141.
38. Burbank, R.D., Acta Cryst., (1965) , 18 , 88.
39. Coppens, P., Acta Cryst., (1968) , A24 , 253.
40. International Tables for X-ray Crystallography, Kynoch Press , (1962) , 3 , 202.
41. Lipson, H. & Cochran, W., "The Determination of Crystal Structures",Bell (London) (1966) , p.131.

42. Wilson, A.J.C., Nature (London) , (1942), 150 , 152.
43. Rogers. D., Computing Methods in Crystallography, Pergamon Press, (1965) , p.129.
44. Rogers. D., Computing Methods in Crystallography, Pergamon Press, (1965) , p.136.
45. Karle, J. & Hauptman, H., Acta Cryst., (1953) , 6 , 473
46. Mellor, I., Ph.D. Thesis, University of Keele , (1969) , p55.
47. Buerger, M.J., "Crystal Structure Analysis, J. Wiley & Sons, Inc. ,(1960) , p.542.
48. Wilson, A.J.C., Acta Cryst., (1949) , 2 , 318.
49. Howells, E.R., Phillips, D.C. & Rogers. D., Acta Cryst., (1950) , 3 , 210.
50. Rogers. D., Computing Methods in Crystallography, Pergamon Press, (1965) , p.123.
51. Collin, R.L., Acta Cryst., (1955) , 8 , 499.
52. Hargreaves, A., Acta Cryst., (1956) , 9 , 191.
53. Lipson, H. & Cochran, W., "The Determination of Crystal Structures",Bell (London) (1966) , p.62.
54. Wilson, A.J.C., Acta Cryst., (1950) , 3 , 397.
55. Lipson, H. & Cochran, W., "The Determination of Crystal Structures",Bell (London) (1966) , p.109.
56. Patterson, A.L., Z.Krist., (1935) , 90 , 517.
57. Buerger, M.J., "Vector Space", J. Wiley & Sons, Inc., New York, (1959)., p.64.
58. Sim, G.A., Acta Cryst., (1957) , 10 , 177.
59. Sim, G.A., Acta Cryst., (1957) , 10 , 536.
60. Beevers, C.A & Robertson, J.H., Acta Cryst., (1950) , 3 , 164.
61. Buerger, M.J., Acta Cryst., (1951) , 4 , 531.
62. Holmes, K.C., Computing Methods in Crystallography, Pergamon Press, (1965) , p.188.
67. Woolfson, M.M., Acta Cryst., (1954) , 7 , 61.
63. Harker, D. & Kasper, J.S.,Acta Cryst., (1948) , 1 , 70.
64. Gillis. J., Acta Cryst., (1948) , 1 , 174.
65. Karle, J. & Hauptman, H., Acta Cryst., (1950) , 3 , 181.

66. Sayre, D., Acta Cryst., (1952) , 5 , 60.
67. Woolfson, M.M., Acta Cryst., (1954) , 7 ,61.
68. Cochran, W. & Woolfson, M.M., Acta Cryst., (1955) , 8 , 1.
69. International Tables for X-ray Crystallography, Kynoch Press (1959) , 2 , 330.
70. Buerger, M.J., "Crystal Structure Analysis, J. Wiley & Sons, Inc. ,(1960) , p.478.
71. Lipson, H. & Cochran, W., "The Determination of Crystal Structures",Bell (London) (1966) , p.323.
72. International Tables for X-ray Crystallography, Kynoch Press , (1959) , 2 , 326.
73. Bhuiya, A.K. & Stanley, E., Acta Cryst., (1963) , 16 , 981.
74. Bhuiya, A.K. & Stanley, E., Acta Cryst., (1964) , 17 , 746.
75. Bracher, B.H. "CELFIT" - A Computer Program to Refine Crystal Unit Cell Dimensions , H.M.S.O. (1967) , AERE-R 5412 S.O. Code No. 91-3-20-78.
76. Wiebenga, E.H. & Smits, D.W., Acta Cryst., (1950) , 3 , 265.
77. International Tables for X-ray Crystallography, Kynoch Press (1959) , 2 , 177.
78. Cochran, W., J.Sci.Instr., (1948) , 25 , 253.
79. International Tables for X-ray Crystallography, Kynoch Press (1958) , 1 , 383.
80. International Tables for X-ray Crystallography, Kynoch Press , (1959) , 2 , 329.
81. International Tables for X-ray Crystallography, Kynoch Press , (1959) , 2 , 330.
82. International Tables for X-ray Crystallography, Kynoch Press , (1959) , 2 , 331.
83. International Tables for X-ray Crystallography, Kynoch Press (1959) , 2 , 333.
84. Schomaker, V., Acta Cryst., (1959) , 12 , 600.
85. Donohue, J., "Structural Chemistry and Molecular Biology", W. H. Freeman & Co.,(1968) , p.459.

86. Cucka,P. & Small, R.W.S., Acta Cryst., (1954) , 7 , 199.
87. Beagley, B. & Small, R.W.S., Proc.Roy.Soc. (London), (1963) ,275A , 469.
88. Krigbaum, W.R., Roe, R.J. & Woods, J.D., Acta Cryst., (1968) , B24 , 1304.
89. Adams, J.M. & Small, R.W.S., Acta Cryst., (1973) , B29 , 2317.
90. Hospital, M. & Housty, J., Acta Cryst., (1966) , 21 , 413.
91. Katsube, Y., Sasada, Y. & Kakudo, M., Bull. Chem. Soc. Japan, (1966) , 39 , 2576.
92. Cobbledick, R.E., Ph.D. Thesis, University of Lancaster (1969).
Cobbledick, R.E. & Small, R.W.S., Acta Cryst., (1972) , B28 , 2894
93. Fujimori, T., Tsukihara, T., Katsube, Y. & Yamamoto, J., Bull. Chem. Soc. Japan , (1972) , 45 , 1564.
94. Mazzarella, L. & Pedone, C. & Puliti, R., Acta Cryst., (1973) , B29 , 2699.
95. Ayerst, E.M. & Duke, J.R.C., Acta Cryst., (1954) , 7 , 588.
96. Takano, T., Sasada, Y. & Kakudo, M., Acta Cryst., (1966) , 21 , 514.
97. Takaki, Y., Sasada, Y. & Watanabe, T., Acta Cryst., (1960) , 13 ,693.
98. Filippakis, S.E., Leiserowitz, L. & Schmidt, G.M.S., J.Chem.Soc.(B), (1967) , 297.
99. Hospital, M. & Housty, J., Acta Cryst., (1966) , 20 , 368.
100. Hughes, D.O. & Small, R.W.S., Acta Cryst., (1972) , B28 , 2520.
101. Bond, W.L., Acta Cryst., (1960) , 13 , 814.
102. Cobbledick, R.E., Ph.D. Thesis University of Lancaster (1969) , p.49.
103. Small, R.W.S. & Travers, S.J., J.Sci.Instr., (1961) , 38 , 205.
104. Furnace, T. & Harker, D., Rev.Sci.Instr., (1956) , 26 , 449.

105. Arndt, U.W. & Phillips, D.C., Acta Cryst., (1958) , 11 , 509.
106. Arndt, U.W. & Willis, B.T.M., "Single Crystal Diffractometry", Cambridge University Press , (1966) , p.45.
107. Cobbledick, R.E., Ph.D. Thesis University of Lancaster (1969) , p.11.
108. Cobbledick, R.E., Ph.D. Thesis University of Lancaster (1969) , p.15.
109. Cobbledick, R.E., Ph.D. Thesis University of Lancaster (1969) , p.16.
110. Powell, M.T.G., "Crystal -" A Suite of Crystallographic Programs for the ELLIOTT 4130 , (1969).
111. Cruickshank, D.W.J., Acta Cryst., (1960) , 13 , 774.
112. Brown, C.J., Acta Cryst., (1966) , 21 , 442.
113. Bracher, B.H. & Taylor, R.I, "FMLS" - A Full-Matrix Least Squares Program for Crystal Structure Refinement." H.M.S.O. (1967) , AERE-R 5478.
114. Lipson, H. & Cochran, W., "The Determination of Crystal Structures",Bell (London) (1966) , p.196.
115. International Tables for X-ray Crystallography, Kynoch Press (1959) , 2 , 107.
116. Andreetti, G.D., Cavalca, L., Domiano, P. & Musatti, A., Acta Cryst., (1968) , B24 , 1195.
117. Subramanian, E., Z.Krist., (1966) , 123 , 222.
118. Sakurai, I., Sundaralingam, M., & Jeffrey, G.A., Acta Cryst., (1963) , 16 , 354.
119. Rollett, J.S., Computing Methods in Crystallography, Pergamon Press, (1965) , p.87.

APPENDICES

APPENDIX 1: COMPUTATIONAL WORK

Since the introduction of computers as a numerical aid, crystallographers have been a major group of users; and during this period many programs have been written to do the well defined crystallographic tasks. A number of these programs have been linked and distributed internationally to provide well proven packages. At the outset of this research, it was decided to write the minimum number of programs to complete the structure determinations, while using the X-RAY 63 system as the basic program package.

All the calculations described for the solution of the Chloroacetamide structure were done using the X-RAY 63 system available on the S.R.C. Chilton ATLAS.

Data collection for Benzanilide, using the Small-Travers diffractometer[103], required a knowledge of the χ, ϕ, 2θ and θ angles for the Furnace-Harker geometry. These angles were calculated using a program written on the Keele University ELLIOTT 4130. The program was specifically written for the space group Ia, and only output angles for unique non-systematically absent reflections. Cell dimensions were refined using a program CELFIT described in a report by Bracher[75].

The data reduction for Benzanilide was done using the X-RAY 63 system described above. Turnround for jobs submitted to the system was, on average, five days. It was decided that it would be advantageous to write a small set of programs for the ELLIOTT 4130, to decrease the turnround time for short analyses, the larger jobs still being sent to ATLAS. The data used on ATLAS was also reduced locally using a program which applied the Lorentz and polarisation factor for a normal beam equatorial geometry. Observed intensities were then scaled using the scale factor calculated by the X-RAY 63 system.

The reduced data, stored on a magnetic tape, could be read into a program, FCLS, which calculated parameter shifts using the diagonal approximation to the Least Squares solution. Using FCLS, selected refinement of overall scale factor, overall or individual isotropic temperature factors and positional parameters was possible. Output of calculated structure factors to magnetic tape, for subsequent input into a program, FOUR, was optional. FOUR, performed two dimensional Fourier syntheses onto any of the cell edges. New parameters were output to paper tape at the end of each run, which could then be used as input to a further run of FCLS and into DIST. DIST was a program to calculate selected distances and all bond angles for the structure.

In 1970 the ELLIOTT 4130 was upgraded to 64K of six microsecond store. This coincided with a heavy demand on the Chilton ATLAS, causing very long turnround on jobs. It was decided to implement a more comprehensive suite of programs locally. This allowed larger scale refinements than were possible using the previously described programs on the old 4130 configuration. The upgraded 4130 still run under a dedicated executive, with which the prime consideration was the real elapsed time of the run. The only magnetic backing store medium was magnetic tape which could only be used to hold sequential files.

A version of FMLS, Bracher[113], was modified for the 4130. The two main modifications being i) the introduction of thermal and positional parameter dumping factors, to reduce the tendency of some solutions to oscillate, and ii) more economic use of storage for data, to allow more parameters to be refined simultaneously. Storage requirements for the matrix of normal equations were reduced by almost half. The two dimensional symmetric full matrix was mapped into a one dimensional form of the upper semi-matrix and diagonal. A further reduction was achieved by only including, in the matrix of normal equations, those elements derived from parameters to

be varied. (Bracher's version always sets up ten parameters for anisotropically defined atoms and five parameters for isotropically defined atoms). This modification also required extensive rewriting of the input and output routines, in order to preserve the Bracher specification. The final version of the program allowed more than double the number of parameters to be varied (in the same core store requirement) and took, in a test run, 6% longer than the original to execute.

Later a suite of FORTRAN programs, CRYSTAL, was acquired from Portsmouth Polytechnic[110]. The Fourier synthesis program, POFOUR, was used in all subsequent syntheses. FMLS was altered to produce structure factors in the form required by POFOUR. The CRYSTAL programs, however, were written for a 32K ELLIOTT 4130, and most of these used 4130 overlay facilities for program code, and extensively used magnetic tapes to supplement the storage available for data. The use of POFOUR, without change, meant that the 64K 4130 at Keele was not being used efficiently. The major consequence of the inefficiency was that many runs exceeded the ten minutes maximum real time allowed during "batch sessions", which gave turnround of about four hours. The alternative arrangement of booked time on the machine gave turnround of up to forty-eight hours.

The aims of the modifications to POFOUR were to

i) reduce the use of work tapes to a minimum

ii) store the data for a full three-dimensional Fourier (for Benzanilide) in core

iii) be capable of producing a 3600 element grid section of the map in one run.

To achieve these aims, Millar Indices were packed into one word using the NEAT (ELLIOTT 4130 Assembler Language) shifting and logical instructions. Initially subroutines were written and all packing and unpacking was done with calls to these subroutines. The overheads in calling the unpacking

routine were removed when it was realised that the 4130 FORTRAN implementation of the logical operators AND, OR and NOT used the corresponding machine instructions directly on their operands. The integer word containing the packed Millar Index was EQUIVALENCEd to a FORTRAN logical variable. Logical expressions were used to mask out the required value, which was then used to control the first or second summations following the scheme suggested by Rollett[119]. The subroutine which did the summations in the calculation of the electron density map was re-written. Additional output of grid co-ordinates, to ease the interpretation of peak positions, was included in the subroutine. It was found in practice that the modified version of POFOUR took one third of the time of the original and met all the modification objectives.

Final attempts to refine the Benzanilide structure were performed using a program, MINIM, written using the "Parameter Shift Method" described by Bhuiya and Stanley[73]. The program required large amounts of core storage for data because of the features of the program design intended to reduce machine time. The following data items were stored in core:

i) Individual parameter contributions to the real and imaginary parts of each calculated structure factor.

ii) Totalled parameter contributions to each structure factor, excluding the parameter being varied, to save summing over N-1 parameters for each shift.

iii) Scattering factors for each atom type, to save interpolation during the calculation of a parameter contribution to the structure factor.

The program allowed any projection, or combination of projections, (with a maximum of 220 planes) to be refined.

A version of MINIM, for three dimensional data, was written later

when a disc was added to the configuration on the ELLIOTT 4130. The new version was achieved with little change to the original program. Essentially blocks of individual atom contributions relating to 220 planes were read into core from a direct access file for calculations, and written back, in situ, in blocks of 220 planes after modification.

During the summer of 1971 the Computer Laboratory at Keele was connected directly into the University of Manchester Regional Computer Centre. In 1972, after the system had become reliable, all the programs were implemented on this machine. Initially the programs were run on the ICL 1906A but were later transformed to the large, powerful CDC 7600. The final least-squares refinement of the benzanilide structure was done using X-RAY 72 which became available on the CDC 7600 in 1974.

APPENDIX 2

OBSERVED AND CALCULATED STRUCTURE FACTORS FOR MONOCHLOROACETAMIDE

The Table lists Millar index $10*|F_o|$ $10*F_c$

h,0,0

1	63	54
2	172	-212
3	30	19
5	117	-128
6	46	25
7	95	-91
8	173	176
9	141	147
10	127	118
11	54	47
12	84	-74
13	75	-72

h,0,2

-13	103	95
-12	124	111
-11	166	147
-10	46	-49
-9	118	-119
-8	173	-165
-7	274	-276
-6	58	62
-5	135	-145
-4	105	114
-2	59	36
-1	349	323
0	12	-9
2	89	-77
3	36	-31
4	89	-73
5	363	398
6	131	144
7	31	43
8	65	68
9	69	-71
10	77	-98
11	65	-80

h,0,4

-12	112	-97
-11	133	-126
-10	228	-200
-9	24	13
-8	73	75
-7	154	151
-6	285	286
-5	20	21
-4	188	163
-3	91	-92
-2	528	-538
-1	94	-77
0	253	-232
1	19	-22
2	531	503
3	103	102
4	46	65
5	49	54
6	156	-154
7	89	-90
8	32	-35
9	29	-47

h,0,6

-11	69	70
-10	99	105
-9	182	192
-8	30	30
-7	22	-25
-6	103	-95
-5	193	-188
-4	81	-76
-3	151	-144
-2	59	38
-1	256	255
0	103	95
1	153	145
2	9	10
3	195	-201
4	65	-61
5	23	-38
6	20	-35
7	41	47
8	30	38

h,0,8

-8	88	-130
-7	36	-44
-6	10	-9
-5	39	37
-4	81	86
-3	66	73
-2	91	106
-1	11	-11
0	89	-102
1	53	-55
2	66	-80
3	7	-8
4	54	71
5	14	22

h,1,0

1	277	-302
2	445	-439
3	425	-425
4	29	-43
5	55	38
6	213	242
7	228	246
8	63	64
9	46	21
10	88	-83
11	115	-124
12	31	-45

h,1,1

-13	25	23
-11	40	-33
-10	62	-53
-9	92	-81
-8	68	-60
-7	116	120
-6	255	264
-5	57	49
-4	102	-90
-3	63	-76
-2	301	-326
0	251	243
1	297	-299
3	298	314
4	76	69
5	68	64
6	19	-22
7	174	-179
8	90	-82
9	45	31
10	43	36
11	26	28
12	28	26

h,1,2

-13	29	46
-12	17	-18
-11	58	-54
-10	192	-170
-9	163	-145
-8	46	-39
-7	62	58
-6	259	259
-5	329	327
-4	186	173
-3	24	-31
-2	278	-296
-1	430	-433
0	404	-396
1	3	7
2	128	89
3	306	296
4	330	310
5	25	37
6	28	30
7	134	-124
8	159	-155
9	44	-53
10	34	-38
11	34	32
12	62	64

h,1,3

-12	57	-45
-11	13	-14
-10	31	31
-9	87	70
-8	132	118
-7	82	75
-6	126	-114
-5	248	-244
-4	71	-63
-3	45	33
-2	4	-4
-1	245	227
0	71	71
1	110	-93
2	181	170
3	18	-26
4	196	-171
5	40	-35
6	30	-45
7	0	-0
8	104	95
9	63	50
10	19	-13

h,1,4

-12	77	-75
-11	17	-17
-10	46	48
-9	179	165
-8	185	173
-7	106	101
-6	30	-30
-5	170	-163
-4	290	-283
-3	225	-221
-2	18	-17
-1	112	97
0	265	268
1	276	274
2	32	29
3	8	5
4	156	-143
5	191	-171
6	32	-44
7	22	-35
8	43	47
9	76	74
10	43	33

h,1,5

-11	70	62
-10	20	24
-9	21	-20
-8	71	-62
-7	113	-117
-6	93	-82
-5	83	70
-4	173	167
-3	49	52
-2	16	15
-1	23	18
0	126	-122
1	40	-30
2	29	23
3	100	-96
4	4	5
5	87	78
6	32	28
7	30	29
8	4	5
9	45	-44

h,1,6

-11	63	87
-10	48	52
-9	20	-28
-8	103	-115
-7	133	-149
-6	110	-121
-5	1	0
-4	71	70
-3	173	172
-2	158	165
-1	34	34
0	10	-10
1	122	-116
2	146	-146
3	40	-40
4	26	-25
5	43	50
6	74	79
7	24	31

h,1,7

-10	47	-62
-9	21	-31
-8	10	7
-7	39	41
-6	72	90
-5	62	71
-4	44	-46
-3	86	-93
-2	18	-18
-1	23	-21
0	15	-14
1	38	48
2	2	3
3	1	1
4	35	53

h,1,8

-7	37	57
-6	65	96

h,1,8

-5	58	95
-4	14	14
-3	18	-18
-2	57	-80
-1	75	-92
0	28	-28
1	13	-13
2	41	39
3	46	63

h,1,9

-5	30	-54
-4	27	-47
-3	27	27
-2	25	38

h,2,0

0	352	-370
1	34	15
2	154	-213
3	60	-65
4	385	397
5	75	90
6	114	152
7	62	41
8	239	-238
9	65	-55
10	42	-24
11	62	-45

h,2,1

-9	76	75
-9	58	75
-8	148	164
-7	98	109
-6	19	-19
-5	53	-68
-4	227	-269
-3	200	-249
-2	52	-62
-1	54	51
0	274	305
1	329	327
2	115	102
3	7	3
4	153	-155
5	194	-215
6	76	-93
7	38	-39
8	58	57
9	85	110

h,2,2

-11	119	-107
-10	57	46
-8	53	73
-7	303	346
-6	48	-43
-5	141	-143
-4	58	-49
-3	436	-427
-2	44	27
-1	130	97
0	94	-76
1	307	287
2	76	66
3	212	193
4	48	46
5	199	-220
6	76	-77
7	124	-121
8	37	-34
9	97	119

h,2,3

-11	132	113
-10	86	67
-9	8	-8
-8	71	-69
-7	183	-182
-6	172	-151
-5	23	-21
-4	52	49
-3	242	217
-2	268	228
-1	94	83
0	12	-11
1	189	-139
2	249	-212
3	125	-108
4	32	-31
5	72	57
6	133	127
7	66	76

h,2,4

-10	147	150
-9	29	-29
-8	21	19
-7	67	-66
-6	342	-347
-5	13	12
-4	106	73
-3	15	15
-2	328	305
-1	30	30
0	16	-18
1	43	45
2	152	-125
3	92	-65
4	146	-127
5	32	-31
6	77	80

h,2,5

-10	119	-113
-9	96	-90
-8	21	-21
-7	45	46
-6	158	142
-5	171	151
-4	74	46
-3	22	-22
-2	148	-113
-1	185	-162
0	87	-74
1	8	-8
2	49	48
3	136	117
4	77	68

h,2,6

-9	153	-146
-8	5	3
-7	47	-48
-6	45	45
-5	255	256
-4	18	21
-3	17	-20

h,2,6

-2	2	-4
-1	162	-154

h,2,7

-9	63	83
-8	81	84
-7	34	33
-6	13	-14
-5	79	-78
-4	103	-109
-3	47	-47
-2	7	-7
-1	47	46
0	91	94

h,3,0

1	23	46
2	58	82
3	77	99
4	7	-6
5	25	27
6	75	-30
7	100	-91
8	16	-17
9	24	-25
10	2	-2
11	27	49

h,3,1

-11	63	62
-10	145	139
-9	44	50
-8	107	-104
-7	23	-23
-6	159	-163
-5	222	-226
-4	18	17
-3	9	15
-2	243	252
-1	371	390
0	95	89
1	84	-59
2	293	-311
3	181	-212
4	37	-54
5	40	-49
6	125	133
7	138	112
8	79	45
9	135	93

h,3,2

-11	58	20
-6	81	-97
-5	43	-48
-4	18	-18
-3	12	-7
-2	89	84
-1	80	75
0	88	70
1	1	-4
2	4	1
3	51	-44
4	98	-87
5	8	-5
6	39	-41
7	12	11
8	89	62
9	40	11

h,3,3

-11	63	-52
-10	60	-59
-9	181	-174
-8	91	-85
-7	93	76
-6	22	-21
-5	160	167
-4	234	265
-3	34	33
-2	27	24
-1	206	-189
0	347	-318
1	149	-113
2	13	15
3	187	174
4	115	136
5	72	71
6	44	45
7	78	-61
8	72	-53

h,3,4

-9	80	-68
-8	16	-17
-7	24	-25
-6	19	18
-5	90	75
-4	44	43
-3	59	50
-2	3	-1
-1	40	-34
0	59	-39
1	94	-69
2	2	-3
3	26	-23
4	19	20
5	47	55

h,3,5

-7	124	93
-6	45	-33
-5	47	50
-4	122	-114
-3	218	-207
-2	45	-63
-1	45	-45
0	90	90
1	197	194
2	92	105
3	2	3
4	45	-75

h,3,6

-7	20	19
-6	43	41
-5	15	-15
-4	36	-35
-3	29	-26
-2	51	-51
-1	0	-2
0	3	2
1	20	19
2	41	42
3	3	4
4	21	21

h,3,7

-7	119	-116
-6	61	-70
-5	2	-1
-4	54	-54
-3	56	54
-2	110	125
-1	57	57
0	35	35
1	29	-29
2	94	-93
3	35	-64
4	31	-3

h,4,0

0	183	173
1	50	-82
2	40	-61
3	60	83
4	35	-48
5	65	50
6	45	43
7	61	-66

h,4,1

-9	70	-74
-8	137	-139
-7	70	-61
-5	74	68
-4	211	217
-3	107	150
-2	28	32
-1	29	-26
0	183	-189
1	248	-230
2	62	-67
3	9	-9
4	99	96
5	189	196

h,4,2

-6	46	76
-5	54	-55
-4	53	-50
-3	35	64
-2	72	-81
-1	61	60
0	79	63
1	168	-144
2	98	75
3	40	45

h,4,3

-10	35	-37
-9	3	4
-8	74	76
-7	142	147
-6	102	100
-5	29	28
-4	44	-42
-4	49	-42
-3	177	-170
-2	180	-166
-1	78	-63
0	10	-11
1	113	113
2	184	186
3	65	68
4	32	33
5	38	-37
6	122	-122
7	39	-50

h,4,4

-9	30	52
-8	36	34
-7	20	-20
-6	30	-31
-5	78	-66
-4	64	56
-3	45	34
-2	62	-49
-1	87	62
0	62	-54
1	34	-35
2	99	89
3	45	-50

h,4,5

-7	36	-53
-6	121	-112
-5	118	-110
-4	42	-50
-3	11	13
-2	120	101
-1	160	129
0	67	61
1	27	25
2	42	-48
3	95	-105

h,5,0

2	120	108
6	75	-72

h,5,1

-7	63	57
-6	154	153
-5	65	61
-4	31	-57
-3	1	-2
-2	174	-169
-1	103	-96
0	73	63
1	97	-94
2	91	80
3	157	153
4	28	28
5	57	65
6	26	-31
7	98	-109

h,5,2

-5	86	-85
-4	14	-15
-3	15	-13
-2	27	27
-1	105	105
0	8	8
1	17	16
2	11	-11
3	86	-84

h,5,3

-6	37	-44
-5	160	-157
-4	73	-72
-3	45	23

h,5,3		
-2	22	-21
-1	129	135
0	91	81
1	16	-17
2	98	89
3	41	-42
4	88	-103

h,5,5		
-4	112	118
-3	68	57
-2	7	8
-1	20	28
0	86	-78
1	44	-47
2	6	-7
3	62	-64

h,6,0		
0	105	99
1	69	68
2	25	-24
3	55	-50
4	56	-48

h,6,1		
-4	45	-47
-3	39	-37
-2	11	-12
-1	28	29
0	35	36
1	42	53
2	22	33

h,6,2		
-4	52	59
-3	58	51
-2	64	64
-1	38	33
0	53	-50
1	74	-87
2	60	-65

APPENDIX 3

OBSERVED AND CALCULATED STRUCTURE FACTORS FOR BENZANILIDE

The Table lists Millar index $10*|F_o|$ $10*|F_c|$ α .

(in millicycles)

h,0,0

2	501	478	999
4	622	580	500
6	662	617	7
8	6*	14	82
10	621	612	4
12	565	555	997
14	29	25	766
16	87	83	76
18	40	46	899
20	45	57	20
22	23	33	989
24	31	30	979
26	63	62	35
28	22	30	935
30	63	60	988

h,0,2

0	817	782	3
2	329	301	9
4	559	528	995
6	36	41	998
8	578	553	997
10	832	806	0
12	63	75	15
14	121	104	990
16	140	137	11
18	53	44	18
20	113	115	990
22	79	73	1000
24	82	80	22
26	18	17	820
28	2*	26	1

h,0,-2

2	1917	1959	2
4	270	277	995
6	363	366	7
8	220	221	26
10	41	44	0
12	246	284	12
14	121	109	982
16	240	245	995
18	166	165	35
20	282	277	993
22	88	83	999
24	62	44	7
26	12*	15	13
28	20	41	34

h,0,4

0	403	394	998
2	296	305	994
4	26	8	803
6	258	256	981
8	377	361	5
10	73	84	14
12	16*	27	870
14	42	44	955
18	90	77	968
16	28	35	32
20	108	99	1
22	82	72	3
24	11*	14	150
26	14	17	47

h,0,-4

2	333	312	7
4	255	246	13
6	369	351	995
8	472	432	8
10	65	70	978
12	11*	14	17
14	91	99	18
16	19	17	935
18	272	249	3
20	61	51	35
22	266	243	999
24	25	33	956
26	14	9	0
28	1*	10	74

h,0,6

0	210	189	994
2	139	122	5
4	83	97	979
6	92	90	12
8	85	88	1
10	229	228	986
12	20	63	22
14	111	122	2
16	13*	20	105
18	63	54	972

h,0,6

20	45	35	962
22	20	21	7

h,0,-6

2	332	332	998
4	59	53	30
6	11*	18	105
8	238	227	996
10	57	165	8
12	76	91	992
14	19	5	193
16	12*	39	4
18	40	22	22
20	80	98	6
22	2*	23	7
24	89	82	999

h,0,8

0	76	68	994
2	14*	16	994
4	34	39	999
6	31	39	982
8	201	198	991
10	39	36	990
12	215	178	4
14	23	25	6
16	11	15	189

h,0,-8

2	109	90	14
4	111	105	992
6	60	46	2
8	65	58	25
10	56	56	990
12	11*	22	15
14	27	30	994
16	10*	6	778
18	2*	36	1

h,0,10

0	11	5	814
2	4*	35	982
4	19	19	964
6	31	67	990

h,0,-10

2	9*	12	41
4	9*	14	77
6	9*	5	791
8	8	70	998

h,1,0

1	233	234	774
3	163	151	793
5	335	334	757
7	204	197	775
9	262	263	765
11	187	176	774
13	176	182	222
15	87	95	771
17	305	309	761
19	50	42	153
21	144	139	244
23	65	67	761
25	45	43	779
27	2*	10	759
29	1*	21	763

h,1,1

0	957	986	1
2	446	463	5
4	32	28	854
6	231	229	15
8	157	154	34
10	290	293	990
12	46	38	242
14	109	94	27
16	104	96	5
18	194	188	18
20	74	71	21
22	107	105	8
24	27	28	61
26	2*	8	76
28	65	70	9

h,1,-1

2	711	720	992
4	300	325	6
6	113	102	34

h,1,-1

8	361	375	12
10	86	85	72
12	255	243	985
14	52	48	143
16	30	38	994
18	116	112	3
20	219	224	14
22	40	39	21
24	64	65	23
26	2*	7	838
28	2*	9	40

h,1,2

1	843	876	756
3	236	244	241
5	72	82	764
7	110	112	784
9	100	91	820
11	186	194	776
13	73	78	239
15	90	79	771
17	72	66	860
19	55	52	218
21	34	31	226
23	45	50	768
25	2*	7	768
27	33	28	776

h,1,-2

1	828	847	248
3	628	664	244
5	102	115	200
7	486	528	761
9	148	134	775
11	140	142	766
13	61	68	768
15	139	135	232
17	119	116	794
19	179	184	762
21	55	61	249
23	52	60	233
25	36	38	784
27	2*	7	865

h,1,3

0	163	149	999
2	39	48	849
4	113	125	20
6	167	153	12
8	207	216	998
10	37	34	920
12	83	81	62
14	82	75	32
16	154	145	12
18	75	71	11
20	138	129	1
22	41	48	37
24	2*	14	17
26	72	67	6
28	15	28	16

h,1,-3

2	480	536	998
4	227	223	982
6	27	28	936
8	77	62	35
10	285	280	13
12	26	23	843
14	75	75	977
16	18	19	764
18	130	117	999
20	124	117	6
22	170	156	5
24	2*	20	14
26	50	45	36
28	16	25	985

h,1,4

1	168	168	242
3	86	89	249
5	94	102	780
7	16	24	172
9	278	314	755
11	157	160	759
13	194	187	242
15	37	34	870
17	111	112	771
19	15*	3	920
21	12*	6	140
23	9*	4	774
25	6*	10	886

h,1,-4

3	274	282	752
5	265	255	246
7	58	57	808
9	193	185	767
11	54	38	804
13	33	34	795
15	16*	29	206
17	28	28	823
19	39	31	883
21	3*	16	242
23	2*	9	245
25	2*	18	775
27	4*	12	213

h,1,5

0	111	95	972
2	62	66	7
4	112	114	3
6	115	110	990
8	35	16	4
10	34	41	896
12	22	19	230
14	173	164	3
16	62	62	1
18	93	83	990
20	45	51	24
22	35	30	983
24	59	57	4

h,1,-5

2	33	36	964
4	148	153	10
6	57	59	991
8	117	109	985
10	12*	7	37
12	134	120	13
14	33	28	973
16	10*	7	942
18	25	33	966
20	75	70	998
22	97	82	4
24	75	64	996
26	8	22	11

h,1,6

1	3*	20	199
3	47	49	783
5	3*	7	164
7	121	135	250
9	133	127	772
11	148	148	238
13	25	41	237
15	133	133	758
17	13*	13	791
19	29	31	779
21	2*	1	250
23	1*	16	170

h,1,-6

1	3*	10	196
3	101	94	752
5	51	43	227
7	72	67	752
9	36	34	817
11	31	23	225
13	19	17	810
15	3*	2	933
17	42	37	221
19	75	67	768
21	58	49	230
23	48	50	751

h,1,7

0	23	22	2
2	86	75	995
4	34	54	969
6	3*	4	992
8	60	62	970
10	63	58	973
12	153	140	1000
14	64	67	11
16	24	28	957
18	30	36	3
20	29	36	971

h,1,-7

2	86	77	7
4	44	40	979
6	78	71	30
8	34	41	4
10	50	39	972

h,1,-7

12	3*	12	983
14	46	38	14
16	15*	20	991
18	18	15	500
20	10*	25	994
22	1*	11	18

h,1,8

1	3*	3	916
3	10*	15	192
5	8*	19	763
7	18	22	853
9	2*	7	984
11	2*	11	763
13	14	19	246
15	15	13	767
17	14	12	242

h,1,-8

1	64	55	231
3	28	34	240
5	71	72	248
7	3*	21	208
9	122	115	751
11	5*	13	170
13	55	43	250
15	12*	10	766
17	10*	8	755
19	11	27	235

h,1,9

0	64	45	982
2	33	33	969
4	20	17	969
6	35	32	977
8	53	49	988
10	79	74	997
12	8*	53	17

h,1,-9

2	2*	7	967
4	19	24	14
6	36	26	981
8	86	67	18
10	13	21	14
12	14	7	47
14	9	9	976

h,1,10

1	1*	9	218
3	11	6	150

h,1,-10

1	1*	5	811
3	45	38	238
5	1*	4	130
7	10	41	247

h,2,0

0	228	228	500
2	96	72	991
4	480	491	995
6	149	137	35
8	315	303	24
10	127	118	966
12	25	19	838
14	100	98	995
16	103	107	972
18	207	204	30
20	50	63	5
22	14*	8	188
24	25	36	55
26	62	55	0
28	12	14	25

h,2,1

1	63	67	249
3	185	182	240
5	173	182	218
7	164	156	214
9	187	191	247
11	57	63	751
13	88	89	242
15	32	29	207
17	25	38	851
19	136	146	249
21	89	103	771
23	4*	18	213
25	39	33	784

h,2,1

27	14	9	94

h,2,-1

1	195	210	754
3	329	342	750
5	97	94	221
7	26	23	33
9	170	165	241
11	79	66	773
13	113	118	755
15	159	153	233
17	75	65	767
19	41	34	242
21	123	129	250
23	40	49	770
25	13*	6	994
27	19	23	787

h,2,2

2	278	250	981
4	41	29	805
6	270	277	11
8	84	80	975
10	54	60	34
12	109	118	956
14	223	224	984
16	270	269	13
18	146	151	14
20	82	90	15
22	29	33	24
24	37	31	960
26	2*	7	3

h,2,-2

2	188	178	985
4	26	30	925
6	164	150	10
8	101	105	34
10	194	203	27
12	159	150	979
14	74	80	969
16	10*	23	10
18	8*	13	774
20	40	38	87
22	3*	16	983
24	70	78	7
26	15	10	130
28	45	53	9

h,2,3

1	79	73	201
3	340	333	241
5	78	82	205
7	153	158	238
9	40	38	224
11	87	88	766
13	125	125	242
15	99	109	208
17	40	43	201
19	75	76	778
21	9*	7	856
23	19	27	784
25	2*	29	786

h,2,-3

1	299	309	236
3	208	207	759
5	314	312	236
7	26	23	50
9	44	42	780
11	39	42	249
13	5*	21	195
15	44	89	759
17	54	59	196
19	22	15	752
21	17	16	826
23	34	32	229
25	10*	11	837
27	11	13	793

h,2,4

2	54	62	926
4	151	137	998
6	33	32	999
8	48	55	964
10	32	39	792
12	162	162	976
14	143	139	998
16	148	161	10
18	62	64	994
20	2*	20	980

h,2,4

22	31	19	906
24	12	10	16

h,2,-4

2	134	120	998
4	359	365	998
6	108	105	20
8	35	39	3
10	20	20	58
12	65	63	36
14	108	107	994
16	28	41	960
18	37	52	25
20	13*	4	95
22	10*	16	966
24	14	20	21
26	57	62	19

h,2,5

1	169	190	244
3	44	49	240
5	81	77	241
7	27	29	204
9	141	132	774
11	77	77	226
13	163	165	239
15	10*	13	917
17	14*	3	782
19	29	28	768
21	9*	18	783
23	32	43	758

h,2,-5

1	37	35	141
3	145	132	225
5	92	81	759
7	52	52	174
9	42	45	207
11	57	56	779
13	12*	15	788
15	3*	6	868
17	3*	12	198
19	8*	20	850
21	55	48	755
23	9*	18	244
25	1*	16	775

h,2,6

2	32	16	893
4	18	7	160
6	95	101	977
8	26	21	139
10	27	18	796
12	17	11	962
14	52	58	9
16	24	16	76
18	13*	33	990
20	31	27	967

h,2,-6

2	179	164	994
4	166	155	6
6	224	215	7
8	103	103	16
10	3*	35	24
12	3*	6	186
14	4*	17	19
16	11*	52	11
18	7*	13	901
20	10*	4	187
22	6*	3	830

h,2,7

1	12*	16	246
3	3*	7	782
5	3*	14	239
7	46	44	817
9	9*	16	96
11	71	72	248
13	8*	12	203
15	11*	8	836
17	16	19	244
19	1*	13	758

h,2,-7

1	32	35	781
3	13*	9	23
5	15*	19	788
7	36	39	233
9	45	53	785

h,2,-7

11	63	57	231
13	13*	26	768
15	2*	6	873
17	9*	10	822
19	50	45	239

h,2,8

0	14*	21	935
2	13*	9	133
4	84	74	970
6	2*	4	952
8	44	36	40
10	13*	6	919
12	19	11	0
14	28	29	26

h,2,-8

2	3*	16	962
4	56	47	995
6	88	81	16
8	69	68	16
10	27	30	22
12	14	7	47
14	25	18	24
16	13	4	980

h,2,9

1	12*	6	191
3	16	5	767
5	2*	15	175
7	15	7	87
9	4*	14	777

h,2,-9

1	2*	6	773
3	2*	15	192
5	5*	22	249
7	32	22	240
9	46	47	232
11	29	25	776

h,3,0

1	54	41	214
3	107	109	756
5	51	39	48
7	68	73	822
9	17	14	963
11	20	24	229
13	147	144	757
15	29	34	873
17	32	34	155
19	80	87	774
21	47	47	766
23	6*	3	971
25	7*	6	243

h,3,1

0	59	42	52
2	253	232	998
4	280	265	988
6	175	161	28
8	39	42	957
10	71	75	997
12	16*	23	67
14	243	262	991
16	42	44	896
18	131	141	10
20	59	65	26
22	9*	13	973
24	42	38	994
26	59	59	13

h,3,-1

2	20	16	862
4	207	200	990
6	166	155	975
8	89	78	35
10	59	60	0
12	48	47	993
14	29	26	984
16	110	109	986
18	26	20	232
20	3*	4	77
22	26	19	52
24	28	36	28
26	53	52	16

h,3,2

1	11*	11	871

h,3,2

3	74	88	795
5	74	71	813
7	16	16	149
9	22	15	102
11	19	113	754
13	84	79	808
15	34	42	904
17	53	54	780
19	3*	15	189
21	31	23	780
23	38	30	761
25	15	20	246

h,3,-2

1	62	64	224
3	161	175	760
5	93	92	782
7	108	110	227
9	31	32	815
11	49	53	792
13	38	41	777
15	85	89	783
17	6*	12	138
19	3*	21	757
21	64	62	797
23	11*	25	778
25	2*	11	82

h,3,3

0	10*	23	949
2	161	148	983
4	76	61	35
6	29	26	86
8	104	108	978
10	45	33	89
12	205	197	985
14	101	101	977
16	185	183	14
18	50	42	993
20	51	67	19
22	12*	15	925
24	78	76	500

h,3,-3

2	128	135	30
4	78	82	17
6	43	43	56
8	52	59	965
10	3*	9	90
12	3*	17	59
14	47	92	995
16	7*	13	918
18	12*	29	5
20	8*	17	932
22	2*	46	995
24	2*	22	8

h,3,4

1	42	40	811
3	50	47	761
5	3*	5	865
7	12*	11	157
9	63	51	797
11	73	63	801
13	60	77	786
15	29	27	826
17	42	43	772
19	46	39	767
21	76	66	770
23	5*	12	218

h,3,-4

1	21	23	871
3	3*	14	246
5	111	119	787
7	38	40	886
9	98	96	752
11	3*	9	202
13	57	47	779
15	12*	21	788
17	26	33	815
19	13*	5	829
21	2*	8	187
23	8*	13	960

h,3,5

0	54	44	55
2	3*	25	987
4	47	47	2
6	94	101	967
8	35	40	923

h,3,5

10	27	25	880
12	47	63	982
14	3*	58	20
16	17	16	832
18	36	42	20
20	11*	6	896
22	56	59	985

h,3,-5

2	83	79	975
4	259	243	11
6	51	49	987
8	136	128	7
10	11*	27	981
12	29	25	42
14	25	13	72
16	86	75	996
18	2*	14	61
20	16	26	975
22	14	9	947

h,3,6

1	3*	12	827
3	18	27	176
5	3*	9	197
7	24	24	875
9	20	27	834
11	59	54	752
13	27	30	791
15	47	47	243
17	24	20	765
19	63	65	772

h,3,-6

1	26	24	828
3	35	32	193
5	18	7	241
7	24	29	843
9	16*	21	975
11	30	37	756
13	10*	1	101
15	2*	14	807
17	2*	5	5
19	10*	11	825
21	9	18	778

h,3,7

0	23	16	11
2	36	35	978
4	49	52	952
6	64	66	978
8	39	42	40
10	17	16	123
12	18	22	12
14	21	18	930
16	1*	8	87

h,3,-7

2	90	81	979
4	14*	28	955
6	149	138	6
8	7*	8	89
10	44	47	994
12	2*	2	821
14	34	35	34
16	26	15	37
18	7*	19	993

h,3,8

1	13*	22	204
3	2*	10	753
5	11*	12	826
7	11*	15	812
9	6*	4	772
11	21	19	782

h,3,-8

1	42	38	231
3	17	20	787
5	28	44	755
7	2*	1	0
9	18	16	237
11	10*	11	952
13	8*	4	189

h,3,9

0	20	19	988
2	15	14	904
4	28	32	994

h,3,-9

2	1*	6	12
4	22	25	987
6	3*	4	750

h,4,0

0	3*	5	500
2	138	131	18
4	104	101	29
6	53	49	54
8	78	87	2
10	44	42	991
12	104	98	21
14	46	48	77
16	20	24	838
18	53	51	14
20	2*	13	37
22	34	34	62
24	24	29	21

h,4,1

1	109	111	237
3	48	49	204
5	65	70	232
7	3*	16	220
9	44	44	762
11	14*	13	793
13	97	73	772
15	19	26	185
17	5*	13	194
19	67	74	763
21	28	23	235
23	21	13	162

h,4,-1

1	93	95	234
3	97	90	784
5	119	120	240
7	142	130	249
9	33	31	797
11	75	75	240
13	50	31	765
15	100	97	762
17	86	83	250
19	13*	10	79
21	81	79	768
23	18	17	143

h,4,2

0	95	92	20
2	80	77	988
4	42	46	15
6	129	132	5
8	36	31	43
10	70	67	34
12	72	78	13
14	33	29	920
16	42	40	61
18	36	41	24
20	45	44	29
22	38	43	24

h,4,-2

2	22	21	791
4	115	118	27
6	87	90	64
8	42	43	69
10	48	53	996
12	27	31	966
14	61	56	33
16	18	18	188
18	23	19	114
20	58	50	21
22	11	12	953

h,4,3

1	48	42	181
3	24	22	849
5	47	49	778
7	28	28	853
9	3*	17	765
11	17*	29	185
13	47	43	800
15	60	57	766
17	13*	6	500
19	11*	5	778
21	37	38	750

h,4,-3

1	210	209	248
3	25	26	120

h,4,-3

5	105	118	772
7	129	143	241
9	87	83	248
11	12*	10	795
13	43	56	242
15	55	45	771
17	32	36	771
19	47	42	758
21	30	21	815

h,4,4

0	43	46	974
2	18	27	980
4	136	131	994
6	30	24	73
8	4*	13	770
10	66	70	996
12	11*	6	870
14	28	34	76
16	47	48	43
18	23	22	12
20	32	38	10

h,4,-4

2	53	46	966
4	3*	12	240
6	74	73	36
8	37	37	82
10	40	40	63
12	42	47	9
14	2*	2	216
16	2*	13	102
18	2*	5	6
20	19	18	51

h,4,5

1	3*	9	85
3	28	33	800
5	18	22	875
7	7*	2	238
9	51	54	221
11	23	22	786
13	105	94	763
15	26	22	797
17	24	29	781

h,4,-5

1	47	50	784
3	94	94	239
5	3*	12	109
7	24	15	862
9	64	62	223
11	34	35	243
13	13*	18	237
15	5*	11	784
17	2*	8	760
19	1*	7	79

h,4,6

0	12*	8	45
2	84	79	986
4	34	27	8
6	30	28	966
8	28	32	998
10	5*	12	131
12	36	32	31
14	36	38	27

h,4,-6

2	41	33	7
4	24	14	983
6	3*	6	167
8	30	27	29
10	8*	6	20
12	44	39	48
14	32	31	29
16	13	16	2

h,4,7

1	19	16	829
3	13*	17	785
5	2*	4	756
7	9*	4	123
9	4*	11	250
11	46	39	769

h,4,-7

1	53	48	249
3	13*	15	772

h,4,-7

5	2*	8	826
7	6*	45	250
9	37	32	218
11	3*	7	0
13	11	17	241

h,4,8

0	24	22	992
2	20	21	973
4	10	10	27
6	1*	7	500

h,4,-8

2	9*	7	921
4	24	25	7
6	8	1	186

h,5,0

1	133	127	227
3	68	65	203
5	160	142	756
7	78	75	765
9	37	40	771
11	86	88	248
13	7*	12	106
15	9*	5	183
17	32	29	769
19	2*	6	866

h,5,1

0	127	117	982
2	72	67	31
4	44	41	500
6	78	73	30
8	9*	10	789
10	57	51	999
12	17	12	986
14	19	20	27
16	15	29	12
18	42	41	15

h,5,-1

2	96	83	983
4	63	62	43
6	55	57	986
8	49	44	6
10	22	24	82
12	31	35	40
14	2*	14	48
16	22	23	980
18	9*	13	2

h,5,2

1	72	79	214
3	110	109	239
5	91	93	754
7	21	30	784
9	45	63	249
11	71	53	213
13	16	16	217
15	10*	15	803
17	14	7	824

h,5,-2

1	140	138	757
3	72	70	224
5	68	60	236
7	117	115	754
9	34	36	766
11	61	61	764
13	61	63	758
15	32	25	754
17	4*	6	205
19	11	13	216

h,5,3

0	12*	2	212
2	39	38	14
4	37	36	48
6	16	13	865
8	47	45	978
10	33	25	15
12	17	15	956
14	13	13	971
16	39	40	15

h,5,-3

2	47	53	28

h,5,-3

4	16*	17	943
6	20	20	932
8	37	36	975
10	13*	8	211
12	42	42	30
14	2*	6	221
16	7*	7	976

h,5,4

1	68	66	221
3	63	67	235
5	32	38	762
7	27	31	757
9	40	44	232
11	43	42	231
13	13	7	52
15	24	23	763

h,5,-4

1	69	74	758
3	94	89	246
5	50	41	773
7	43	54	755
9	43	50	231
11	15	19	751
13	55	52	765
15	13	19	809
17	1*	15	755

h,5,5

0	50	46	10
2	16	5	27
4	12*	10	862
6	35	30	10
8	2*	6	115
10	15	18	35
12	19	14	941

h,5,-5

2	31	30	962
4	10*	18	992
6	13*	4	781
8	55	56	999
10	13	7	903
12	15	17	72
14	24	27	13

h,5,6

1	27	29	227
3	27	35	233
5	34	28	245
7	9*	11	769
9	27	33	245

h,5,-6

1	45	41	772
3	38	42	243
5	48	42	248
7	43	37	784
9	31	28	243

h,5,7

0	7	8	135

h,5,-7

2	30	29	981

h,6,0

0	60	64	0
2	18	11	198
4	15	8	978
6	52	51	14
8	2*	8	890
10	10*	20	51
12	19	20	21
14	6*	14	965

h,6,1

1	24	20	870
3	14*	7	150
5	22	22	227
7	33	23	758
9	13	9	213
11	13	15	930
13	16	19	847

h,6,-1

3	19	17	143
5	16	12	845
7	12*	6	975
9	9*	4	165
11	12	2	208
13	14	12	880

h,6,2

0	17	23	962
2	7*	8	206
4	47	46	5

h,6,-2

2	36	39	971
4	12*	12	65
6	35	33	40
8	14	20	997
10	8*	1	56
12	31	33	31

h,6,3

1	4*	11	244
3	34	36	245
5	39	30	794

h,6,-3

1	28	22	198
3	48	39	765
5	2*	23	242
7	18	16	819

h,6,4

0	13	9	969
2	19	21	962
4	14	16	51

h,6,-4

2	12	22	994
4	10	5	845
6	9*	9	0
8	38	32	31